AD-A011 760

GLOBAL WEATHER MODELING WITH VECTOR SPHERICAL HARMONICS

Sven Biorklund, et al

IBM Federal Systems Division

Prepared for:

Air Force Office of Scientific Research
Advanced Research Projects Agency

28 April 1975

DISTRIBUTED BY:

NTIS

National Technical Information Service
U. S. DEPARTMENT OF COMMERCE

SECURITY CLASSIFICATION OF THIS PAGE (*When Data Entered*)

REPORT DOCUMENTATION PAGE		READ INSTRUCTIONS BEFORE COMPLETING FORM
1. REPORT NUMBER AFOSR - TR - 75 - 0674	2. GOVT ACCESSION NO.	3. RECIPIENT'S CATALOG NUMBER AD-A011 760
4. TITLE (*and Subtitle*) GLOBAL WEATHER MODELING WITH VECTOR SPHERICAL HARMONICS		5. TYPE OF REPORT & PERIOD COVERED 11/30/73 - 2/28/75 FINAL REPORT 6. PERFORMING ORG. REPORT NUMBER
7. AUTHOR(s) Sven Bjorklund, N. Pleszkoch, F. Testa		8. CONTRACT OR GRANT NUMBER(s) F44620-74-C0036
9. PERFORMING ORGANIZATION NAME AND ADDRESS INTERNATIONAL BUSINESS MACHINES CORP. 18100 FREDERICK PIKE GAITHERSBURG, MARYLAND 20760		10. PROGRAM ELEMENT, PROJECT, TASK AREA & WORK UNIT NUMBERS 64706E (Program Element) ARPA Order 2633
11. CONTROLLING OFFICE NAME AND ADDRESS Advanced Research Projects Agency/IPT 1400 Wilson Boulevard Arlington, Virginia 22209		12. REPORT DATE April 28, 1975 13. NUMBER OF PAGES 142
14. MONITORING AGENCY NAME & ADDRESS(*if different from Controlling Office*) Air Force Office of Scientific Research/NP 1400 Wilson Boulevard Arlington, Virginia 22209		15. SECURITY CLASS. (*of this report*) Unclassified 15a. DECLASSIFICATION/DOWNGRADING SCHEDULE

16. DISTRIBUTION STATEMENT (*of this Report*)

Approved for public release;
distribution unlimited.

17. DISTRIBUTION STATEMENT (*of the abstract entered in Block 20, if different from Report*)

Approved for public release;
distribution unlimited.

18. SUPPLEMENTARY NOTES

19. KEY WORDS (*Continue on reverse side if necessary and identify by block number*)

Vector spherical harmonics, three-dimensional spectral model

20. ABSTRACT (*Continue on reverse side if necessary and identify by block number*)

A three-dimensional spectral global weather prediction model based on the Mintz-Arakawa model, using vector spherical harmonics has been used for prediction with real data.

DD FORM 1 JAN 73 1473 EDITION OF 1 NOV 65 IS OBSOLETE

SECURITY CLASSIFICATION OF THIS PAGE (*When Data Entered*)

FINAL REPORT

GLOBAL WEATHER MODELING WITH
VECTOR SPHERICAL HARMONICS

Submitted to
DEPARTMENT OF THE AIR FORCE
Air Force Office of Scientific Research (AFSC)
1400 Wilson Boulevard
Arlington, Virginia 22209

28 April 1975

Principal Investigator: Sven Bjorklund
Phone: (301) 840-6946
Weather Systems Department
Federal System Division
International Business Machines Corporation
Gaithersburg, Maryland

Program Manager: William J. Best
Phone: (202) 694-5454

Effective Date: 11/30/75
Expiration Date: 02/28/75
ARPA Order: 2633
Contract No:F44620-74-C-0036

Sponsored by
ADVANCED RESEARCH PROJECTS AGENCY
ARPA Order No. 2633

INTRODUCTION

This final report on global weather modeling with vector spherical harmonics supported by the Air Force Office of Scientific Research Contract No.F44620-74-C-0036 under ARPA order 2633 describes a third dimensional spectral model based on the use of vector spherical harmonics and scalar spherical harmonics in the horizontal and Legendre Polynomials in the vertical direction. Thus at each time step no spatial derivatives but only time-derivatives need to be computed. The vector spherical harmonics have two distinct advantages: no horizontal derivatives appear at any point of the formulation and the functions have a clearly defined direction at the poles. The model implemented is what corresponds to and eight layer version of Gates'Mintz-Arakawa model. The first chapter is a review of the mathematics which has been an attempt at a formulation which is new in the sence that it tries to make the presentation as simple as possible by not starting with the usual group theoretical approach. The chapter on the program design has been included for completeness, although it was not supported by this contract but thru several IRAD (Independent Research and Development) tasks by IBM. This includes both design and implementation of the general program system. The programming done under the contract has been for specific interface programs to enable us to make computer runs with real data.

ACKNOWLEDGEMENTS

We are indebted to a great number of people for advice, constructive criticism and support. Foremost we have to thank Dr. F. Shuman, Director of the National Meteorological Center for very generously supplying us with data-tapes, input and output programs and access to the computer and his continuing advise throughout the various phases of the work. We also want to thank Drs. N. Phillips, J. Brown, J. Sela, J. Stackpole of N.M.C., Dr. J. Smagorimsky for invitations to give two seminars at the geophysical Fluid Dynamics Laboratory. Princeton, N.J. and Drs. A. Gordon and K. Miyakoda of G.F.D.L. for useful discussions. Dr. C. Leith of the National Center for Atmospheric Research for invitations to give three seminars at NCAR and for an invitation to one of us (S.B.) to spend some time there as a guest researcher. We also want to thank Drs. A. Kasahara and W. Washington of NCAR for advice. Dr. J. Perry of ARPA for support. Drs. A. Wiin - Nielsen, L. Bengtsson, T. Laevastu, Prof. G. Haltiner, Dr. L. Gates and Prof. Y. Mintz for advice. P. Chase and J. McDonnell for help and advice in giving the facilities of N.M.C. Finally we want to thank Drs. H. Mills, H. Kolsky and J. Cooley of IBM for their continuous support, encouragement and advice.

MATHEMATICAL BACKGROUND

Since the mathematical formulation used in this paper is not commonly used in meteorology, it is useful to include a discussion of the mathematical tools used.

There are several reasons why it is natural to express scalar fields such as pressure, temperature and so on in spherical coordinates in terms of spherical harmonics. The most compelling reasons are group theoretical and we will not discuss them here. The spherical harmonics $Y_{\ell}^{m}(\theta,\varphi)$ form a complete orthonormal set of functions in the co-latitude θ and longitude φ. This means that any scalar function, i.e., one where one number is associated with the physical variable at each point in space, can be expressed as a series in terms of the spherical harmonics. Consider, for example, the pressure p to be a function of θ and φ. Then one can write

$$p(\theta,\varphi) = \sum_{m,\ell} p_{\ell}^{m} Y_{\ell}^{m}(\theta,\varphi) \tag{1}$$

where p_{ℓ}^{m} are constant coefficients, not to be confused with the Legendre functions introduced later.

The functions $Y_{\ell}^{m}(\theta,\varphi)$ are defined in the following way:

$$Y_{\ell}^{m}(\theta,\varphi) = (-1)^{m} \left[\frac{2\ell+1}{4\pi} \frac{(\ell-m)!}{(\ell+m)!}\right]^{\frac{1}{2}} P_{\ell}^{m}(\cos\theta) e^{im\varphi} \tag{2}$$

It should be pointed out that the spherical harmonics and the Legendre functions are defined in slightly different ways in different papers and that it is important to adhere to the definitions used here for the subsequent equations to be correct.

ℓ takes on integral positive values or zero.

$\ell = 0, 1, 2, \cdots$. For a given value of ℓ, m can have $2\ell + 1$ values $0, \pm 1, \pm 2, \cdots \pm \ell$.

$P_\ell^m (\cos \theta)$ is an associated Legendre function and has the form

$$P_\ell^m (\cos \theta) \equiv \sin^m \theta \frac{d^m}{d(\cos \theta)^m} [P_\ell (\cos \theta)] \tag{3}$$

Where $P_\ell (\cos \theta)$ is a Legendre Polynomial defined by

$$P_\ell (\cos \theta) \equiv \frac{1}{2^\ell \ell!} \frac{d^\ell}{d(\cos \theta)^\ell} [\cos^2 \theta - 1]^\ell \tag{4}$$

The first few Legendre Polynomials are

$P_0 (\cos \theta) = 1$ $\quad$ $P_1 (\cos \theta) = \cos \theta$ $\quad$ $P_2 (\cos \theta) = \dfrac{3 \cos^2 \theta - 1}{2}$

$P_3 (\cos \theta) = \dfrac{5 \cos^3 \theta - 3 \cos \theta}{2}$

The first few associated Legendre functions are:

$$P_1^1(\cos\theta) = \sin\theta\,, \quad P_2^1(\cos\theta) = 3\cos\theta\sin\theta$$

$$P_2^2(\cos\theta) = 3\sin^2\theta\,, \quad P_3^1 = \frac{3}{2}\sin\theta\,(5\cos^2\theta - 1)$$

$$P_3^2(\cos\theta) = 15\sin^2\theta\cos\theta\,, \quad P_3^3 = 15\sin^3\theta$$

$$P_\ell^0 = P_\ell$$

The spherical harmonics $Y_\ell^m(\theta,\varphi)$ satisfy the following orthogonality conditions.

$$\int_0^{2\pi}\int_0^{\pi} Y_\ell^{m*}(\theta,\varphi)\, Y_{\ell^1}^{m^1}(\theta,\varphi)\sin\theta\, d\theta\, d\varphi = \delta_{m\,m^1}\,\delta_{\ell\,\ell^1}\,.$$

The symbol $\delta_{m\,m^1}$ is a Kronicker delta and is equal to zero if $m \neq m^1$ and equal to one if $m = m^1$.

The functions $Y_{\ell}^{m}(\theta,\varphi)$ can then be formed from the examples above by the use of equation (2). The spherical harmonics satisfy the equation

$$\nabla^2 Y_{\ell}^{m}(\theta,\varphi) = \frac{-\ell(\ell+1)}{r^2} Y_{\ell}^{m}(\theta,\varphi) \tag{5}$$

If a scalar field is a function of the three spherical coordinates r, θ, φ, and of time it can be expanded in the following form

$$p(r,\theta,\varphi,t) = \sum_{m,\ell} p_{\ell}^{m}(r,t)\; Y_{\ell}^{m}(\theta,\varphi) \tag{6}$$

Now the expansion coefficients are functions of r and t.

The gradient of the pressure is a vector field so it is appropriate to look for a representation of a vector field in terms of functions of θ and φ which are the logical counterparts of the scalar spherical harmonics $Y_{\ell}^{m}(\theta,\varphi)$.

Let us form the gradient of a typical term in the expansion for the pressure. We will for the time being omit the time dependence which has no influence on the contents of the next few pages. Consider a term of the form

The functions $Y_{\ell}^{m}(\theta,\varphi)$ can then be formed from the examples above by the use of equation (2). The spherical harmonics satisfy the equation

$$\nabla^2 Y_{\ell}^{m}(\theta,\varphi) = \frac{-\ell(\ell+1)}{r^2} Y_{\ell}^{m}(\theta,\varphi) \tag{5}$$

If a scalar field is a function of the three spherical coordinates r, θ, φ, and of time it can be expanded in the following form

$$p(r,\theta,\varphi,t) = \sum_{m,\ell} p_{\ell}^{m}(r,t)\; Y_{\ell}^{m}(\theta,\varphi) \tag{6}$$

Now the expansion coefficients are functions of r and t.

The gradient of the pressure is a vector field so it is appropriate to look for a representation of a vector field in terms of functions of θ and φ which are the logical counterparts of the scalar spherical harmonics $Y_{\ell}^{m}(\theta,\varphi)$.

Let us form the gradient of a typical term in the expansion for the pressure. We will for the time being omit the time dependence which has no influence on the contents of the next few pages. Consider a term of the form

$f(r)\ Y_{\ell}^{m}(\theta,\varphi)$

The gradient in spherical coordinates is formed by applying the operator

$$\nabla = \hat{e}_r \frac{\partial}{\partial r} + \frac{\hat{e}_\theta}{r} \frac{\partial}{\partial \theta} + \frac{\hat{e}_\varphi}{r \sin\theta} \frac{\partial}{\partial \varphi} \tag{7}$$

Where $\hat{e}_r$, $\hat{e}_\theta$, and $\hat{e}_\varphi$ are an orthogonal set of unit vectors pointing in the direction of increasing r , θ , and φ .

First, consider only the term $Y_{\ell}^{m}(\theta,\varphi)$

$$\nabla Y_{\ell}^{m}(\theta,\varphi) = \frac{1}{r} \left[\hat{e}_\theta \frac{\partial Y_{\ell}^{m}}{\partial \theta} + \hat{e}_\varphi \frac{1}{\sin\theta} \frac{\partial Y_{\ell}^{m}}{\partial \varphi} \right] \tag{8}$$

The result is a vector field that has θ and φ components, i.e., which is tangential to the surface of a sphere. We can then use this as a part of a general vector field. Let us define a field $B_{L}^{M}(\theta,\varphi)$ by

$$B_{L}^{M}(\theta,\varphi) \equiv \frac{r}{\sqrt{L(L+1)}} \nabla Y_{L}^{M} = \frac{1}{\sqrt{L(L+1)}} \left[\hat{e}_\theta \frac{\partial Y_{L}^{M}}{\partial \theta} + \hat{e}_\varphi \frac{1}{\sin\theta} \frac{\partial Y_{L}^{M}}{\partial \varphi} \right] \tag{9}$$

The reason for the factor $\frac{1}{\sqrt{L(L+1)}}$ will be discussed later.

We will use the notation

$$\gamma_L \equiv \sqrt{L(L+1)} \tag{10}$$

$B_L^M(\theta,\varphi)$ will now be one of our basic fields. One can see from equations (2), (3) and (9) that if $M = 0$, $B_L^0(\theta,\varphi)$ is only a function θ and only has a component in the θ direction. $B_L^0(\theta)$ thus has the same value on any point on a longitude circle and everywhere points in a direction parallel to the lines of constant longitude.

Now consider the gradient of $f(r)\, Y_L^M(\theta,\varphi)$

$$\nabla f(r)\, Y_L^M(\theta,\varphi) = \hat{e}_r \frac{df(r)}{dr} Y_L^M(\theta,\varphi) + f(r)\, \nabla Y_L^M(\theta,\varphi)$$

$$= \frac{df(r)}{dr} \hat{e}_r Y_L^M(\theta,\varphi) + \frac{\gamma_L}{r} f(r)\, B_L^M(\theta,\varphi) \tag{11}$$

We will now define another vector field $A_L^M(\theta,\varphi) \equiv \hat{e}_r Y_L^M(\theta,\varphi)$ (12)

$A_L^M(\theta,\varphi)$ is a vector field which points in the radial direction. We can then rewrite (12) in the form

$$\nabla f(r)\, Y_L^M(\theta,\varphi) = \frac{df(r)}{dr} A_L^M(\theta,\varphi) + \frac{\gamma_L}{r} f(r)\, B_L^M(\theta,\varphi) \tag{13}$$

$A_L^M(\theta,\varphi)$ and $B_L^M(\theta,\varphi)$ are not sufficient to form the basis for the representation of a general vector field which is a function of θ and φ, simply because vector fields are not all expressible as gradients of

scalars. This can also be seen by looking at the special case A_L^0 and B_L^0. As we have seen, A_L^0 points in the radial direction and B_L^0 points in the north south direction, so in general, we in addition need an east-west component.

This leads us to look for an additional field which is perpendicular to both A_L^M and B_L^M. The vector product of two vectors is perpendicular to each. A_L^M is proportional to $\hat{e}_r$ so let us define a new vector field $C_L^M(\theta,\varphi)$ by

$$C_L^M(\theta,\varphi) \equiv -i\,\hat{e}_r \times B_L^M(\theta,\varphi) \tag{14}$$

(The reason for the factor i will become apparent later.) Now,

$$C_L^M(\theta,\varphi) = -i\,\frac{\hat{e}_r}{Y_L} \times \left[\hat{e}_\theta \frac{\partial Y_L^M}{\partial \theta} + \hat{e}_\varphi \frac{1}{\sin\theta} \frac{\partial Y_L^M}{\partial \theta}\right] \tag{15}$$

$$\hat{e}_r \times \hat{e}_\theta = \hat{e}_\varphi \qquad \hat{e}_r \times \hat{e}_\varphi = -\hat{e}_\theta \tag{16}$$

Thus

$$C_L^M(\theta,\varphi) = \frac{-i}{Y_L}\left[\hat{e}_\varphi \frac{\partial Y_L^M}{\partial \theta} - \hat{e}_\theta \frac{1}{\sin\theta} \frac{\partial Y_I^M}{\partial \varphi}\right] \tag{17}$$

We see that C_L^0 only has a φ component. We will show later that the set of $A_L^M(\theta,\varphi)$, $B_L^M(\theta,\varphi)$ and $C_L^M(\theta,\varphi)$ form a complete orthonormal set of vector functions in θ and φ and consequently any mathematically well-behaved vector field which is a function of the independent variables θ and φ can be expressed as a series of these functions. As an example, take the velocity field $\overline{V}$ of a fluid. Let $\overline{V}$ be a function of the spherical coordinates r , θ and φ and of time t . Then $\overline{V}(r,\theta,\varphi,t)$ can be expressed as

$$\overline{V}(r,\theta,\varphi,t) = \sum_{M,L} a_L^M(r,t)\, A_L^M(\theta,\varphi) + \sum_{M,L} b_L^M(r,t)\, B_L^M(\theta,\varphi) + \sum_{M,L} c_L^M(r,t)\, C_L^M(\theta,\varphi) \qquad (18)$$

Now that we have found a representation that can be related in a simple and logical way to the gradient of a scalar field, we must test its utility.

In order to do this we will examine the curl and divergence operations in terms of our representation. Since the curl of a vector field is itself a vector field, the result of the curl operation should be in terms of the A_L^M , B_L^M and C_L^M functions. Since the divergence of a vector field is a scalar field, the divergence of A_L^M , B_L^M and C_L^M should be in terms of scalar spherical harmonics Y_L^M . It is not clear at this point how

simple the results will be in comparison with the conventional way of doing these operations in spherical coordinates where all the derivatives with respect to the independent variables occur. In addition, the conventional formulation contains numerous trigonometric expressions.

We begin with the divergence.

Consider $\quad f(r)\, A_L^M(\theta,\varphi) = f(r)\, \hat{e}_r\, Y_L^M(\theta,\varphi)$

$$\nabla \cdot f(r)\, A_L^M(\theta,\varphi) = \left[\hat{e}_r \frac{\partial}{\partial r} + \frac{\hat{e}_\theta}{r}\frac{\partial}{\partial \theta} + \frac{\hat{e}_\theta}{r \sin\theta}\frac{\partial}{\partial\varphi}\right]\cdot \hat{e}_r\, f(r)\, Y_L^M(\theta,\varphi) \qquad (19)$$

One must note that there is an important difference between Cartesian and spherical coordinates. In Cartesian coordinates the derivatives of the unit vectors $\hat{i}$, $\hat{j}$, $\hat{k}$ are zero. In spherical coordinates the derivatives of $\hat{e}_r$, $\hat{e}_\theta$ and $\hat{e}_\varphi$ are in general not zero since $\hat{e}_r$, $\hat{e}_\rho$ and $\hat{e}_\varphi$ change direction from point to point. It is customary in meteorological work when going to spherical coordinates to write

$$\frac{\partial}{\partial x} = \frac{1}{r \sin\theta}\frac{\partial}{\partial\varphi} \qquad\qquad \frac{\partial}{\partial\varphi} = -\frac{\partial}{r\,\partial\varphi}$$

This is a dangerous practice since it ignores the above-mentioned fact.

We will here list the derivatives for future reference:

$$\frac{\partial \hat{e}_r}{\partial r} = 0 \qquad \frac{\partial \hat{e}_r}{\partial \theta} = \hat{e}_\theta \qquad \frac{\partial \hat{e}_r}{\partial \varphi} = \hat{e}_\varphi \sin\theta$$

$$\frac{\partial \hat{e}_\theta}{\partial r} = 0 \qquad \frac{\partial \hat{e}_\theta}{\partial \theta} = -\hat{e}_r \qquad \frac{\partial \hat{e}_\theta}{\partial \varphi} = \hat{e}_\varphi \cos\theta$$

$$\frac{\partial \hat{e}_\varphi}{\partial r} = 0 \qquad \frac{\partial \hat{e}_\varphi}{\partial \theta} = 0 \qquad \frac{\partial \hat{e}_\varphi}{\partial \varphi} = -\hat{e}_r \sin\theta - \hat{e}_\theta \cos\theta$$

Now, returning to $\nabla \cdot f(r)\, A_L^M(\theta,\varphi)$ using the above equations, one has

$$\nabla \cdot f(r)\, A_L^M = \frac{df(r)}{dr} Y_L^M + \frac{f(r)}{r}\left[\hat{e}_\theta \cdot \frac{\partial \hat{e}_r}{\partial \theta} + \hat{e}_\varphi \frac{1}{\sin\theta} \cdot \frac{\partial \hat{e}_r}{\partial \varphi}\right] Y_L^M$$

or

$$\nabla \cdot f(r)\, A_L^M(\theta,\varphi) = D(2)\, f(r)\, Y_L^M(\theta,\varphi) \tag{20}$$

Now consider $f(r)\, B_L^M(\theta,\varphi)$

$$\nabla \cdot f(r)\, B_L^M = \nabla \cdot f(r) \frac{r}{Y_L} \nabla Y_L^M$$

$$= \nabla \cdot \left\{ f(r) \frac{1}{Y_L} \left[\hat{e}_\theta \frac{\partial Y_L^M}{\partial \theta} + \hat{e}_\varphi \frac{1}{\sin\theta} \frac{\partial Y_L^M}{\partial \varphi}\right]\right\} \tag{21}$$

If we break the operator ∇ into two parts

$$\nabla = \hat{e}_r \frac{\partial}{\partial r} + \frac{1}{r}\left[\hat{e}_\theta \frac{\partial}{\partial \theta} + \frac{\hat{e}_\varphi}{\sin\theta}\frac{\partial}{\partial \varphi}\right] = \nabla_1 + \nabla_2 \tag{22}$$

where

$$\nabla_1 = \hat{e}_r \frac{\partial}{\partial r} \quad \text{and} \quad \nabla_2 = \frac{1}{r}\left[\hat{e}_\theta \frac{\partial}{\partial \theta} + \frac{\hat{e}_\varphi}{\sin\theta}\frac{\partial}{\partial \varphi}\right] \tag{23}$$

We find $\nabla \cdot \left[f(r)\, B_L^M(\theta,\varphi)\right] = (\nabla_1 f(r)) \cdot B_L^M(\theta,\varphi) + f(r)\nabla_2 \cdot B_L^M(\theta,\varphi)$

We kn that

$$\nabla^2 Y_L^M(\theta,\varphi) = -\frac{\gamma_L^2}{r^2} Y_L^M(\theta,\varphi) = \nabla_2^2\, Y_L^M(\theta,\varphi)$$

Thus $\nabla_2 \cdot B_L^M = \frac{1}{\gamma_L}\nabla_2 \cdot \left[r\nabla_2 Y_L^M\right] = \frac{1}{\gamma_L} r\nabla_2^2 Y_L^M = -\frac{\gamma_L}{r} Y_L^M$

and consequently, since $\nabla_1 f(r) = \hat{e}_r \frac{\partial f}{\partial r}$ and B_L^M are perpendicular we get

$$\nabla \cdot f(r)\, B_L^M(\theta,\varphi) = -\frac{\gamma_L}{r} f(r)\, Y_L^M(\theta,\varphi) \tag{24}$$

Lastly, we want to find $\nabla \cdot f(r)\, C_L^M(\theta,\varphi)$

Since

$$\nabla \cdot (\alpha \overline{A}) = \alpha \nabla \cdot \overline{A} + \overline{A} \cdot \nabla \alpha \tag{25}$$

$$\nabla \cdot (f(r)\, C_L^M) = f(r) \nabla \cdot C_L^M + C_L^M \cdot \nabla f(r)$$

But $\nabla f(r) = \frac{\partial f}{\partial r} \hat{e}_r$ and C_L^M is tangential so $C_L^M \cdot \nabla f(r) = 0$ and $\nabla \cdot (f(r)\, C_L^M) = f(r) \nabla \cdot C_L^M$

Now consider

$$\nabla \cdot C_L^M = -\frac{i}{Y_L} \nabla \cdot (r \hat{e}_r \times \nabla Y_L^M) . \tag{26}$$

Using the identity

$$\nabla \cdot (\overline{A} \times \overline{B}) = \overline{B} \cdot \nabla \times \overline{A} - \overline{A} \cdot \nabla \times \overline{B} \tag{27}$$

we get

$$\nabla \cdot C_L^M = -\frac{i}{Y_L} \left[\left(\nabla Y_L^M\right) \cdot \left(\nabla \times r \hat{e}_r\right) - r \hat{e}_r \cdot \left(\nabla \times \nabla Y_L^M\right) \right] \tag{28}$$

where

$$\nabla \times r \hat{e}_r = \nabla \times \overline{r} = 0 \qquad \text{and} \qquad \nabla \times (\nabla \alpha) = 0$$

thus

$$\nabla \cdot C_L^M = 0 \tag{29}$$

and

$$\nabla \cdot f(r)\, C_L^M(\theta,\varphi) = 0 \tag{30}$$

We collect the results here

$$\nabla \cdot f(r)\, A_L^M(\theta,\varphi) = D(2)\, f(r)\, Y_L^M(\theta,\varphi) \tag{20}$$

$$\nabla \cdot f(r)\, B_L^M(\theta,\varphi) = \frac{-\gamma_L}{r}\, f(r)\, Y_L^M(\theta,\varphi) \tag{24}$$

$$\nabla \cdot f(r)\, C_L^M(\theta,\varphi) = 0 \tag{30}$$

when $$D(L) \equiv \left(\frac{d}{dr} + \frac{L}{r} \right) \tag{31}$$

We have now found the divergence expressions and they do indeed meet the criteria of simplicity. They also show the logical interrelationship between Y_L^M on one hand and A_L^M B_L^M and C_L^M on the other.

We have found two very important results. The gradient on a scalar field expressed in terms of scalar spherical harmonics Y_L^M gives vector spherical harmonics A_L^M and B_L^M and the divergence of the vector A_L^M's spherical harmonics, and B_L^M's give scalar spherical harmonics.

Furthermore, the simplicity of these expressions is striking, since only derivatives with respect to r occur and the angular part of the functions just occur as multiplying factors. No derivatives of the angular part

or trigonometric factors enter anywhere. This makes it very easy to eliminate the angular part from equations.

If we can now show something similar for the curl, we will have established both the connection between the scalar and the vector functions and between the vector functions themselves.

We start with

$$\nabla \times f(r)\, A_L^M(\theta,\varphi)$$

$$\nabla \times f(r)\, A_L^M(\theta,\varphi) = \nabla \times [f(r)\, \hat{e}_r\, Y_L^M]$$

$$\nabla \times (\varphi, \overline{A}) = \nabla\varphi \times \overline{A} + \varphi \nabla \times \overline{A}$$

$$\overline{A} = f(r)\, \hat{e}_r \qquad \varphi = Y_L^M$$

$$\nabla \times (f(r)\, A_L^M) = \nabla Y_L^M \times \hat{e}_r\, f(r) + Y_L^M\, \nabla \times (\hat{e}_r\, f(r))$$

$$\nabla \times (\hat{e}_r\, f(r)) = \nabla f(r) \times \hat{e}_r + f(r)\, \nabla \times \hat{e}_r$$

$$\nabla f(r) = \hat{e}_r \frac{df}{dr} \qquad \nabla \times \hat{e}_r = 0$$

Thus

$$\nabla \times f(r)\, A_L^M = -f(r)\,\hat{e}_r \times \nabla Y_L^M = i f(r) \frac{\gamma_L}{r}\, C_L^M(\theta,\varphi) \tag{31}$$

Now we derive curl of $f(r)\ B_L^M$

$$\nabla \times f(r)\ B_L^M(\theta,\varphi) = \nabla \times [f(r) \frac{r}{\gamma_L} \nabla Y_L^M]$$

$$= \frac{1}{\gamma_L} [\nabla (r f(r)) \times \nabla Y_L^M + r f(r) \nabla \times (\nabla Y_L^M)]$$

Curl of a gradient is zero

so $\nabla \times (f(r)\ B_L^M) = \frac{1}{\gamma_L} (\nabla (r f(r)) \times Y_L^M$

$$\nabla (r f(r)) = \hat{e}_r \frac{d}{dr}(r f(r)) = \hat{e}_r \left(\frac{df(r)}{dr} + \frac{f(r)}{r}\right) \times \nabla Y_L^M$$

$$C_L^M = -i \frac{\overline{r} \times \nabla Y_L^M}{\gamma_L}$$

Thus

$$\nabla \times f(r)\ B_L^M(\theta,\varphi) = i \left(\frac{d}{dr} + \frac{1}{r}\right) f(r)\ C_L^M(\theta,\varphi) \qquad (32)$$

Finally we need $\nabla \times f(r)\ C_L^M$

$$\nabla \times [f(r)\ C_L^M(\theta,\varphi)] = \nabla f(r) \times C_L^M + f(r) \nabla \times C_L^M$$

$$= \hat{e}_r \frac{df}{dr} \times C_L^M + f(r) \nabla \times \left(- \frac{i\ \overline{r} \times \nabla Y_L^M}{\gamma_L}\right)$$

$$\nabla \times (\overline{A} \times \overline{B}) = \overline{A}\, \nabla \cdot \overline{B} - \overline{B}\, \nabla \cdot \overline{A} + (\overline{B} \cdot \nabla)\, \overline{A} - (\overline{A} \cdot \nabla)\, \overline{B}$$

$$\nabla \times \; -i\,(\hat{e}_r \times B_L^M)$$

$$\nabla \times (\hat{e}_r \times B_L^M) = \hat{e}_r\, \nabla \cdot B_L^M - B_L^M\, \nabla \cdot \hat{e}_r + (B_L^M \cdot \nabla)\, \hat{e}_r - (\hat{e}_r \cdot \nabla)\, B_L^M$$

$$\hat{e}_r \cdot \nabla = \frac{\partial}{\partial r} \qquad (\hat{e}_r \cdot \nabla)\, B_L^M = 0$$

$$\nabla \cdot \hat{e}_r = \frac{2}{r} \qquad \nabla \cdot B_L^M = \frac{-\gamma_L Y_L^M}{r}$$

$$(B_L^M \cdot \nabla)\, \hat{e}_r = \frac{1}{r}\left[\hat{e}_\theta \frac{\partial}{\partial \theta} Y_L^M + \hat{e}_\varphi \frac{1}{\sin\theta} \frac{\partial Y_L^M}{\partial \varphi}\right] \cdot \frac{1}{r}\left[\hat{e}_\theta \frac{\partial}{\partial \varphi} + \hat{e}_\varphi \frac{1}{\sin\theta} \frac{\partial}{\partial \varphi}\right]\hat{e}_r$$

$$= \frac{1}{r^2}\left[\frac{\partial Y_L^M}{\partial \theta} \frac{\partial}{\partial \theta} + \frac{1}{\sin^2\theta} \frac{\partial Y_L^M}{\partial \varphi} \frac{\partial}{\partial \varphi}\right]\hat{e}_r = \frac{1}{r^2}\left[\hat{e}_\theta \frac{\partial Y_L^M}{\partial \theta} + \hat{e}_\varphi \frac{1}{\sin\theta} \frac{\partial Y_L^M}{\partial \varphi}\right]$$

$$= \frac{\gamma_L}{r} B_L^M$$

Thus

$$\nabla \times f(r)\, C_L^M(\theta,\varphi) = i\gamma_L \frac{f(r)}{r} A_L^M(\theta,\varphi) + i\left(\left(\frac{d}{dr} + \frac{1}{r}\right) f(r)\, B_L^M(\theta,\varphi)\right) \qquad (33)$$

We have thus derived the gradient divergence and curl expressions. We list them here for reference.

$$\nabla \; f(r)\, Y_L^M(\theta,\varphi) = \frac{d}{dr} f(r)\, A_L^M(\theta,\varphi) + \frac{\gamma_L}{r} f(r)\, B_L^M(\theta,\varphi)$$

$$\nabla \cdot f(r)\, A_L^M(\theta,\varphi) = \left(\frac{d}{dr} + \frac{2}{r}\right) f(r)\, Y_L^M(\theta,\varphi)$$

$$\nabla \cdot f(r)\, B_L^M(\theta,\varphi) = -\frac{\gamma_L}{r} f(r)\, Y_L^M(\theta,\varphi)$$

$$\nabla \cdot f(r)\, C_L^M(\theta,\varphi) = 0$$

$$\nabla \times f(r)\, A_L^M(\theta,\varphi) = -\frac{i\gamma_L}{r} f(r)\, C_L^M(\theta,\varphi)$$

$$\nabla \times f(r)\, B_L^M(\theta,\varphi) = i\left(\frac{d}{dr} + \frac{1}{r}\right) f(r)\, C_L^M(\theta,\varphi)$$

$$\nabla \times f(r)\, C_L^M(\theta,\varphi) = \frac{i\gamma_L}{r} f(r)\, A_L^M(\theta,\varphi) + i\left(\frac{d}{dr} + \frac{1}{r}\right) f(r)\, B_L^M(\theta,\varphi)$$

It is difficult to imagine a simpler set of expressions in spherical coordinates than this. It has been customary to use a set of the form

$$\overline{V} = \sum f_L^M(r,t)\, Y_L^M(\theta,\varphi)\, \hat{e}_\theta + \sum g_L^M(r,t)\, Y_L^M(\theta,\varphi)\, \hat{e}_\varphi \; .$$

The reader is urged to try the above derivations in terms of these functions. Two things happen; it is not possible (at least in our experience) to eliminate derivatives in θ and various trigonometric expressions; the functions do not reproduce the way, for example, the curl expressions above do.

The functions above; A_1^m, B_1^m and C_1^m have the advantage that it is possible to visualize their appearance. They are, however, not what one calls vector spherical harmonics at all but linear combinations of these. So, while they are a convenient way of representing real data and in a very economical way express the characteristic features atmospheric motion, for example C_1^0 represent the zonal motion and C_1^m's ($M \neq 0$) represent Rossby waves, they are not easy to use when one deals with non-linearities. For these it is more convenient to use the actual vector spherical harmonics, the derivation of which from the A_1^m's, B_1^m's and C_1^m's we sketch below.

Introducing the following operators

$$\partial_{-1} = \frac{1}{\sqrt{2}}\left(\frac{\partial}{\partial x} - i\frac{\partial}{\partial y}\right), \quad \partial_0 = \frac{\partial}{\partial z}, \quad \partial_{+1} = -\frac{1}{\sqrt{2}}\left(\frac{\partial}{\partial x} + i\frac{\partial}{\partial y}\right) \tag{34}$$

one can show (1) that

$$\partial_{-1} f(r) Y_L^M = -\left[\frac{(L-M+2)(L-M+1)}{2(2L+3)(2L+1)}\right]^{\frac{1}{2}} Y_{L+1}^{M-1}\left(\frac{d}{dr} - \frac{L}{r}\right) f + \left[\frac{(L-M)(L-M-1)}{2(2L+1)(2L-1)}\right]^{\frac{1}{2}} Y_{L-1}^{M-1}\left(\frac{d}{dr} + \frac{L+1}{r}\right) f$$

$$\partial_0 f(r) Y_L^M = \left[\frac{(L+M+1)(L-M+1)}{(2L+3)(2L+1)}\right]^{\frac{1}{2}} Y_{L+1}^{M}\left(\frac{d}{dr} - \frac{L}{r}\right) f - \left[\frac{(L+M)(L-M)}{(2L+1)(2L-1)}\right]^{\frac{1}{2}} Y_{L-1}^{M}\left(\frac{d}{dr} + \frac{L+1}{r}\right) f$$

$$\partial_{+1} f(r) Y_L^M = \left[\frac{(L-M+2)(L-M+1)}{2(2L+3)(2L+1)}\right]^{\frac{1}{2}} Y_{L+1}^{M+1}\left(\frac{d}{dr} - \frac{L}{r}\right) f - \left[\frac{(L+M+2)(L+M+1)}{2(2L+3)(2L+1)}\right]^{\frac{1}{2}} Y_{L-1}^{M+1}\left(\frac{d}{dr} + \frac{L+1}{r}\right) f$$

if one then introduces the following basis vectors

$$\hat{e}_{-1} = \frac{1}{\sqrt{2}}(\hat{i} - i\hat{j}) \qquad \hat{e}_0 = \hat{k} \qquad \hat{e}_{+1} = -\frac{1}{\sqrt{2}}(\hat{i} + i\hat{j}) \tag{38}$$

the del-operator can be written

$$\nabla = \sum \hat{e}^{*}_{\mu} \partial_{\mu} = \sum (-1)^{\mu} \hat{e}_{-\mu} \partial_{\mu} = \sum (-1)^{\mu} \hat{e}_{\mu} \partial_{-\mu} \tag{39}$$

Remembering that B_l^m is defined as

$$B^M_l = \frac{r\nabla Y^M_L}{\sqrt{L}}$$

and using (39) in conjunction with (35)-(37) one finds after some straight forward but tedious manipulations that B_l^m can be written the the form

$$B_l^m = \left(\frac{L+1}{2L+1}\right)^{\frac{1}{2}} T^M_{LL-1} + \left(\frac{L}{2L+1}\right)^{\frac{1}{2}} T^M_{LL+1} \tag{40}$$

Where

$$T^m_{LL-1} = \left[\frac{(L-M-1)(L-M)}{2L(2L-1)}\right]^{\frac{1}{2}} Y^{M+1}_{L-1}\,\hat{e}_{-1} - \left[\frac{(L-M)(L+M)}{L(2L-1)}\right]^{\frac{1}{2}} Y^{M}_{L-1}\,\hat{e}_{0}$$
$$+ \left[\frac{(L+M-1)(L+M)}{2L(2L-1)}\right]^{\frac{1}{2}} Y^{M-1}_{L-1}\,\hat{e}_{-1} \tag{41}$$

and

$$T^m_{LL+1} = \left[\frac{(L+M+1)(L+M+2)}{2(L+1)(2L+3)}\right]^{\frac{1}{2}} Y^{M+1}_{L+1}\,\hat{e}_{-1} - \left[\frac{(L-M+1)(L+M+1)}{(L+1)(2L+3)}\right]^{\frac{1}{2}} Y^{M}_{L+1}\,\hat{e}_{0}$$
$$+ \left[\frac{(L-M+1)(L-M+2)}{2(L+1)(2L+3)}\right]^{\frac{1}{2}} Y^{M-1}_{L+1}\,\hat{e}_{+1} \tag{42}$$

If one now repeats the above procedure for the expression $\nabla f(r)\, Y_1^m$ in eq. (13) one finds that A_1^m can be written

$$A_1^m = \left(\frac{L}{2L+1}\right)^{1/2} T^M_{LL+1} - \left(\frac{L+1}{2L+1}\right)^{1/2} T^M_{LL-1} \tag{43}$$

Remembering that $\nabla \times f(r)\, A_1^m$ is given by (31) one can by using the curl operator (39) on f(r) times (43) find C_1^m. The result is

$$C_1^m = T_{LL}^m = \left[\frac{(L-M)(L+M+1)}{2L(L+1)}\right]^{1/2} Y_L^{M+1}\, \hat{e}_{-1} + \frac{M}{[L(L+1)]^{1/2}} Y_L^M\, \hat{e}_0 - \left[\frac{(L+M)(L-M+1)}{2L(L+1)}\right]^{1/2} Y_L^{M-1}\, \hat{e}_{+1} \tag{44}$$

We will call T_{LL-1}^m T_{LL}^m and T_{LL+1}^m collectively T_{JL}^m. One can then write

$$T^M_{JL} = \sum_{\mu=-1}^{+1} \langle L\, M-\mu\, 1\, \mu | J\, M \rangle\, Y_L^{M-\mu}\, \hat{e}_\mu \tag{45}$$

when the coefficients $\langle L\, M-\mu\, 1\, \mu | J\, M\rangle$ are defined by equations (41), (42) and (44) T_L^m are what is conventionally called vector spherical harmonics. The coefficients $\langle L\, M-\mu\, 1\, \mu | J\, M\rangle$ are special cases of what is called Clebsh-Gordan coefficients. Recognizing this one can then call upon the very powerful machinery if the three-dimensional rotation group to perform computations. We will here only briefly sketch how one deals with non-linearities. In addition to the equations above one needs two more. Equation (45) can be inverted and written

$$Y_L^{M-\mu} = \sum_{J=L-1}^{L+1} \langle L\, M-\mu\, 1\, \mu | J\, M \rangle\, T^M_{JL} \tag{46}$$

and the product of two spherical harmonics can be written

$$Y_l^m \, Y_{l'}^{m'} = \sum_{L''} \left[\frac{2L''+1}{4\pi(2l+1)(2L''+1)} \right]^{\frac{1}{2}}$$

$$\cdot \langle l\, 0\, l'\, 0 \mid L''\, 0 \rangle \langle l\, m\, l'\, m' \mid L''\, m+m' \rangle \, Y_{L''}^{m+m'} \tag{47}$$

The above equation and the orthonormality condition on the T_{Jl}^{m} namely

$$\int_0^{2\pi}\!\!\int_0^{\pi} T_{JL}^{M*} \cdot T_{J'L'}^{M'} \sin\theta \, d\theta \, d\varphi = \delta_{MM'} \, \delta_{LL'} \, \delta_{JJ'} \tag{48}$$

together with rules for dealing with sums of products of Clebsch-Gordan coefficients form the complete mathematical machinery for applying vector spherical harmonics to meteorology.

Section 3. ON A POSSIBLY NEW MODE OF ATMOSPHERIC WAVE MOTION

In order to show the relative ease with which the vector spherical harmonics can be used to produce analytic results we will do an anlaysis of the conventional way of expressing two-dimensional motion in terms of a non-divergent and an irrotational part. We might mention that we have tried to repeat this analysis using the usual expressions for the differential operations of vector calculus in spherical coordinates but not been able to get any results due to the complexity of the expressions.

One customary way of representing the two-dimensional motion of the atmosphere is to break the velocity field up into two parts

$$\vec{V}_1 = \hat{k} \times \nabla \psi \qquad \vec{V}_2 = \nabla \chi \tag{1,2}$$

$\hat{k}$ is a unit vector in the radial direction or in our rotation $\hat{k} = \hat{e}_r$ ∇ is the two-dimensional del-operator $\vec{V}_1$ and $\vec{V}_2$ are then tangential to the surface of a spherical earth. From the definition $\vec{V}_1$ and $\vec{V}_2$ one finds

$$\nabla \cdot \vec{V}_1 = 0 \qquad \nabla \times \vec{V}_2 = 0 \tag{3,4}$$

We will now look at the problem in three dimensions, and will allow initially a vertical or radial component which we eventually will suppress. Let us then write down to three-dimensional velocity fields, the first one non-divergent and the second one irrotational

$$\vec{V}_1 = \sum_{M,L} a^M_L(r,t)\, A^M_L(\theta,\varphi) + \sum_{M,L} b^M_L(r,t)\, B^M_L(\theta,\varphi) + \sum_{M,L} c^M_L(r,t)\, C^M_L(\theta,\varphi) \tag{5}$$

with $\qquad \nabla \cdot \vec{V}_1 = 0 \qquad (6)$

and

$$\vec{V}_2 = \sum_{M,L} \alpha^M_L(r,t)\, A^M_L(\theta,\varphi) + \sum_{M,L} \beta^M_L(r,t)\, B^M_L(\theta,\varphi) + \sum_{M,L} \gamma^M_L(r,t)\, C^M_L(\theta,\varphi) \tag{7}$$

with $\nabla \times \vec{V}_2 = 0$ (8)

using equ. (20), (24), (30), (31), (32), and (33) from Section 1, namely

$$\nabla \cdot f(r) A^M_L(\theta,\varphi) = \left(\frac{d}{dr} + \frac{2}{r}\right) f(r) Y^M_L(\theta,\varphi) \tag{9}$$

$$\nabla \cdot f(r) B^M_L(\theta,\varphi) = -\frac{\gamma_L}{r} f(r) Y^M_L(\theta,\varphi) \tag{10}$$

$$\nabla \cdot f(r) C^M_L(\theta,\varphi) = 0 \tag{11}$$

and

$$\nabla \times f(r) A^M_L(\theta,\varphi) = -\frac{i\gamma_L}{r} f(r) C^M_L(\theta,\varphi) \tag{12}$$

$$\nabla \times f(r) B^M_L(\theta,\varphi) = i\left(\frac{d}{dr} + \frac{1}{r}\right) f(r) C^M_L(\theta,\varphi) \tag{13}$$

$$\nabla \times f(r) C^M_L(\theta,\varphi) = \frac{i\gamma_L}{r} f(r) A^M_L(\theta,\varphi) + i\left(\frac{d}{dr} + \frac{1}{r}\right) f(r) B^M_L(\theta,\varphi) \tag{14}$$

to form (6) and (8) respectively we have

$$\nabla \cdot \vec{V}_1 = 0 \Rightarrow \left(\frac{d}{dr} + \frac{2}{r}\right) a^M_L = \frac{\gamma_L}{r} b^M_L \tag{15}$$

and

$$\nabla \times \vec{V}_2 = 0 \Rightarrow \Sigma \frac{i\gamma_L}{r} \alpha^M_L C^M_L + \Sigma i\left(\frac{d}{dr} + \frac{1}{r}\right) \beta^M_L C^M_L + \Sigma \frac{i\gamma_L}{r} A^M_L$$

$$+ \Sigma i\left(\frac{d}{dr} + \frac{1}{r}\right) \gamma^M_L B^M_L = 0 \tag{16}$$

The radial part must be zero all by itself or

$$Y^M_L(\theta,\varphi) = 0 \tag{17}$$

Consequently the irrotational part contains no C_1^m. In addition (16) gives:

$$\frac{\gamma_L}{r}\alpha^m_L = \left(\frac{d}{dr} + \frac{1}{r}\right)\beta^m_L \tag{18}$$

First we notice that since C_1^m is defined by

$$C^m_L(\theta,\varphi) = -i\,\frac{\vec{r}\times\nabla Y^m_L(\theta,\varphi)}{\gamma_L}$$

it corresponds to

$$\hat{r}\times\nabla\psi$$

It then follows that the horizontal part in V_1, represented by

$$\sum b^m_L(r,t)\,B^m_L(\theta,\varphi)$$

is not contained in the conventional way of representing the divergence-less part of the velocity.

Now if we want to impose the condition that there is absolutely no vertical motion allowed equ. (15) leads to the conclusion that

$$b_1^m(r,t) = 0$$

Thus this condition eliminates the new field. In addition it imposes on the irrotational part i.e.

$$\sum \beta^m_L(r,t)\,B^m_L(\theta,\varphi)$$

the condition

$$\left(\frac{d}{dr} + \frac{1}{r}\right)\beta^m_L = 0 \tag{20}$$

or that

$$\beta^m_L \propto \frac{1}{r} \tag{21}$$

Now, since in reality there is a small vertical motion let us allow this and see what conclusions can be made about the magnitudes of b_1^m and $^m_1$.

First consider b_1^m, form (15) we have

$$\left(\frac{d}{dr} + \frac{2}{r}\right)a^m_L = \frac{\gamma_L}{r}b^m_L$$

Let us assume that a_1^m is proportional to the distance from the surface of the earth z.

$$a_l^m = k_l^m z \qquad \frac{da_l^m}{dr} = k_l^m \qquad \frac{2a_l^m}{r} = \frac{k_l^m}{r} z$$

Since $r \approx r_e$, the radius of the earth

$$\frac{da_l^m}{dr} \gg \frac{2a_l^m}{r}$$ and we ignore the second term. Thus

$$\frac{da_l^m}{dr} = \frac{\gamma_l}{r} b_l^m \approx \frac{\gamma_l}{r_e} b_l^m \approx k_l^m = \frac{a_l^m}{z}$$

or

$$b_l^m \approx \frac{r_e}{\gamma_l z} a_l^m$$

Now

$$\frac{r_e}{z} \approx 300$$

and

$$\gamma_l = \sqrt{l(l+1)} \approx l$$

Thus b_1^m is one to two orders of magnitude larger than a_1^m. So if the vertical motion represented by a_1^m is of the order of cm/s. b_1^m can be of the order of m/s and does not appear neglible.

On the other hand we have from equation (18)

$$\left(\frac{d}{dr} + \frac{1}{r}\right) \beta_l^m = \frac{\gamma_l}{r} \alpha_l^m$$

A repetition of the previous arguments indicates that β_1^m is an order or two of magnitude smaller than α_1^m.

Thus without having actual numbers for a_1^m and α_1^m it appears safe to conjecture that

$$\alpha_l^m > b_l^m > \beta_l^m$$

Consequently it appears that by using the conventional apprach outlined above one neglects a mode of motion which may in fact not be negligible

Section 3. EXPRESSIONS FOR A_1^m, B_1^m, and C_1^m IN TERMS OF SPHERICAL BASISVECTORS BUT WITHOUT DERIVATIVES

We recall the defintions:

$$A_1^m(\theta,\varphi) = \hat{e}_r \, Y_L^M(\theta,\varphi)$$

$$B_1^m(\theta,\varphi) = \frac{1}{\gamma_L}\left[\hat{e}_\theta \frac{\partial Y_L^M}{\partial\theta} + \hat{e}_\varphi \frac{1}{\sin\theta}\frac{\partial Y_L^M}{\partial\varphi}\right]$$

$$C_1^m(\theta,\varphi) = -\frac{1}{\gamma_L}\left[\hat{e}_\varphi \frac{\partial Y}{\partial\theta} - \hat{e}_\theta \frac{1}{\sin\theta}\frac{\partial Y_L^M}{\partial\varphi}\right]$$

For computational purposes it is desirable express B_1^m and C_1^m without derivatives and without trigonometric expressions. We thus need to express

$\frac{1}{\sin\theta}\frac{\partial Y_L^M}{\partial\varphi}$ and $\frac{\partial Y_L^M}{\partial\theta}$ in such a manner

that they contain no derivatives. From the quantum mechanical theory of angular momentum (1) one has the two operators

$$L_+ = e^{i\varphi}\left(\frac{\partial}{\partial\theta} + i\frac{\cos\theta}{\sin\theta}\frac{\partial}{\partial\varphi}\right)$$

$$L_- = -e^{-i\varphi}\left(\frac{\partial}{\partial\theta} - i\frac{\cos\theta}{\sin\theta}\frac{\partial}{\partial\varphi}\right)$$

These operators when they operate on spherical harmonics give

$$L_+ Y_L^M = [(L-M)(L+M+1)]^{\frac{1}{2}}\, Y_L^{M+1}$$

$$L_- Y_L^M = [(L+M)(L-M+1)]^{\frac{1}{2}}\, Y_L^{M-1}$$

now

$$\frac{\partial}{\partial\theta} = \frac{1}{2}e^{-i\varphi}L_+ - \frac{1}{2}e^{+i\varphi}L_-$$

and thus

$$\frac{\partial Y_L^M}{\partial\theta} = \frac{1}{2}\left\{[(L-M)(L+M+1)]^{\frac{1}{2}}\, Y_L^{M+1} e^{-i\varphi} - [(L+M)(L-M+1)]^{\frac{1}{2}}\, Y_L^{M-1} e^{i\varphi}\right\}$$

On the other hand

$$i\frac{\cos\theta}{\sin\theta}\frac{\partial}{\partial\varphi} = \frac{1}{2}e^{-i\varphi}L_{+} + \frac{1}{2}e^{+i\varphi}L_{-}$$

We have $P_L^m = \cos\theta\, P_{L+1}^m - (L-M+2)\sin\theta\, P_{L+1}^{m-1}$

$$Y_L^M = (-1)^M\left[\frac{2L+1}{4\pi}\frac{(L-M)!}{(L+M)!}\right]^{\frac{1}{2}} P_L^M e^{iM\varphi} = (-1)^M\left[\frac{2L+1}{2L+3}\right]^{\frac{1}{2}}\left[\frac{2L+3}{4\pi}\frac{(L+1-M)!}{(L+1+M)!}\right]^{\frac{1}{2}}\left[\frac{L+M+1}{L-M+1}\right]^{\frac{1}{2}}\cos\theta\, P_{L+1}^M e^{iM\varphi}$$

$$-(L-M+2)\left[\frac{2L+1}{2L+3}\right]^{\frac{1}{2}}\left[\frac{2L+3}{4\pi}\frac{(L+1-(M-1))!}{(L+1+(M-1))!}\right]^{\frac{1}{2}}\frac{1}{[(L-M+1)(L-M+2)]^{\frac{1}{2}}}\sin\theta\, P_{L+1}^{M-1} e^{iM\varphi}$$

or

$$Y_L^M = \left[\frac{2L+1}{2L+3}\right]^{\frac{1}{2}}\left[\frac{(L+M+1)}{(L-M+1)}\right]^{\frac{1}{2}}\cos\theta\, Y_{L+1}^M$$

$$+\left[\frac{2L+1}{2L+3}\right]^{\frac{1}{2}}\left[\frac{(L-M+2)}{(L-M+1)}\right]^{\frac{1}{2}}\sin\theta\, Y_{L+1}^{M-1}e^{i\varphi}$$

Then

$$\frac{1}{\sin\theta}\frac{\partial Y_L^M}{\partial\varphi} = \left[\frac{2L+1}{2L+3}\right]^{\frac{1}{2}}\left\{\left[\frac{(L+M+1)}{(L-M+1)}\right]^{\frac{1}{2}}\frac{\cos\theta}{\sin\theta}\frac{\partial Y_{L+1}^M}{\partial\varphi} + \left[\frac{L-M+2}{(L-M+1)}\right]^{\frac{1}{2}}\frac{\partial}{\partial\varphi}\left(Y_{L+1}^{M-1}e^{i\varphi}\right)\right\}$$

$$\frac{\cos\theta}{\sin\theta}\frac{\partial Y_{L+1}^M}{\partial\varphi} = \left(-\frac{i}{2}e^{-i\varphi}L_{+} - \frac{i}{2}e^{i\varphi}L_{-}\right)Y_{L+1}^M$$

$$= -\frac{i}{2}\left\{[(L-M+1)(L+M+2)]^{\frac{1}{2}}e^{-i\varphi}Y_{L+1}^{M+1} + [(L+M+1)(L-M+2)]^{\frac{1}{2}}e^{i\varphi}Y_{L+1}^{M-1}\right\}$$

so

$$\frac{1}{\sin\theta}\frac{\partial Y_L^M}{\partial\varphi} = \left[\frac{2L+1}{2L+3}\right]^{\frac{1}{2}}\left\{-\frac{i}{2}[(L+M+1)(L+M+2)]^{\frac{1}{2}}e^{-i\varphi}Y_{L+1}^{M+1}\right.$$

$$\left.-\frac{i}{2}(L+M+1)\left[\frac{(L-M+2)}{(L-M+1)}\right]^{\frac{1}{2}}e^{i\varphi}Y_{L+1}^{M-1} + iM\left[\frac{(L-M+2)}{(L-M+1)}\right]^{\frac{1}{2}}Y_{L+1}^{M-1}e^{i\varphi}\right.$$

or $$\frac{1}{\sin\theta}\frac{\partial Y_L^M}{\partial\varphi} = -\frac{i}{2}\left[\frac{2L+1}{2L+3}\right]^{\frac{1}{2}}\Big\{[(L+M+1)(L+M+2)]^{\frac{1}{2}} e^{-i\varphi} Y_{L+1}^{M+1}$$

$$+ [(L-M+1)(L-M+2)]^{\frac{1}{2}} e^{i\varphi} Y_{L+1}^{M-1}\Big\}$$

so finally

$$B_L^M = \frac{1}{\sqrt{L(L+1)}}\Big[\frac{\hat e_\theta}{2}\Big\{[(L-M)(L+M+1)]^{\frac{1}{2}} Y_L^{M+1} e^{-i\varphi} - [(L+M)(L-M+1)]^{\frac{1}{2}} Y_L^{M-1} e^{i\varphi}\Big\}$$

$$- \frac{i\hat e_\varphi}{2}\left[\frac{2L+1}{2L+3}\right]^{\frac{1}{2}}\Big\{[(L+M+1)(L+M+2)]^{\frac{1}{2}} e^{-i\varphi} Y_{L+1}^{M+1} - [(L-M+1)(L-M+2)]^{\frac{1}{2}} e^{i\varphi} Y_{L+1}^{M-1}\Big\}\Big]$$

$$C_L^M = -i\left[-\hat e_\theta (B_L^M)_\theta + \hat e_\varphi (B_L^M)_\varphi\right]$$

For a purely zonal motion one then has terms of the form

$$C_L^0 = -i\hat e_\varphi \frac{1}{2}\left[Y_L^1 e^{-i\varphi} - Y_L^{-1} e^{+i\varphi}\right]$$

one can note that this formulation has no problem with the direction at the pole since Y_1^1 and Y_1^{-1} are zero there. The θ component vanishes since it is proportionate to $\frac{\partial Y_L^0}{\partial\varphi} = 0$

For purely meridional motion one has terms of the form

$$B_L^0 = \frac{1}{2}\hat e_\theta\left[Y_L^1 e^{-i\varphi} - Y_L^{-1} e^{+i\varphi}\right]$$

Section 4. DIRECTION OF THE VECTOR SPHERICAL HARMONICS AT THE POLES

The three sets of vector spherical harmonics can be written:

$$A^M_L(\theta,\varphi) \equiv \hat{e}_r Y^M_L(\theta,\varphi) \tag{1}$$

$$B^M_L(\theta,\varphi) \equiv \frac{r\nabla Y^M_L(\theta,\varphi)}{\gamma_L} \tag{2}$$

$$C^M_L(\theta,\varphi) \equiv -i\frac{\vec{r}\times\nabla Y^M_L(\theta,\varphi)}{\gamma_L} \tag{3}$$

$$\gamma_L = \sqrt{L(L+1)} \tag{4}$$

One can immediately see that the A^m_l have a well defined direction everywhere on the sphere i.e., in the radial direction.

Since the B^m_l's and the C^m_l's are related to each other by

$$C^M_L = -i\,\hat{e}_r \times B^M_L \tag{5}$$

it is clear that M and L being the same for each set, one set is perpendicular to the other. We will thus investigate the behavior of C^m_l at the poles. The behavior of B^m_l's then follow form (5).

C^m_l can be written

$$C^M_L(\theta,\varphi) = \overline{T}^M_{LL}(\theta,\varphi) = \left[\frac{(L-M)(L+M+1)}{2L(L+1)}\right]^{\frac{1}{2}} Y^{M+1}_L \hat{e}_-$$

$$+\frac{M}{[L(L+1)]^{\frac{1}{2}}} Y^M_L \hat{e}_0 - \left[\frac{(L+M)(L-M+1)}{2L(L+1)}\right]^{\frac{1}{2}} Y^{M-1}_L \hat{e}_+$$

The only spherical harmonics which are non-zero at the pole are Y_1^o. Consequently the only C_1^m that can be non-zero at the poles are those which contain Y_1^o, i.e.

$$C_L^1 = \left[\frac{(L-1)(L+2)}{2L(L+1)}\right]^{\frac{1}{2}} Y_L^2 \hat{e}_- + \left[\frac{1}{L(L+1)}\right]^{\frac{1}{2}} Y_L^1 e_0 - \left[\frac{L(L+1)}{2L(L+1)}\right]^{\frac{1}{2}} Y_L^0 \hat{e}_+$$

and

$$C_L^{-1} = \left[\frac{L(L+1)}{2L(L+1)}\right]^{\frac{1}{2}} Y_L^0 \hat{e}_- + \left[\frac{1}{L(L+1)}\right]^{\frac{1}{2}} Y_L^{-1} \hat{e}_0 - \left[\frac{(L-1)(L+2)}{2L(L+1)}\right]^{\frac{1}{2}} Y_L^{-2} \hat{e}_+$$

Since $Y_1^2 = Y_1^1 = 0$ at the pole we only consider the non-vanishing terms, which contain Y_1^o

$$C_L^1(0,0) = -\frac{1}{\sqrt{2}} Y_L^0(0,0)\hat{e}_+ = -\frac{1}{\sqrt{2}}\left[\frac{2L+1}{4\pi}\right]^{\frac{1}{2}} \hat{e}_+$$

$$C_L^{-1}(0,0) = \frac{1}{\sqrt{2}} Y_L^0(0,0)\hat{e}_- = \frac{1}{\sqrt{2}}\left[\frac{2L+1}{4\pi}\right]^{\frac{1}{2}} \hat{e}_-$$

The velocity field can then be written in the form (at the pole)

$$\vec{V} = \sum_{L=1}^{\infty} c_L^1 C_L^1(0,0) + \sum_{L=1}^{\infty} c_L^{-1} C_L^{-1}(0,0)$$

Now, $\vec{V}$ is real

$$\vec{V} = \sum c_L^1 C_L^1 + \sum c_L^{-1} C_L^{-1} = \vec{V}^* = \sum c_L^{1*} C_L^{1*} + \sum c_L^{-1*} C_L^{-1*}$$

We have the following relationship

$$T^{M*}_{JL} = (-1)^{M+L-J+1}\, T^{-M}_{JL}$$

or

$$C^{1*}_{L} = T^{1*}_{LL} = (-1)^{1+L-L+1}\, T^{-1}_{LL} = C^{-1}_{L}$$

and

$$\sum_L C^{1}_{L} C^{1}_{L} + \sum C^{-1}_{L} C^{-1}_{L} = \sum_L C^{1*}_{L} C^{-1}_{L} + \sum C^{-1*}_{L} C^{1}_{L}$$

or

$$C^{1*}_{L} = C^{-1}_{L}$$

Thus

$$\vec{V} = \sum_L C^{1}_{L} C^{1}_{L} + \sum_L C^{1*}_{L} C^{-1}_{L}$$

Write

$$C^{1}_{L} = \alpha_L + i\beta_L$$

Thus

$$\vec{V} = -\left[\sum_L (\alpha_L + i\beta_L)\,\hat{e}_+ + \sum_L (\alpha_L - i\beta_L)\,\hat{e}_-\right]\left[\frac{2L+1}{8\pi}\right]^{\frac{1}{2}}$$

$$\hat{e}_+ = -\frac{1}{\sqrt{2}}(\hat{i} + i\hat{j}) \qquad \hat{e}_- = \frac{1}{\sqrt{2}}(\hat{i} - i\hat{j})$$

$$\vec{V} = \sum_L \left[(\alpha_L + i\beta_L)(\hat{i} + i\hat{j}) + (\alpha_L - i\beta_L)(\hat{i} - i\hat{j})\right]\left[\frac{2L+1}{8\pi}\right]^{\frac{1}{2}}$$

$$= \sum_L (\alpha_L \hat{i} - \beta_L \hat{j})\left[\frac{2L+1}{8\pi}\right]^{\frac{1}{2}}$$

This is the value of the velocity at the north pole. The significance is that it is not necessary to take any particular computational or transformational steps to avoid difficulties at the poles when dealing with the velocity field expressed in terms of vector spherical harmonics.

Section 5. THE MODEL

This section will describe the model currently implemented. It is a global, dry-air, hydrostatic balance set of equations in spherical coordinates, without orography. The independent variables and domains are:

σ, (the radial variable $= \frac{p}{\pi}$)

$$1 \geqslant \sigma \geqslant 0 \longleftrightarrow r_e \leqslant r \leqslant \infty$$

θ, colatitude $\quad 0 \leqslant \theta \leqslant \pi$

φ, longitude $\quad 0 \leqslant \varphi \leqslant 2\pi$

The dependent variables are:

$\bar{V}(\sigma, \theta, \varphi, t)$, the horizontal velocity field

$T(\sigma, \theta, \varphi, t)$, temperature field

$\gamma(\theta, \varphi, t)$, log surface pressure

$\Phi(\sigma, \theta, \varphi, t)$, geopotential

$\dot{\sigma}(\sigma, \theta, \varphi, t)$, $\frac{d\sigma}{dt}$

Other symbols are:

$p(\sigma,\theta,\varphi,t)$, pressure

$\pi(\sigma,\theta,\varphi,t)$, surface pressure

g , acceleration due to gravity (constant)

Ω , earth's angular velocity

R , gas constant

K , ratio of specific heats

$\hat{e}_\sigma$, radial unit vector

$\overline{F}(\sigma,\theta,\varphi,t)$, friction field

$\dot{H}(\sigma,\theta,\varphi,t)$, heat forcing function

c_p , specific heat at constant pressure

$r(\sigma,\theta,\varphi,t)$, distance from earths center

r_e , radius of earth

∇ , $\left(\frac{\hat{e}_\theta}{r_e}\frac{\partial}{\partial\theta} + \frac{\hat{e}_\varphi}{r_e \sin\theta}\frac{\partial}{\partial\varphi}\right)_{\sigma \text{ constant}}$

$\delta_\odot(t)$, latitude of earth-sun line

$\varphi_\odot(t)$, longitude of earth-sun line

k_F , friction constant

$k_H(\sigma)$, heat term constants, one per σ layer.

The equations are:

$$\frac{\partial \bar{V}}{\partial t} = \bar{F} - \left(\frac{\dot{\sigma}}{\sigma}\right)\left(\sigma\frac{\partial \bar{V}}{\partial \sigma}\right) - (\bar{V}\cdot\nabla)\bar{V} - 2\Omega\cos\theta(\hat{e}_\sigma \times \bar{V})$$
$$- \nabla\Phi - R\sigma\left(\frac{T}{\sigma}\right)\nabla\gamma$$

$$\frac{\partial(T/\sigma)}{\partial t} = \frac{\dot{H}}{c_p\sigma} - \bar{V}\cdot\nabla(T/\sigma) + K(T/\sigma)\frac{\partial\gamma}{\partial t} + K(T/\sigma)\bar{V}\cdot\nabla\gamma$$
$$-\left(\frac{\dot{\sigma}}{\sigma}\right)\left[\left(\sigma\frac{\partial(T/\sigma)}{\partial\sigma}\right) + (1-K)(T/\sigma)\right]$$

The quantity in brakets is constrained to be $\leqslant 0$. This is attempting to indirectly enforce

$$\frac{\partial(T/\sigma)}{\partial\sigma} \leqslant -\frac{T}{\sigma^2}(1-K)$$

which avoids convective instability.

$$\frac{\partial\Phi}{\partial\sigma} = -R(T/\sigma)$$

$$\frac{\partial\gamma}{\partial t} = \int_1^0 (\nabla\cdot\bar{V} + \bar{V}\cdot\nabla\gamma)\,d\sigma$$

$$\frac{\partial\dot{\sigma}}{\partial\sigma} = -\frac{\partial\gamma}{\partial t} - \nabla\cdot\bar{V} - \bar{V}\cdot\nabla\gamma$$

$$r = r_e + \Phi/g$$

$$\pi = e^{\gamma}$$

$$p = \sigma\pi$$

$$\bar{F} = \begin{cases} -k_F|\bar{V}|\bar{V} & , \sigma = 1 \\ \bar{0} & , \sigma \neq 1 \end{cases}$$

$$\dot{H} = k_H\left[\sin\delta_\odot\cos\theta + \cos\delta_\odot\sin\theta\cos(\varphi_\odot - \varphi)\right]$$

The required initial conditions are:

$$\bar{v}(\sigma, \theta, \varphi, t_o)$$

$$T(\sigma, \theta, \varphi, t_o)$$

$$\psi(\theta, \varphi, t_o)$$

The boundary conditions are:

$$\Phi(1, \theta, \varphi, t) = 0$$

$$\dot{\sigma}(1, \theta, \varphi, t) = \dot{\sigma}(0, \theta, \varphi, t) = 0$$

$$T(1, \theta, \varphi, t) = T(1, \theta, \varphi, t_o)$$

The terms $\left(\frac{\dot{\sigma}}{\sigma}\right), \left(\frac{T}{\sigma}\right), \left(\sigma\frac{\partial}{\partial\sigma}\right)$ are in parenthesis to highlight the fact that these quantities are computed and used most naturally in the form. See section on radial functions for additional discussion of $\left(T/\sigma\right)$.

Section 6. PROGRAM SYSTEM DESIGN CONSIDERATIONS

INTRODUCTION

A program system has been designed and implemented to support research into the application of Vector Spherical Harmonics (VSH) to global weather models expressed as sets of partial differential equations in spherical coordinates. This section presents considerations affecting the design philosophy and the tools and techniques used in attempting to carry it out.

Because the system is intended as a general framework to support research, it is desirable that it be easy to use and easy to change. A user should be required to specify only the minimum amount of information necessary to define a given run. He should be able to specify both simple and fundamental alternatives - from integration time step through integration algorithm to the set of equations to be solved.

Furthermore, using appropriate conventions, many aspects of code changes become mechanical. This is particularly true of those changes - storage structures, loop control - that distribute over the system as the result of a change in a specific part of the system. These distributed changes, if possible, should be automated to save the user time and eliminate the possibility of error. These considerations imply that the system be highly parameterized. Further, distinction should be made between independent and dependent parameters. Only those parameters that were not computable from other parameters would be independent and require user specification.

The dynamic systems to be investigated generally require large amounts of data and computation. One of the objectives of the program system is to demonstrate VSH advantages in terms of computational efficiency. Thus the system, while being general, must execute efficiently. Also, occasions will arise when efficiencies must be compared against existing

models and implementations. These other implementations are generally written in FORTRAN. In order to allow the most direct comparison of efficiency, and for other reasons, it is desired that the portions of the system applying VSH to solve equations be written in FORTRAN.

This gives rise to a conflict. The high degree of parameterization desired for generality, ease of use and ease of change is not compatible with the efficiently executing streamlined code necessary to best demonstrate efficiency.

The conflict is resolved using the PL/I precompiler extended to FORTRAN. Using the precompiler the system can be highly parameterized. The parameters will be precompiler variables and the parameterization will be resolved at compilation. The precompiler "IF" clause and "INCLUDE" features allow source code segments to be brought in line for compilation by appropriate precompiler variable settings. The precompiler "macro" feature allows "code generators" to be written that produce FORTRAN code as a function of precompiler variables. The precompiler is also used to generate the Job Control Language procedure to execute a given configuration of the system, insuring consistency between data definition statements and executing code.

VSH Functional Flow

The figure on the next page shows the basic functional flow of VSH incorporating transform methods. Consider the boxes to be data resevoirs, or data sets, and the numbered lines to indicate data flow paths and a sequence of algorithms.

Computations are done both in the physical domain, using "physical" variables-velocity, density, etc-arrayed on layered spherical grids and in the spectral domain, using spectral expansion coefficients of the

VSH Flow Diagram

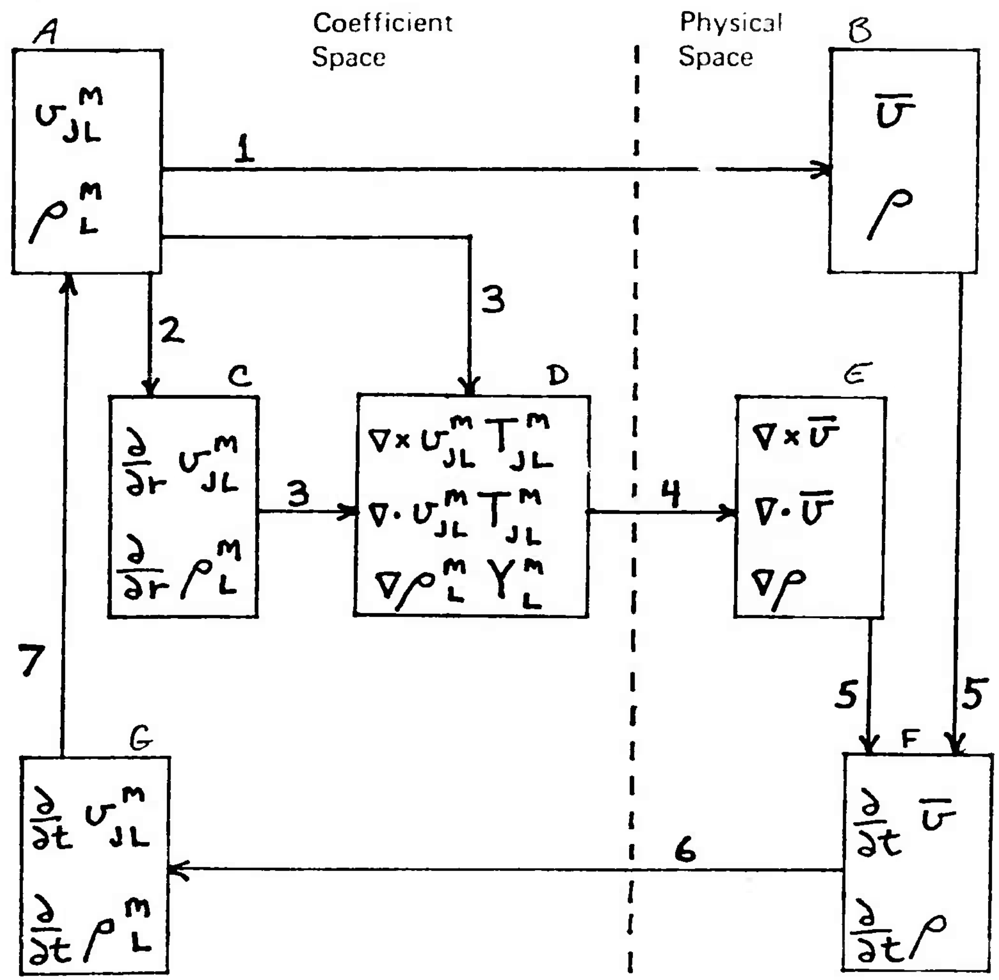

39

physical variables. The data is transformed as appropriate to take advantage of computational and formulational efficiencies in spectral or physical space.

The flow begins and ends with spectral expansion coefficients, represented in box A.

The sequence of functional steps is:

1. Transform coefficients to obtain corresponding values over the physical grid - Function line 1 from box A to box B.

2. Numerically expand each coefficient over all layers into radial derivatives - Function line 2 from box A to box C.

3. Form the appropriate spatial derivatives term by term. - Function lines 3 from boxes A and C to box D.

4. Transform to get values of spatial derivatives over the physical grid. - Function line 4 from box D to box E.

5. Form the model equations and apply boundary conditions. Function lines 5 from boxes B and E to box F.

6. Transform the temporal derivatives to coefficient space. Function line 6 from box F to box G.

7. Integrate to update coefficients. Function line 7 from box G to box A.

Some of the areas subject to change in the course of research include:

1. The model-box F and function lines 5.

2. Various algorithms - obtaining the initial set of coefficients, mechanizing the transformations, integration techniques, etc.

3. The method - the radial fitting functions, the number of terms in the spectral expansions.

All of the possible changes and categories of change cannot be anticipated apriori. In general, the primary change must be implemented by recoding. Therefore, the individual algorithms and the model equations have been isolated.

However, a change that can "analytically" be thought of as isolated often necessitates associated changes distributed throughout the system.

For example, adding curl of curl to modify the friction term in the model requires a coding change along function lines 5. But then the curl of curl must also be formed in spectral space (function line 2 and box C), and curl of curl must be transformed to physical space (function line 4 and box E). The addition of curl of curl in the model is the primary, or independent change and can be made in isolation. The other changes follow from, and are dependent on, the primary change.

As another example, consider changing the number of terms in the spectral expansion for given variables. This can be effected by setting limits of computational loops in the various transforms (lines 1, 4, and 6). But storage areas - both core and direct access - are also affected. Note also that the first example implies changes to various storage area.

In both of these examples the primary change requires action by the person making the change and is visible and manageable. The secondary, dependent changes are often not so visible, and consistency between the primary and secondary changes, which is essentially mechanical, is often difficult to implement. An objective of the program design is to automate where-ever possible these secondary changes, relieving the user/changer of a major burdern and assuring consistency throughout the system.

In short, the functional flow given in Figure 1 is to be implemented to execute efficiently, but in a manner that allows for easy recoding of primary changes and automates the mechanical aspects of a secondary change.

This gives rise to a conflict, as summarized in the figure below. Generality, ease of use and ease of change imply a high degree of parameterization in the system. Execution time efficiency implies minimizing execution time decision and writing streamlined, highly linear code. The implications of the objectives are not, on the face of it, compatible.

Conflict

Generality	
Ease Of Change	Execution Time
Ease Of Use	Efficiency
High Degree Of	No Execution Time
Parameterization	Decisions
	Streamlined Code

Use of a Precompiler

The solution chosen is to pay the price of flexibility at compile time. Each change will involve a recompilation; not only of the routine

containing the change, but of all impacted routines. All control decisions will be resolved and all storage allocations will be established at compile time.

The tools to implement this approach are provided by the PL/I precompiler (or preprocessor) and by a prototype FORTRAN preprocessor developed as an extension of the PL/I preprocessor.[1] The capabilities of the PL/I FORTRAN preprocessor are:

- Program Libraries
- 'Includes'
- Macros
- Preprocessor Variables

To maximize the utility of these tools, all programs are organized into libraries on direct access storage devices. Libraries are maintained for the following program elements:

- Source Code
- Object Modules
- Load Modules
- Job Control Language Procedures
- Linkage Editor Code

1 Developed by Juan Rivero, Wesley Gray, Barry Beals of IBM Federal Systems Division.

Each library is organized as a partitioned data set containing individually accessible elements, called members. For example, an integration algorithm would be a member of the source library, while all of the source members necessary to implement the VSH functional flow are compiled and linked together to produce one member of the load library.

Utility programs have been developed for performing housekeeping in the libraries-editing, deleting, adding selecting members.

The INCLUDE capability is a preprocessor feature that allows source library members to be brought in line at compile time. For example, the statement "INCLUDE INTEG" would be replaced by the source code contained in member INTEG. This code may contain the statement "INCLUDE DERIV" and similar nesting can occur indefinitely.

The Primary advantage of the INCLUDE feature is that the source code can be broken into logical or functional units without unnecessary subroutine linkages.

Macros are PL/I procedures that execute at compile time. Their chief attraction is as code generators. A macro can return FORTRAN code that is functionally dependent on the input argument values. Macros combined with preprocessor variables are the means by which distributed changes are automated.

Preprocessor variables are PL/I variable that are active at compile time. They are of two types, character strings and integers. They are used in preporcessor and non-preporcessor statements. Preprocessor statements (assignment, if then else, do loops) are executed at compile time. Preprocessor variables are used in these statements in the same way that PL/I variables are used in PL/I statements. The Preprocessor IF statement allows selective execution of INCLUDE statements.

Where preprocessor variables appear in non-preprocessor statements (FORTRAN code) they are replaced by their current value.

For example, the dimension of a FORTRAN array may be coded with a preprocessor variable in place of a literal size specification. When the preprocessor encounters this statement the varible will be replaced with its current value. The following figure gives an example of a preprocessor macro that produces FORTRAN code.

MACRO CALL

```
@EQUIVALENCE(V#B#,2,3,$DIMENSIONS, WORK,201)
```

GENERATED CODE

```
 EQUIVALENCE(V1B1(1),WORK(201)),(V1B2(1),WORK(301)),
X (V1B3(1),WORK(401))
 EQUIVALENCE (V2B1(1),WORK(201)),(V2B2(1),WORK(3201)),
X (V2B3(1),WORK(6201))
```

@Equivalence is the macro name. The arguments V#B# and WORK are literals. The remaining four arguments can be literals or preprocessor variables. In actual use they are usually preprocessor variables whose values have been set from some compile time control parameters.

Storage is arranged in blocks according to the function being performed. Naming conventions have been established for the blocks. In this example, V#B# is the "name base" for allocating blocks of storage for vector variables. The second and third arguments in the macro call give the number of vector variables and the number of storage blocks to be allocated to each variable. There are thus two vector variables and each has three blocks. The $DIMENSIONS string has two entries - 100 and 3000. The size of all blocks for vector variable 1 will be 100 words and the size of all blocks for vector variable 2 will be 3000 words.

Allocation and alignment of storage - the number, size, and relative locations of various blocks - can be automated using similar naming conventions for other types of storage blocks. Also, the preprocessor variables that act as parameters to the macro calls can themselves be computed at compile time from some minimal set of independent preprocessor variables. This double level of automation reduces the load on the user/changer and assures consistency.

Section 7. PROGRAM SYSTEM FUNCTIONAL DESCRIPTION

The main function of the program system is to apply Vector Spherical Harmonics (VSH) to global weather modeling. This is done in the PREDICT module. This implies the need for several support functions such as initialization, (the Input module) report generation (the Output and Polar modules) and tabular data construction (the TABLE module).

The weather model currently implemented is a Mintz-Arakawa dry air formulation in sigma coordinates on eight layers. The Richardson two step scheme is used for time integration.

Since the major portion of the computations are done with spectral expansion coefficients, an interface - the Standard Format - has been developed. Initialization data derived from any source must be put into the Standard Format before being passed to the PREDICT module. Similarly, the time history generated by PREDICT is in the Standard Format, which must be converted into desired report format.

The current source of initialization data is the National Meteorotogical Center (NMC) GLOPEP data set. This is "live" global meteorological data updated on a daily basis, and thus it also provides a means of evaluating forecasts produced by PREDICT.

System Components

The program system consists of the following major components:

- **Input**

  Converts data from GLOPEP format to an initial Mintz-Arakawa model state. Also, on option, selects an initializing state, or set of states, from a Standard Format PREDICT time history.

- Predict

  Applies VSH techniques to a Mintz-Arakawa cast of a global weather model to produce predictive estimates of weather behavior.

- Output

  Converts selected samples from a PREDICT time history in Standard Format into GLOPEP format for subsequent mapping and analysis. Prints user selected data in various spectral and physical representations from the PREDICT Standard Format time history.

- Polar

  Produces user selected polar stereographic contour plots of GLOPEP data.

- Table

  Prepares various time invariant data tables used in the VSH protions of PREDICT.

Input

An initial state, or states, must be prepared for PREDICT. There are two possible sources - GLOPEP or a PREDICT time history. The state must contain the following data in spectral expansion coefficient form.

- wind velocity ($\bar{V}$), on all layers
- temperature over sigma ($\overline{T/\sigma}$) on all layers
- natural logarithm of sea surface pressure (ψ)

If the source of the initializing data is a PREDICT time history, the necessary variables are simply selected at, or within a specified tolerance of, the desired time. If the source of the initializing data is a GLOPEP data set, conversions must be made to obtain the variables $\bar{\sigma}$, T/σ and ψ.

This is a three step process:

- o Convert GLOPEP variables to PREDICT variables
- o Convert from GLOPEP radial layers to PREDICT radial layers
- o Convert from physical variables on latitude longitude grids to spectral expansion coefficients.

Applicable GLOPEP data consists of:

U = horizontal component of wind from West to East

V = horizontal component of wind from South to North

T = temperature

Z = pressure height

This data is given in pressure coordinates on concentric spherical grids, equally spaced in latitude (Θ) and longitude (ϕ) at 2.5°. The grids are set at pressure heights of 1000, 850, 700, 500, 400, 300, 250, 200, 150, 100, 70, 50 millibars.

o Conversion to PREDICT variables

GLOPEP velocity is transformed to rectangular coordinates at each GLOPEP (θ, ϕ) point by

$$\begin{bmatrix} x \\ x \\ z \end{bmatrix} = \begin{bmatrix} -\sin\phi & -\cos\phi\cos\theta \\ \cos\phi & -\sin\phi\cos\theta \\ o & \sin\theta \end{bmatrix} \begin{bmatrix} U \\ V \end{bmatrix}$$

GLOPEP temperature is simply copied at this step. It will be divided by sigma after conversion to spectral expansion coefficients.

Sea surface temperature is currently taken to be 1000 mb temperature. It may optionally be taken as GLOPEP surface temperature, but this includes orography, and the current Mintz-Arakawa model is a spherical model.

Sea surface pressure, π, is obtained using the hydrostatic balance condition $\partial p/\partial r = -gp/RT$

where p is pressure, r is radius, g is gravity, T is temperature and R is the universal gas constant.

Since sea surface is very near 1000 mb pressure, one takes the slope of pressure versus r at 1000 mb from the hydrostatic balance condition to use in a point slope form for linear extrapolation from 1000 mb to sea surface pressure

$$\pi - 1000\text{mb} = \left.\frac{-gp}{RT}\right|_{1000\text{mb}} (r_e - r_{1000\text{mb}})$$

where re-r1000mb = Z 1000mb, the first layer GLOPEP pressure height. Adjusting for conversion from GLOPEP to PREDICT units,

$$\pi = \frac{10^8 g Z_{1000\text{mb}}}{RT_{1000\text{mb}}} + 10^8$$

and

$$\psi - e^{\pi}$$

- Conversion to PREDICT radial layers.

  The GLOPEP data are given at the 12 pressure heights listed previously. PREDICT requires data on a number (currently 8) of Gaussian spaced layers corresponding to the number of orthogonal polynomials used in radial expansions. Data for the PREDICT layers are derived from the given data on the GLOPEP layers by:

  - Define a function on the GLOPEP data by fitting straight lines between the GLOPEP data points.

  - Expand this function in orthogonal polynomials.

  - Evaluate this expansion on the PREDICT layers.

- Conversion from physical to spectral representation.

  As detailed elsewhere in this report, spectral expansion coefficients x^m_l for given m, l truncation limits are obtained from physical data $x(\theta,\varphi)$ by

$$X_\ell^m = \int_0^{\pi}\int_0^{2\pi} x(\theta,\varphi)\, Y_\ell^{m\,*}(\theta,\varphi) \sin\theta \, d\varphi \, d\theta$$

Integration over φ is by the trapezoidal rule, while integration over θ is by Simpson's rule with end point correction.

PREDICT

The PREDICT module generates numerical solutions of a global weather model. The current weather model is a Mintz-Arakawa hydrostatic balance, dry air, smooth earth model expressed in sigma coordinates. It is described in greater detail elsewhere in this report.

PREDICT has been built to apply VSH techniques to the solution of weather models. These techniques have been described in general in "Weather Systems Department IRAD Report 1972" and in application to the Mintz-Arakawa model in "Global Weather Modeling with Vector Spherical Harmonics Report No. 2" ARPA order number 2089, program code number G270GE.

Brief descriptions of the PREDICT functional components will be given here, along with a somewhat more detailed exposition of the steps taken to form the Mintz-Arakawa model.

The organization of PREDICT's functional components is shown in the diagram below.

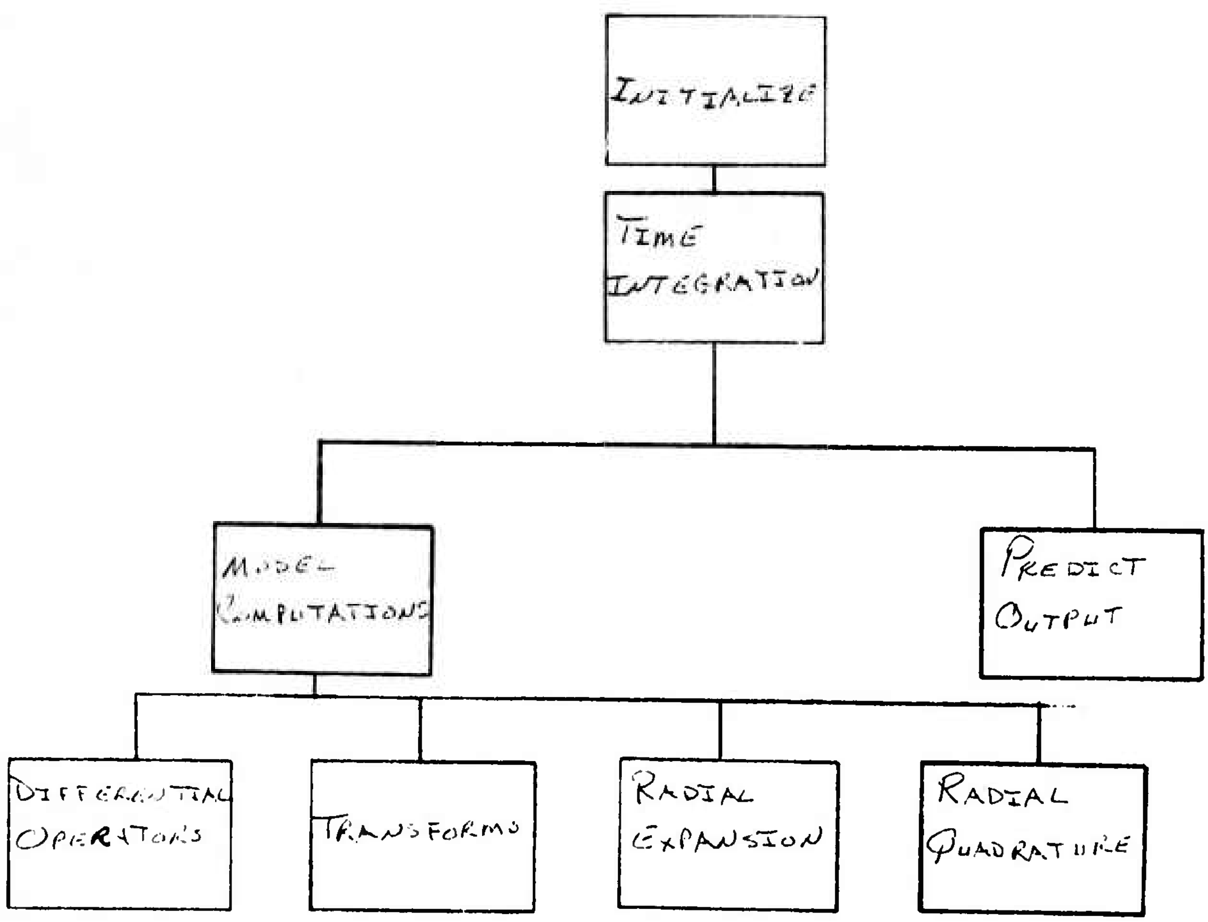

Initialization

The initialization section reads in the initial state, or states, for the model, and various constants and tables and run control data, such as integration time step and time span. Requisite data not supplied as input are, where possible, given default values. After various validity and consistency checks, control is passed to the time integration module.

Time Integration

PREDICT currently uses Richardson's method

$$X_{n+1} = X_{n-1} + 2\Delta t\,\dot{X}_n$$

for time integration. This is a two step method. When only one initial state has been input, a standard fourth order Runge-Kutta integration is used to provide the other starting value. The program is written so that Runge-Kutta can optionally be used as the only integration scheme, but this option has not to date been exercised due to the computational cost of Runge-Kutta.

All time integrations are performed in spectral space. For each time update, the integration section calls the model computation routine to form the temporal differential equations.

Model Computations

The sequence of steps to form the Mintz-Arakawa model is outlined below. This sequence is performed four times for a Runge-Kutta integration step and once for a Richardson integration step.

In spectral space:

- o Do radial truncation on $\tilde{\sigma}$, T/σ. This involves fitting data computed by the previous integration step with the number of polynomials used to represent radial behavior. It is done to avoid aliasing in subsequent computations.

- Set radial component of velocity to zero on all layers, assuming only horizontal velocities.

- Form $\nabla\psi$ on layer 1 and transform to physical space.

On all layers:

- Compute the components of kinetic energy for this layer and sum into total kinetic energy for this time.

- Transform $\bar{v}$ to physical space.

- Compute $\nabla \cdot \bar{v}$ and $(\bar{v} \cdot \nabla)\bar{v}$ and transform to physical space.

- If not layer 1, where (T/σ) is held constant, form $\nabla(T/\sigma)$ and transform it and (T/σ) to physical space.

- Form $\partial\phi/\partial\sigma$ in spectral space.

- Form $\bar{v} \cdot \nabla\psi$ and the integral equation for $\partial\psi/\partial t$ in physical space.

- Transform $\bar{v} \cdot \nabla\psi$ from physical space to spectral space and back to physical space for proper truncation to avoid aliasing when forming the triple product $(T/\sigma)\bar{v} \cdot \nabla\psi$ in the $\partial(T/\sigma)/\partial t$ equation. This is done since the physical grid is sized for simple products.

- Transform the integral for $\partial\psi/\partial t$ to spectral space.

In spectral space:

- Compute ϕ on all layers by radial quadrature.

- Compute $\partial\psi/\partial t$ on layer 1 by radial quadrature and transform to physical space.

- o Form $\partial \dot{\sigma}/\partial \sigma$ on all layers, solve for $\dot{\sigma}/\sigma$ by radial quadrature and transform $\dot{\sigma}/\sigma$ to physical space.

- o Compute $\partial \bar{v}/\partial \sigma$ and $\partial (T/\sigma)/\partial \sigma$ on all layers and transform to physical space.

- o Compute $\nabla \phi$ on all layers and transform to physical space.

In physical space:

- o Form $\partial \bar{v}/\partial t$ on all layers and transform to spectral space.

- o Form $\partial (T/\sigma)/\partial t$ on all layers but the first and transform to spectral space.

In order to perform these computations, the model calls on the Differential Operators, Radial Quadrature and Transforms sections.

Differential Operators

This program section performs vector and scalar differential operations on given variables according to formulae given by VSH. For the Mintz-Arakawa model, only horizontal differential operators are used, so no radial derivatives appear. The various operators-curl, divergence, gradient, advection - are formed as combinations of the numerical constants α_χ, β_χ, 1/r and the spectral expansion coefficients. The exact VSH formulation for these operators is given in "Global Weather Modeling with Vector Spherical Harmonics, Report No. 2" referenced earlier at the beginning of the discussion of the PREDICT module.

In the event of a three dimensional model, radial derivatives of the expansion coefficients would be used in forming the differential operators. These would be supplied by the Radial Expansion section.

Transforms

This section performs the transformations of quantities from spectral expansion coefficients to physical grid representations and vice-versa. For computational efficiency, the model forms equations involving products in physical space, first computing the individual terms in spectral space and then transforming them. The resulting equation is then transformed back to a spectral representation for a subsequent integration or quadrature.

The form for transforming from physical to spectral space is

$$X_l^m = \int_0^{\pi} \int_0^{2\pi} X(\theta, \phi)\, Y_l^{m*}(\theta, \phi) \sin\theta \, d\phi \, d\theta$$

The form for transforming from spectral to physical space is given by the truncated harmonic expansion

$$X(\theta, \phi) = \sum_{m=-(M-1)}^{M-1} \sum_{l=|m|}^{L-1} X_l^m \, Y_l^m(\theta, \phi)$$

The transforms and the exact techniques used are discussed in greater detail elsewhere in this report.

Radial Quadrature

The solution of the Mintz-Arakawa model involves integrations over the radial variable sigma. This is done by Gaussian quadrature on spectral expansion coefficients. The PREDICT radial layers are Gaussian spaced. The initial data prepared in Input is derived radially using the orthogonal polynomial set to be used in PREDICT. This assures that the PREDICT data is exactly representable radially by a polynomial of highest degree consistent with the number of layers in PREDICT.

Radial Expansion

In the Mintz-Arakawa model, the equations for $\partial\bar{\sigma}/\partial t$ and $\partial(T/\sigma)/\partial t$ require the terms $\partial\bar{\sigma}/\partial\sigma$ and $\partial(T/\sigma)/\partial\sigma$. The radial derivatives of $\bar{\sigma}$ and T/σ are computed in spectral space by analytically differentiating the radial function expansions of the variables. This is possible since, as mentioned above, the data are derived to be exactly representable by the orthogonal polynomial set, currently Legendre Polynomials of the first kind, which are differentiable.

Predict Output

At the conclusion of the time step, the Integration section calls the PREDICT OUTPUT section (not to be confused with the OUTPUT program, which is a separate entity). Here various user selected data are printed, and the Standard Format time history data set containing user selected data at user selected intervals is prepared.

Output

The Output module has two main functions:

- Print selected data in selected formats from the Standard Format time history.
- Prepare a GLOPEP data set at a selected time instant from data on the Standard Format time history.

Print

Any data on the time history data set may be printed. Fields may be printed in the following forms an selected layers

Scalar Spectral:	Coefficients of Y_l^m
Vector Spectral	Coefficients of A_l^m, B_l^m, C_l^m T_{jl}^m
Vector Physical:	at (θ,ϕ) grid points in θ,ϕ components R,θ,ϕ components X,Y,Z components
Scalar Physical	at (θ,ϕ) grid points

No capability currently exists in OUTPUT to transform fields from physical to spectral space or vice versa for printing. The only transforms done are from one representation to another in the given space. The Standard Format time history carries fields in the following forms:

Scalar Spectral:	Coefficients of Y_l^m
Vector Spectral:	Coefficients of T_{jl}^m
Vector physical:	X,Y,Z coordinates at (θ,ϕ) grid points
Scalar physical:	at (θ,ϕ) grid points

Glopep

Output can prepare a GLOPEP data set at a selected time. This is done in three steps:

- o Transform PREDICT spectral fields to physical data on GLOPEP θ, φ grid at PREDICT layers.

- o Transform from PREDICT layers to GLOPEP layers.

- o Transform from PREDICT variable to GLOPEP variables.

<u>Spectral to Physical Transformation</u>

Physical data $X(\theta,\varphi)$ is computed from spectral expansion coefficients X_l^m by

$$X(\theta,\varphi) = \sum_{m=-(M-1)}^{M-1} \sum_{l=|m|}^{L-1} X_l^m Y_l^m(\theta,\varphi)$$

<u>Radial Transformation</u>

Obtaining data on GLOPEP layers from data on PREDICT layers involves two steps:

- o Determine the coefficeints of a Legendre Polynomial expansion of the data on the PREDICT layers by Gaussian Quadrature.

- o Evaluate the Legendre Polynomial expansion on the Glopep layers.

<u>Transform to GLOPEP Variables</u>

The GLOPEP data set requires the variables:

U horizontal component of velocity from West to East

V horizontal component of velocity from North to South

Z	Pressure height
T	Temperature
TSURF	Surface Temperature
PTROP	Tropopause Pressure
RH	Relative Humidity

These data are obtained from PREDICT data as follows:

- o Velocity

$$\begin{bmatrix} U \\ V \end{bmatrix} = \begin{bmatrix} -\sin\phi & \cos\phi & 0 \\ -\cos\phi\cos\theta & -\sin\phi\cos\theta & \sin\theta \end{bmatrix} \begin{bmatrix} V_x \\ V_y \\ V_z \end{bmatrix}$$

- o Pressure height

$$Z = \emptyset/g$$

where $\emptyset$ is PREDICT geopotential and g is gravity

- o Temperature is simply set equal to PREDICT temperature that has been carried thru the previous two transformations

- o Surface temperature is set equal to 1000 millibar temperature

- o Tropopause pressure is made to carry PREDICT surface pressure for subsequent mapping via POLAR. Relative humidity is set to zero.

Polar

Polar generates contour maps of selected data from a GLOPEP data set. User controlled parameters allow control of such things as map size,

data scaling, contour interval, hemisphere, layer and variable selection. The program defaults to produce hemispheric polar stereographic projections, but any desired projection may be generated by suitable choice of control parameters.

Table

TABLE generates various time invariant data required by PREDICT. Among these data are:

- α_ℓ, β_ℓ, 1/r sets for use in differntial operators
- Y_1^m and F_1^m sets for use in transforms
- Matrices of Legendre Polynomials with appropriate factors for use in radial expansion and radial guadrature

Section 8. RADIAL FUNCTION CONSIDERATIONS

The first program runs exhibited disappointing reconstructions of initial condition data fields. This was primarily due to poor radial expansions, described here. See also the section on vector/scalar spherical harmonic expansions.

Briefly the situation was:

1. Given data fields, on a 2.5^o latitude, longitude grid on twelve pressure surfaces (1000, 850, 700, 500, 400, 300, 250, 200, 150, 100, 70, 50 mb.). The NMC at Suitland, Md. kindly supplied these data fields.

2. Expand the fields in truncated expansions of Legendre polynomials time vector/scalar spherical harmonics

$$P_k(s)\, Y_\ell^m(\theta, \varphi)$$

or $$P_k(s)\, T_{j\ell}^m(\theta, \varphi)$$

Note that s is a linear mapping of σ (our true radial variable) such that $1+\epsilon \geqslant \sigma \geqslant 0$ is equivalent to $-1 \leqslant s \leqslant 1$ (the interval of orthogonality of Legendre polynomials). The ϵ is because the lowest layer for Gausian quadrature over s is made to correspond to $\sigma = 1$. See Figure 8-1.

σ: 0– .1– .2– .3– .4– .5– .6– .7– .8 .9– 1.0–

NMC Initial Data Layers

σ_{NOM}	p mb	h_{NOM} km
.05	50	20.6
.07	70	18.5
.10	100	16.2
15	150	13.6
.20	200	11.8
.25	250	10.4
.30	300	9.2
.40	400	7.2
.50	500	5.6
.70	700	3.0
.85	850	1.5
1.0	1000	0

Gaussian Computation Layers (5 Layer Case)

σ	S	p_{NOM} mb	h_{NOM} km
.049	.906	49	20.7
.243	.538	243	10.6
.525	0	525	5.2
.807	−.538	807	1.9
1.0	−.906	1000	0

Gaussian Computation Layers (8 Layer Case)

σ	S	p_{NOM} mb	h_{NOM} km
.020	.960	20	26.6
.104	.797	104	15.9
.242	.526	242	10.6
.416	.183	416	6.9
.604	−.183	604	4.2
.778	−.526	778	2.2
.916	−.797	916	0.8
1.0	−.960	1000	0

Figure 8-1. Radial layers.

3. Evaluate the spectral expansions

$$\text{field} = \begin{cases} \sum_{k,m,\ell} c(k,m,\ell) P_k(s) Y_\ell^m(\theta,\varphi) \\ \sum_{k,m,j,\ell} c(k,m,j,\ell) P_k(s) T_{j\ell}^m(\theta,\varphi) \end{cases}$$

at the grid points of the given data fields.

4. Compare given field vs. reconstructed fields.

These first program runs performed radial expansions truncated to four Legendre polynomials (P_0 thru P_3). This requries five Gaussian spaced layers over $-1 \leqslant s \leqslant 1$ to handle product non-linearities without aliasing. In general, expansions in P_k, for k = 0,1, ...K, the minimum number of layers (to avoid aliasing with a product nonlinearity) is

K	Number of Layers
3	5
4	7
5	8
6	10
7	11
8	13
9	14
10	16
11	17

The most isolated major discrepancy in the reconstructed data fields involved temperature. In this case, step 2 above included dividing the given temperature field (T) by σ, then expanding (T/σ). Step 3 included a multiplication by σ to recover the desired field. The problem was

simply that (T/σ) could not be fit well enough (radially) with a reasonable number of polynomials, even though T could be. The sketch in Figure 8-2 illustrates this problem. The solution adopted was to expand the field T instead of (T/σ). In implementing the change it was easiest to form T/σ and use this quantity in the computations even though the ultimate spectral expansion is now of the field T.

The quantity (T/σ) was originally chosen for two reasons.

a. Implicit upper boundary condition on T. - That is for any m,l the Y_ℓ^m coefficient in the expansion of (T/σ) is of the form $\sum_{k=0}^{K} c(k,m,\ell)P_k(s)$. This polynomial, when evaluated at s = 1 (corresponding to $\sigma = 0$, $r = \infty$) will have a possibly large but finite value. Hence T at $\sigma = 0$ must be equal to zero. The current expansion of T removes this boundary condition.

b. Maximum aliasing control. - With expansion of (T/σ) the sources of aliasing error are limited to the forcing functions (friction and heating terms) and the application of the lower boundary condition on temperature. Now the equation of motion is subject to radial aliasing through the term $\nabla\Phi$.

We then studied radial variations for several time samples of NMC initial condition data. This was done by expanding the data (temperature, pressure height, velocity) in spherical harmonics on the NMC pressure surfaces. Examinations of the radial variations of particular harmonic coefficients, with significant magnitudes, revealed three characteristic shapes. These are:

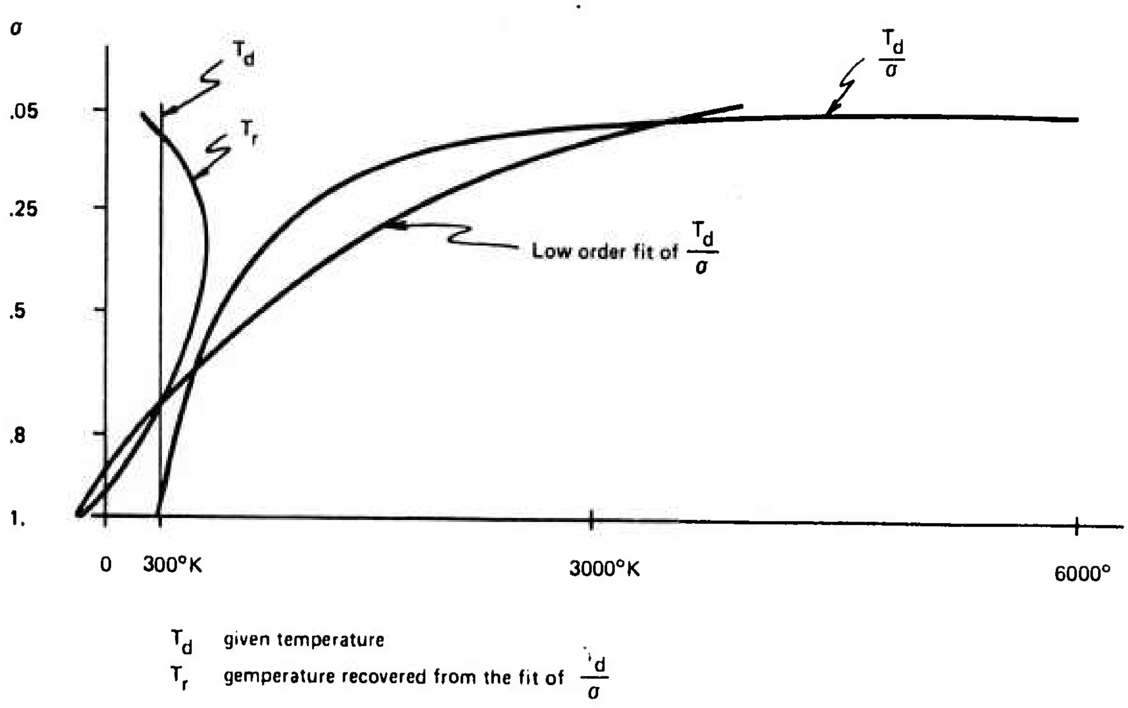

Figure 8-2. Temperature fitting problem.

a. The Y_o^o coefficient of pressure height. Figure 8-3.

b. The Y_o^o coefficient of temperature. Figure 8-4.

c. Most other coefficients, real & imaginary parts. (e.g., the Y_2^o coeficient of pressure height. Figure 8-5.)

The remaining coefficients tended to be either of insignificant amplitude (in which case measurement or computational noise could be the cause of the radial structure variation) or more smooth than (c) above. Because of their dominance, cases (a) & (b) are singled out even though they have less extreme variation over σ then (c). Figures 8-3, 8-4 and 8-5 illustrates typical values of these coefficients and their reconstruction after expanding in $P_k(\varsigma)$, k = 0,1,...K for selected values of K.

Observe, in Figure 8-3, the relatively good expansion with K = 3, of the Y_o^o coefficient of pressure height. But even for moderately large K, the errors are very significant because of the extreme magnitude of this coefficient (compare with the next largest coefficient for this field, Y_2^o, in Figure 8-5). These errors are:

K	Maximum error in Y_o^o	σ at which max error occurs	average error over 12 sample points
3	1.02 km	.10	.47 km
5	.37	.10	.14
7	.25	.05	.07

Now in our model, pressure height (actually geopotential, Φ) reenters the computations only via $\nabla\Phi$ in the equation of motion. It so happens that Y_o^o has no horizontal component, hence our prediction process is not corrupted by this sizable error. The error will ultimately be fixed by expanding (for this coefficient only) the deviation from the nominal, computing this quantity over time, and then adding the

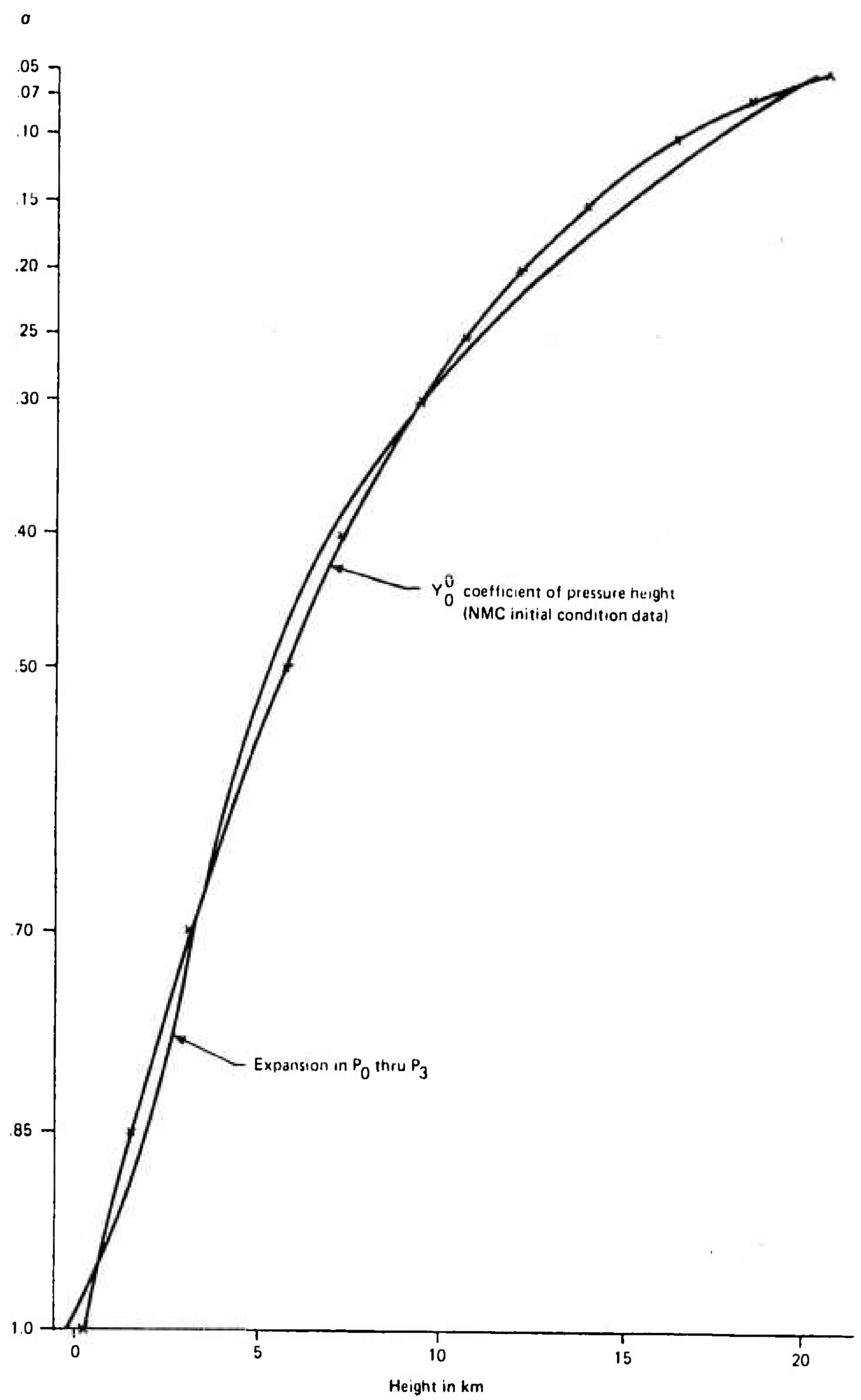

Figure 8-3. Radial structure of Y_0^0 coefficient of pressure height.

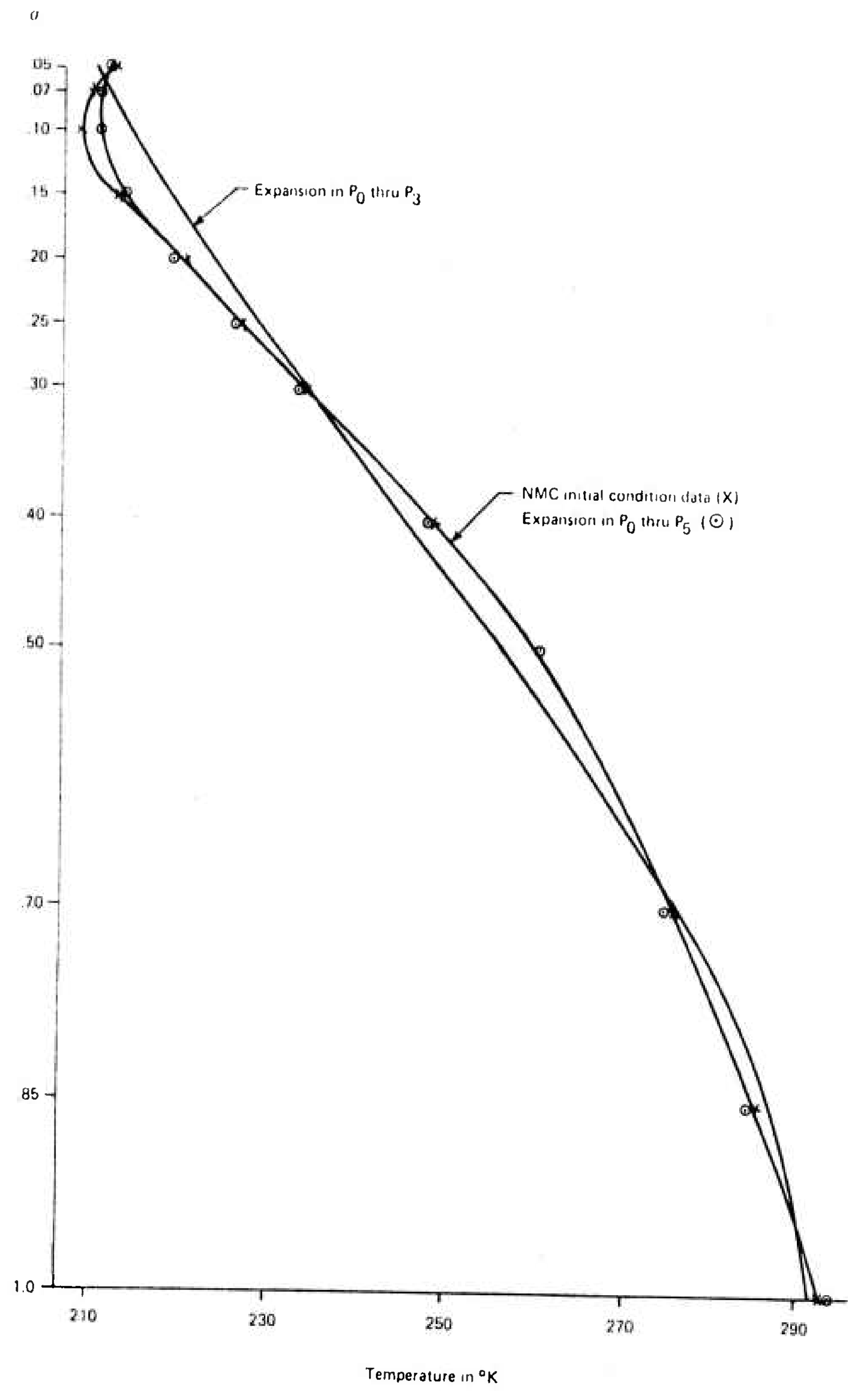

Figure 8-4. Radial structure of Y_0^0 coefficient of temperature.

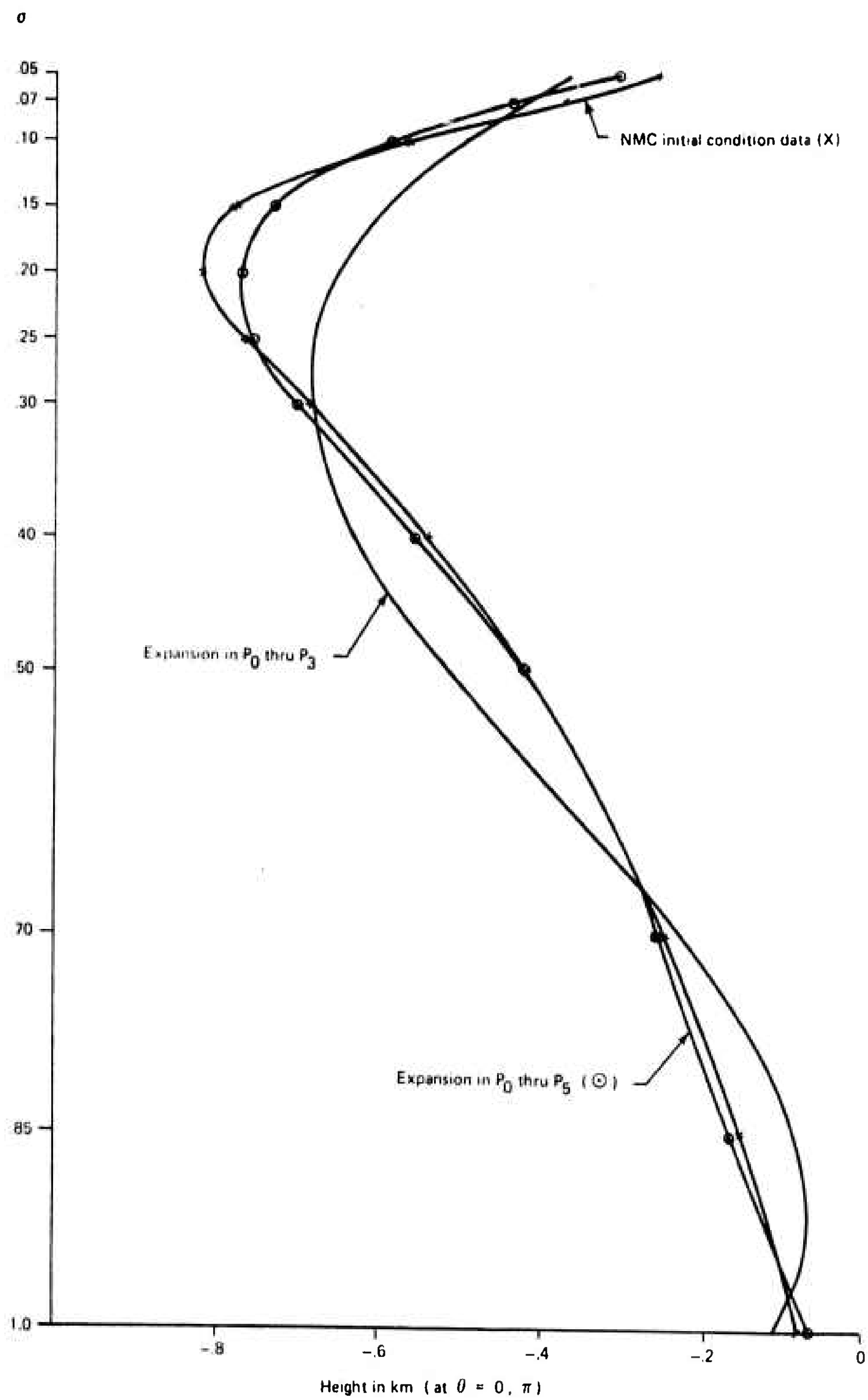

Figure 8-5. Radial structure of Y_2^0 coefficient of pressure height.

deviations to the nominal for output. For the time being our maps of pressure height contain this error which appears as a bias at each output level. Typical values of this bias error (K=5) are:

Pressure Level	(True height - computed height)	
1000 mb	-87	meters
850	3	
700	67	
500	-197	
400	-113	
300	118	
250	186	
200	140	
150	- 64	
100	-374	
70	-365	
50	17	

In Figure 8-4, we see an acceptable fit for K = 3 and a good fit for K = 5, with respect to the Y_o^o coefficient of temperature. The errors are:

K	Maximum error	σ at which max error occurs	average error over 12 points
3	5.42 ^oK	.10	2.48 ^oK
5	2.28 ^oK	.10	.77 ^oK
7	1.02 ^oK	.05	.56 ^oK

Figure 8-5 shows several expansions of the Y_2^0 coefficient of pressure height. The independent axis labels (and errors below) represent the situation at the poles, where Y_2^0 assumes it's greatest value. The error summary for this coefficient,

K	Maximum error	σ at which max error occurs	average error aver 12 points
3	192 m.	.15	83 m.
5	67 m.	.07	26 m.
7	51 m.	.15	20 m.

It is interesting to note that the (K=5) expansion is superior to the (K=7) expansion, for this coefficient, over the lower layers. The errors in meters, by layer are:

σ ↓	K → 3	5	7
1.0	32	9	15
.85	71	9	10
.70	23	4	16
.50	95	3	11
.40	91	16	0
.30	3	21	26
.25	82	5	12
.20	169	46	28
.15	192	56	51
.10	69	18	1
.07	52	67	42
.05	110	53	32

Based on these investigations it appeared reasonable to start our prediction runs using radial expansions up to and including P_5, which requires eight computational layers. Clearly cubic expansions are not adequate, and the improvement of seventh degree expansions seems small compared to the 38% increase of computational effort over the fifth degree expansion (i.e., 8 layers $\rightarrow$ 11 layers).

After making the changes described here, our data, reconstructed after three dimensional expansion, was in much better agreement with the source fields. Except for pressure height bias, we feel that the bulk of any discrepancies is due to fairly low spherical harmonic truncation limits we have used to date.

Section 9. VECTOR/SCALAR SPHERICAL HARMONIC EXPANSIONS

In our spectral method, a scalar field is approximated by a three-dimensional truncated spectral expansion,

$$x(r,\theta,\varphi) \cong \sum_{k=0}^{K} \sum_{m=-M}^{M} \sum_{\ell=|m|}^{L} c(k,\ell,m) P_k(s) Y_\ell^m(\theta,\varphi) \quad ,$$

and a vector field by,

$$\bar{V}(r,\theta,\varphi) \cong \sum_{k=0}^{K} \sum_{m=-M}^{M} \sum_{\ell=|m|}^{L} \sum_{j=\ell-1}^{\ell+1} c(k,j,\ell,m) P_k(s) T_{j\ell}^m(\theta,\varphi) \; .$$

The radial expansions are discussed in another section of this report. Here we will address only the horizontal expansions

$$x(\theta,\varphi) \cong \sum_{m=-M}^{M} \sum_{\ell=|m|}^{L} c(\ell,m) Y_\ell^m(\theta,\varphi) \quad ,$$

$$\bar{V}(\theta,\varphi) \cong \sum_{m=-M}^{M} \sum_{\ell=|m|}^{L} \sum_{j=\ell-1}^{\ell+1} c(j,\ell,m) T_{j\ell}^m(\theta,\varphi) \; .$$

The scalar expansion is the key item, since the vector transformations are handled as follows. Represent the vector field

$$\bar{V}(\theta,\varphi) = V_x(\theta,\varphi)\,\hat{\imath} + V_y(\theta,\varphi)\,\hat{\jmath} + V_z(\theta,\varphi)\,\hat{k} \; .$$

Perform a triple scalar transform on the components

$$V_x(\theta,\varphi) \cong \sum_{m=-M}^{M} \sum_{\ell=|m|}^{L} c_x(m,\ell) Y_\ell^m(\theta,\varphi) \quad , \text{ etc.}$$

These components are then mapped to the T_{jl}^m basis by

$$\hat{\imath} = \frac{1}{\sqrt{2}}(\hat{e}_{-1} - \hat{e}_{+1})$$

$$\hat{\jmath} = \frac{i}{\sqrt{2}}(\hat{e}_{-1} + \hat{e}_{+1})$$

$$\hat{k} = \hat{e}_0$$

The vector spherical harmonic coefficients are then obtained using the relationship

$$T_{j\ell}^m(\theta,\varphi) = \sum_{\mu=-1}^{1} \langle \ell \; m-\mu \; 1 \; \mu | j \; m \rangle \, Y_\ell^{m-\mu}(\theta,\varphi)\, \hat{e}_\mu$$

and its inverse

$$Y_\ell^{m-\mu}(\theta,\varphi)\,\hat{e}_\mu = \sum_{j=\ell-1}^{\ell+1} \langle \ell \; m-\mu \; 1 \; \mu \,|\, j \; m \rangle \, T_{j\ell}^{m}(\theta,\varphi).$$

Now let's examine some of the details of a scalar expansion. The expansion coefficients are found, from the orthonormality of the Y_l^m's by

$$x(\ell,m) = \int_0^{\pi}\int_0^{2\pi} Y_\ell^{m*}(\theta,\varphi)\, x(\theta,\varphi) \sin\theta \, d\varphi \, d\theta$$

where

$$Y_\ell^{m*}(\theta,\varphi) = K_\ell^m \, P_\ell^m(\cos\theta)\, e^{-im\varphi}$$

$$K_\ell^m = (-1)^m \left[\frac{2\ell+1}{4\pi}\,\frac{(\ell-m)!}{(\ell+m)!}\right]^{1/2}$$

This is implemented by integrating

$$h(\theta,m) = \int_0^{2\pi} x(\theta,\varphi)\, e^{-im\varphi}\, d\varphi$$

followed by

$$x(\ell,m) = K_\ell^m \int_0^{\pi} h(\theta,m)\, P_\ell^m(\cos\theta) \sin\theta \, d\theta$$

During the prediction steps, these quadratures are exact since the fields are truncated. The φ integration is trapezoidal and the θ integration is Gaussian. For expanding initial condition data, supplied on a uniform mesh θ/φ grid, we first tried trapezoidal quadrature for both integrations. This resulted in significant errors near the poles. The errors were removed by using Simpsons quadrature with end point correction

for the θ integration. This was easy to do because of the $\sin\theta$ factor. That is, end point correction requires

$$\frac{d}{d\theta}\left[h(\theta,m)\, P_\ell^m(\cos\theta)\sin\theta\right]\Big|_{0,\pi}$$

$$= \left\{\sin\theta\frac{d}{d\theta}\left[h(\theta,m)\, P_\ell^m(\cos\theta)\right] + h(\theta,m)\, P_\ell^m(\cos\theta)\frac{d}{d\theta}\sin\theta\right\}\Big|_{0,\pi}$$

$$= \left[h(\theta,m)\, P_\ell^m(\cos\theta)\cos\theta\right]\Big|_{0,\pi}$$

and no explicit differentiation is required.

In parallel with prediction runs, made with fairly low truncation limits (M=L=9), we studied the effect of horizontal truncation limit variation on a scalar field (1000 mb pressure height).

For a real field, one doesn't need to compute the expansion coefficients with negative m, since

$$c(l,-m) = (-1)^m \; c(l,m)^*$$

and for real vector fields

$$c(j,l,-m) = (-1)^{m+j+l+1} \; c(j,l,m)^*.$$

Hence we can represent our expansion coefficients schematically as the shaded portion of:

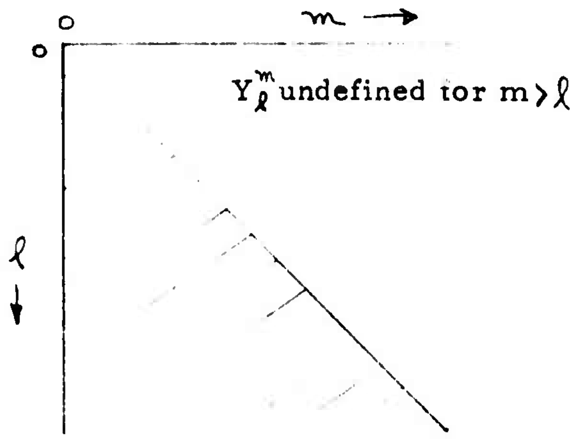

We have chosen to implement a truncation policy that can be called trapezoidal. That is, given M,L ($L \geq M$) we retain the coefficients indicated by,

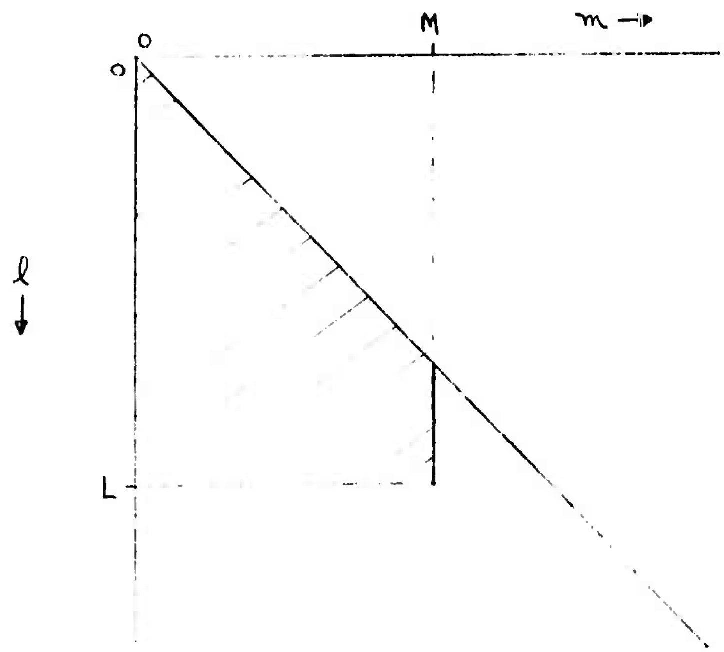

Other spectral modelers seem to prefer a rhombiodal truncation policy, based on two parameters M,J. This truncation is illustrated by

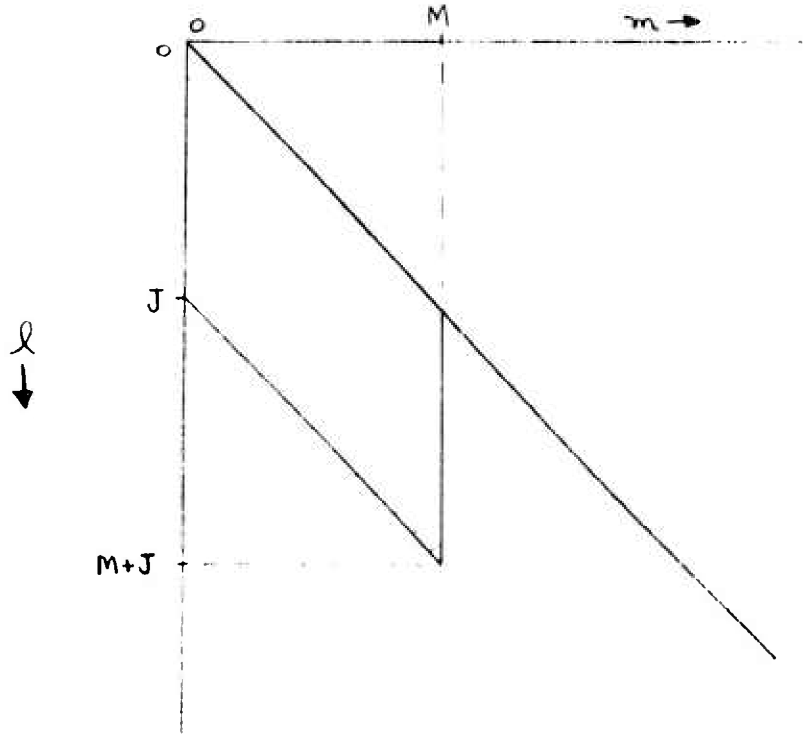

Now let's list some of the factors associated with variations of the truncation parameters of the two truncation policies.

		Trapezoidal	Rhombiodal
a.	Number of coefficients	$(\frac{M+1}{2})(2L-M+2)$	$(M+1)(J+1)$
b.	Minimum number of uniformly spaced φ points required to transform a product non-linearity without aliasing	3M+1	3M+1
c.	Minimum number of Gaussian spaced θ points required to transform a product non-linearity without aliasing	$\frac{3L+1}{2}$	$\frac{3J+2M+1}{2}$

d. Approximate operation count for the Legendre step in a Y_1^m transform, either direction. (Minimum physical grid).	(3L+1)(M+1)(2L-M+1)/4	(J+1)(M+1)(3J+2M+1)/2

The Fourier part of a Y_1^m transform can be implemented in various fashions with both truncation policies. Its operation count could range from one to a small fraction times (d) above.

Let's now look at two ways to define equivalence between the truncation policies, and compare the 'quality' of equivalent truncated expansions of a particular field. This field (1000 mb pressure height, hour 0, 25 July 1974) was used only because it was the field with the most 'structure' on the first data tape we received from the National Meteorological Center.

Because of the similarity of the parameter M, we shall require equivalent truncation limits to have the same value for M. One possible way to relate the parameters L and J would be to produce the same number of coefficients. That is from (a) above,

$$(M+L)(2L-M+2)/2 = (M+1)(J+1)$$

$$\text{or} \quad J_1 = L - \frac{M}{2}$$

Another possiblity is to equate the operation counts given in (d) above, since the spectral $\longleftrightarrow$ physical transformations dominate the computation effort in spectral methods. In this case

$$J_2 = \frac{1}{12}\left[144L^2 + 192L + 16M^2 - 56M - 72LM + 64\right]^{1/2} - \frac{M+2}{3}$$

For $12 \leqslant M \leqslant 20$ and $M < L \leqslant 40$

$$J_2 \cong J_1 - 1 = L - \frac{M}{2} - 1$$

We will split the difference and say that

J = L - (M+1)/2 are equivalent.

One measure of the truncation error can be formed by the sum of the magnitudes squared of the unretained coefficients. This is proportional to the surface integral of the error field squared.

$$\epsilon = \sum_{\substack{l,m \\ \text{unretained}}} |c(\ell,m)|^2 = k \int_0^{\pi}\int_0^{2\pi} (X - X_t)^2 \sin\theta \, d\varphi \, d\theta$$

where X_t is the truncated expansion of X.

Figure 9-1 is 60 meter contour plot of the untruncated 1000 mb pressure height. Note that this plot (and the others in this section) do not quite wrap-around in φ.

Figure 9-2 tabulates the coefficient magnitudes (1 and m up to 25) obtained by expanding the 1000 mb pressure height. These have been multiplied by 10 and rounded to integers. Note that the RSS and RMS figures are with respect to the rows and columns of the triangular array printed except that the M=L=0 term has been excluded. That is, the factor of 10 is included and the implied coefficients (with m negative) have not been included in the RSS, RMS computations.

Figures 9-3 show the reconstructed field (trapezoidal truncation, M=25, L=25). Let's denote its measure of error by

$$\epsilon_{25,25} = \sum_{\ell, |m| > 25} |c(m,\ell)|^2$$

an unknown quantity.

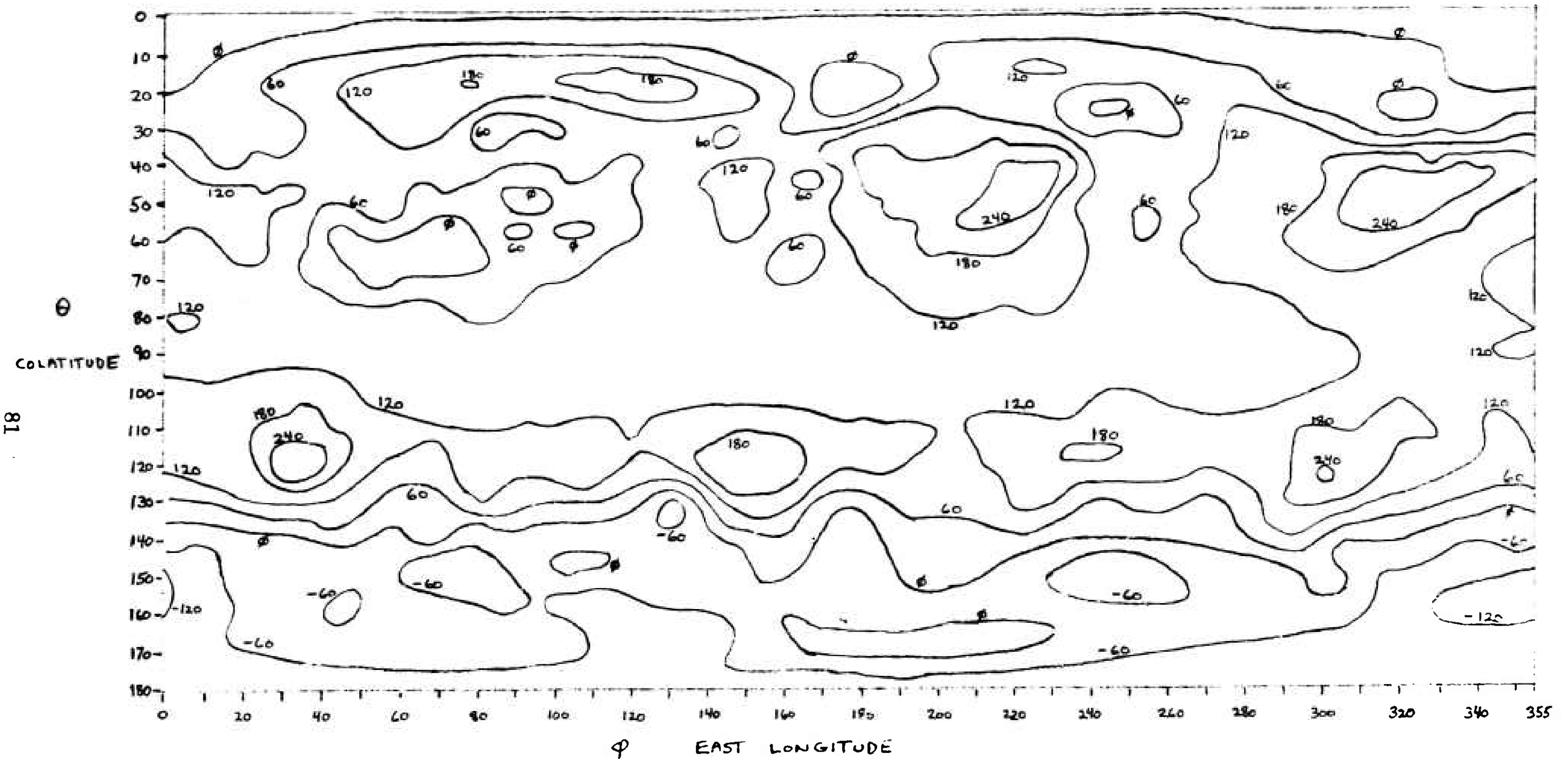

Figure 9-1

Contour Map of Untruncated Test Field
1000 mb pressure height
Hour 0, 25 July 1974
60 meter contour interval

m →

ℓ ↓	0	1	2	3	4	5	6	7	8	9	10	11	12	13	14	15	16	17	18	19	20	21	22	23	24	25	RSS	RMS
0	3243	-	-	-	-	-	-	-	-	-	-	-	-	-	-	-	-	-	-	-	-	-	-	-	-	-		
1	910	467	-	-	-	-	-	-	-	-	-	-	-	-	-	-	-	-	-	-	-	-	-	-	-	-	1023	723
2	1247	275	226	-	-	-	-	-	-	-	-	-	-	-	-	-	-	-	-	-	-	-	-	-	-	-	1297	749
3	767	206	235	50	-	-	-	-	-	-	-	-	-	-	-	-	-	-	-	-	-	-	-	-	-	-	830	415
4	642	253	70	253	212	-	-	-	-	-	-	-	-	-	-	-	-	-	-	-	-	-	-	-	-	-	768	344
5	549	325	47	170	91	89	-	-	-	-	-	-	-	-	-	-	-	-	-	-	-	-	-	-	-	-	674	275
6	409	113	162	66	238	155	54	-	-	-	-	-	-	-	-	-	-	-	-	-	-	-	-	-	-	-	542	205
7	188	123	179	100	91	148	51	19	-	-	-	-	-	-	-	-	-	-	-	-	-	-	-	-	-	-	354	125
8	61	13	121	42	16	112	131	81	16	-	-	-	-	-	-	-	-	-	-	-	-	-	-	-	-	-	239	80
9	268	35	96	65	65	109	52	44	25	25	-	-	-	-	-	-	-	-	-	-	-	-	-	-	-	-	329	104
10	92	62	65	35	76	13	81	64	19	45	22	-	-	-	-	-	-	-	-	-	-	-	-	-	-	-	193	58
11	117	41	27	57	50	93	50	24	66	70	55	12	-	-	-	-	-	-	-	-	-	-	-	-	-	-	214	62
12	72	35	63	30	73	56	58	37	35	25	61	12	24	-	-	-	-	-	-	-	-	-	-	-	-	-	175	49
13	54	67	61	15	20	27	36	15	49	53	66	18	12	6	-	-	-	-	-	-	-	-	-	-	-	-	155	41
14	117	46	55	70	46	79	19	53	33	38	69	38	49	22	10	-	-	-	-	-	-	-	-	-	-	-	217	56
15	9	22	28	33	45	41	4	17	17	31	30	54	22	19	19	6	-	-	-	-	-	-	-	-	-	-	113	28
16	65	21	20	48	54	64	19	11	4	46	41	16	19	27	11	12	5	-	-	-	-	-	-	-	-	-	143	35
17	1	15	40	28	36	44	2	32	4	20	24	44	19	12	16	11	10	9	-	-	-	-	-	-	-	-	104	25
18	15	21	19	16	33	39	45	32	15	15	13	31	26	6	9	6	8	3	3	-	-	-	-	-	-	-	97	22
19	20	24	14	39	24	21	24	27	8	14	13	23	25	9	13	12	19	12	4	3	-	-	-	-	-	-	87	19
20	8	7	33	31	9	14	24	11	25	30	23	24	24	22	18	20	11	6	12	9	2	-	-	-	-	-	89	19
21	7	22	6	17	24	45	47	13	4	8	10	24	9	8	21	12	14	12	4	6	4	3	-	-	-	-	88	19
22	16	12	14	8	23	11	14	14	13	14	16	19	10	14	19	18	15	6	9	17	5	4	4	-	-	-	66	14
23	15	10	9	14	18	27	13	4	15	17	26	19	13	24	26	3	12	15	2	11	13	6	3	1	-	-	74	15
24	0	8	8	16	18	17	8	13	7	24	31	4	10	7	3	12	11	2	12	14	5	10	10	4	2	-	62	12
25	8	4	10	26	12	12	14	26	10	16	6	5	22	10	16	14	11	8	12	10	12	7	2	3	4	0	64	13
RSS	2004	743	465	367	386	332	214	150	110	136	150	103	84	58	56	41	38	27	24	29	20	14	11	5	4	0		
RMS	401	149	95	77	82	72	48	34	26	33	37	27	23	16	16	12	12	9	8	11	8	6	6	3	3	0		

Figure 9-2

Magnitudes of Test Field Expansion Coefficients (x10)

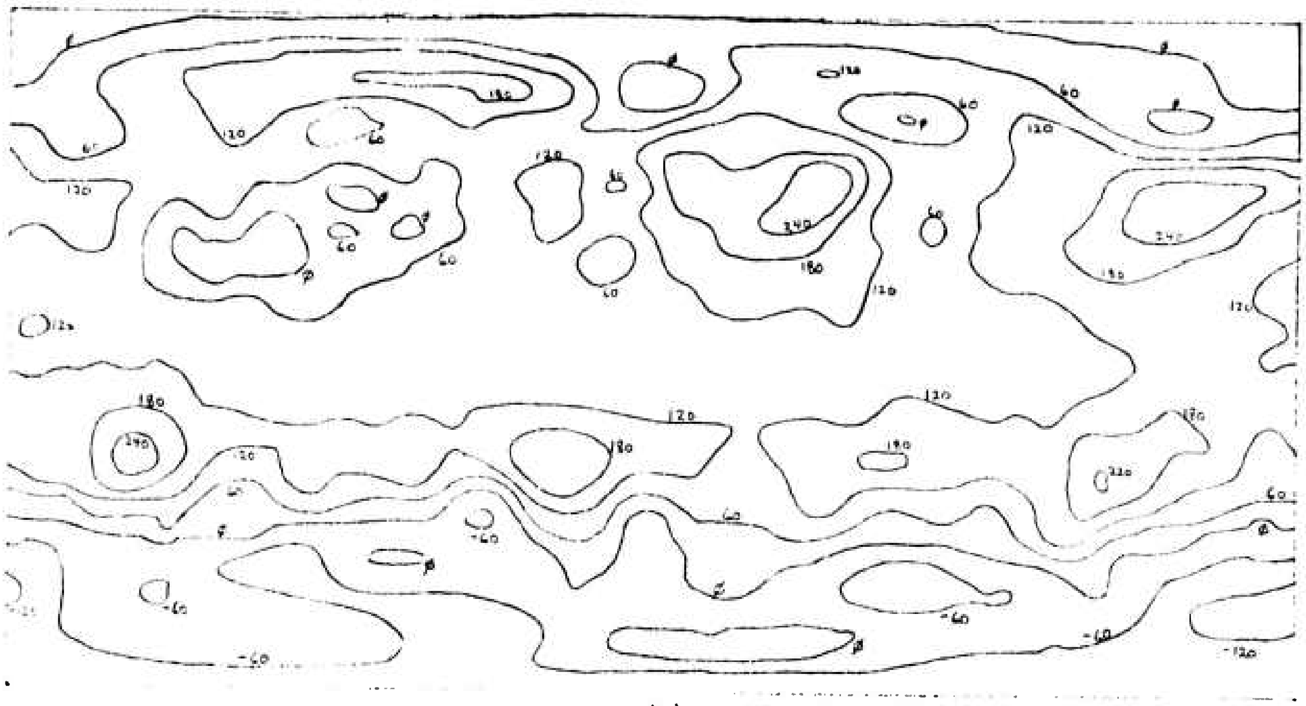

(a)

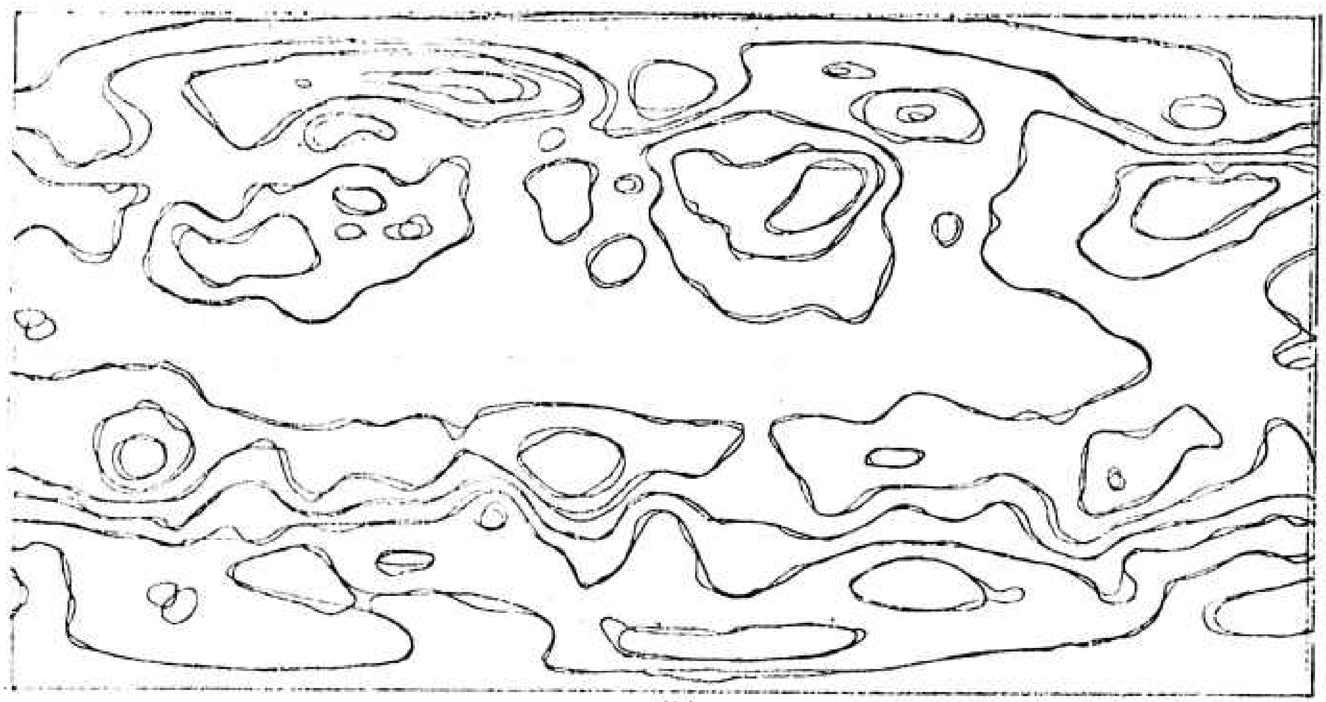

(b)

Figure 9-3

(a) Test Field, Trapezoidal Truncation (M=25, L=25)
(b) With Untruncated Map Overlay

Figures 9-4 illustrate the reconstruction with the truncation used for the predictions made to date. Trapezoidal, M=9, L=9. The error, in terms of true coefficient values including negative m's is

$$\epsilon = \epsilon_{25,25} + 5094.$$

Figures 9-5 thru 9-10 show some reconstructions with varying truncation parameters. They are summarized below.

Figures	Truncation Policy	M	L or J	Equivalent J or L	ϵ increment
9-5	Trapezoidal	9	L = 15	J = 10.5	2122.
9-6	Rhomboidal	9	J = 9	L = 14.	3175.
9-7	Trapezoidal	15	L = 15	J = 7.5	1578.
9-8	Rhomboidal	15	J = 9	L = 17.	2328.
9-9	Trapezoidal	15	L = 25	J = 17.5	88.
9-10	Trapezoidal	12	L = 20	J = 13.5	623.

The error measures for these reconstructed fields are equal to $\epsilon_{25,25}$ + ϵ increment from the table.

We feel that the case illustrated in Figure 9-10 is a reasonable policy to try on our next series of runs (trapezoidal, M=12, L=20). The ϵ increment for the equivalent rhombiodal policy is

985. , (Rhomboidal, M=12, J=13)
or 730. , (Rhomboidal, M=12, J=14)

which are similar to the ϵ increment (623.) for the trapezoidal case.

Since our programs are not set up for rhomboidal truncation, we have pursued the rhombiodal/trapezoidal comparison only to the extent of demonstrating that our trapezoidal policy is a reasonable alternative.

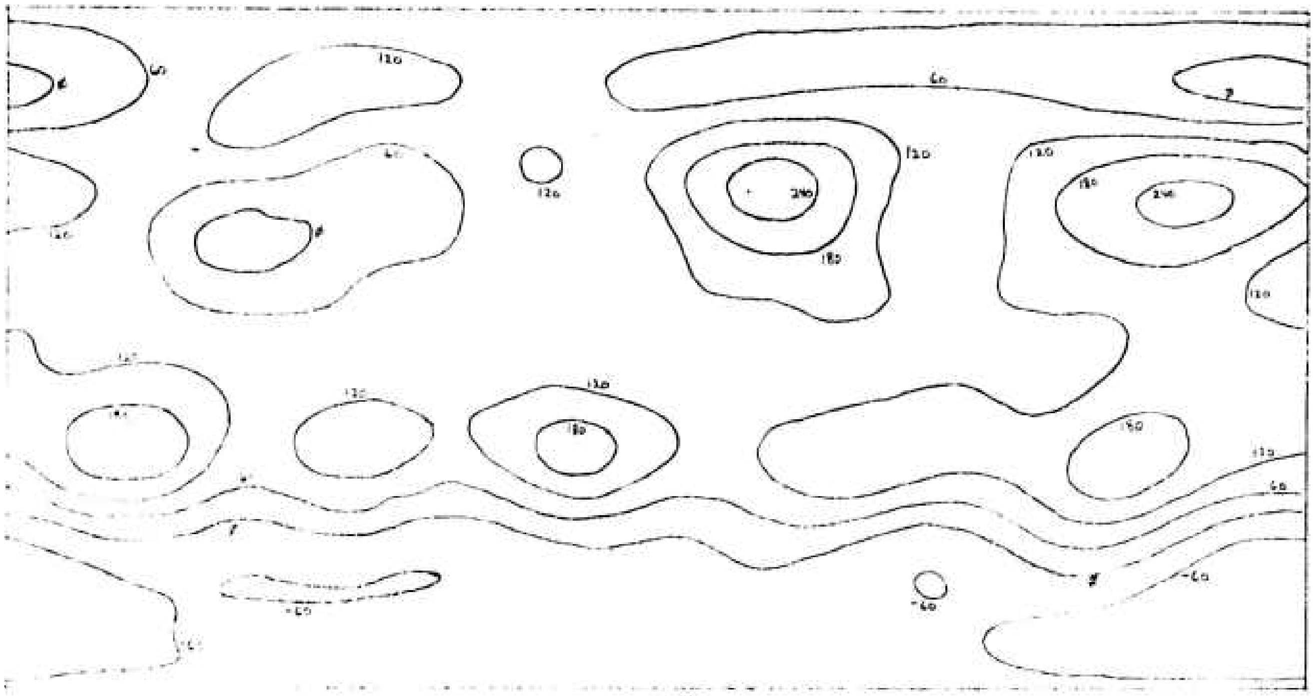

(a)

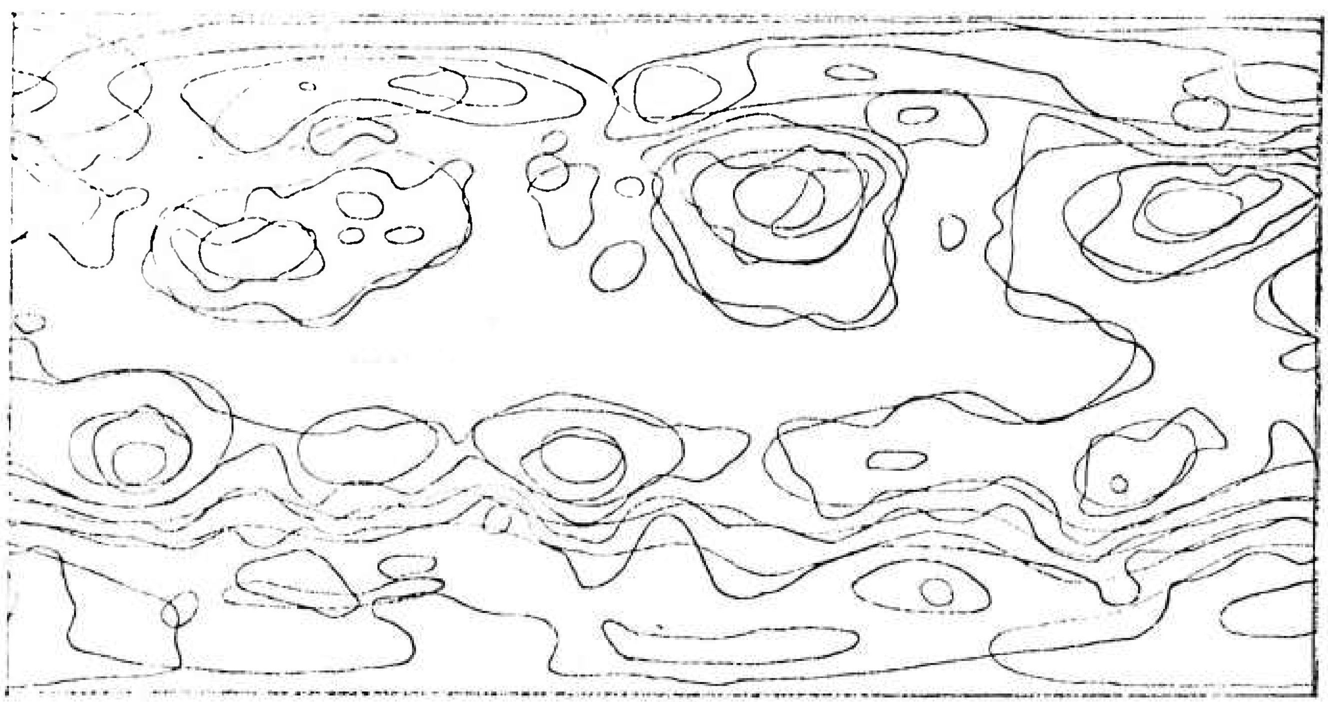

(b)

Figure 9-4

(a) Test Field, Trapezoidal Truncation (M= 9, L= 9)
(b) With Untruncated Map Overlay

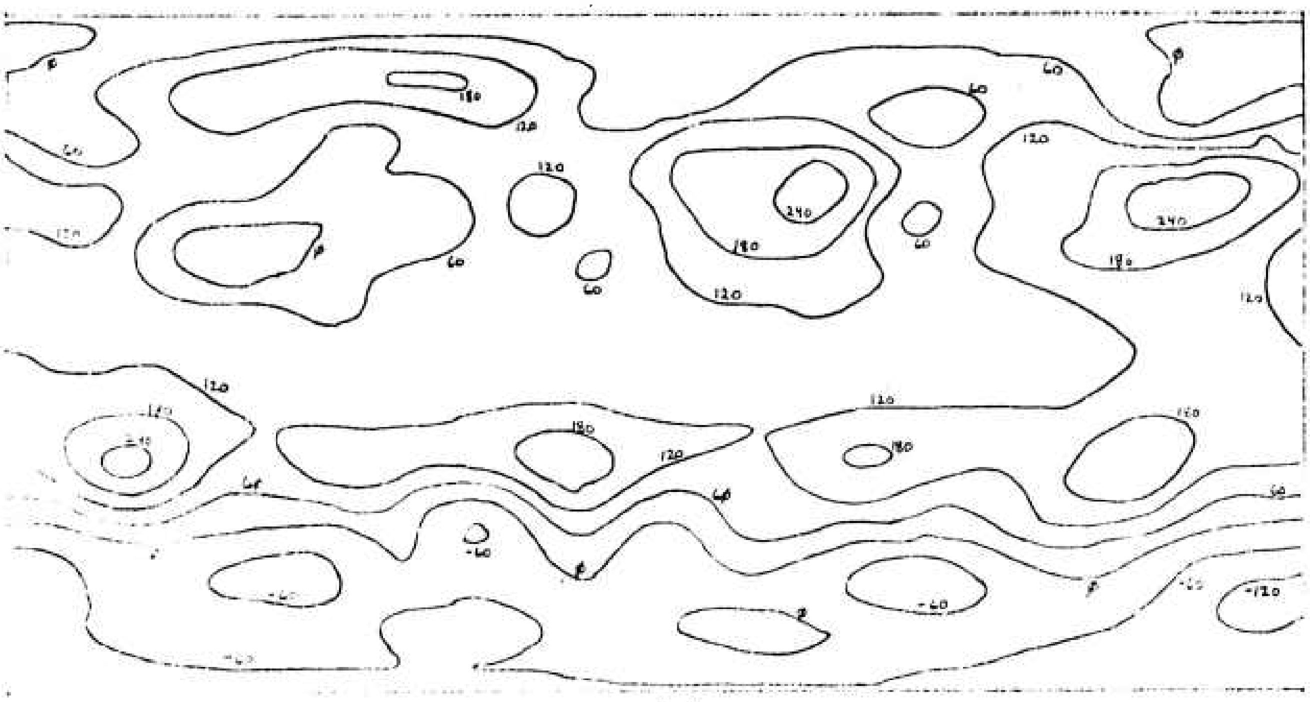

(a)

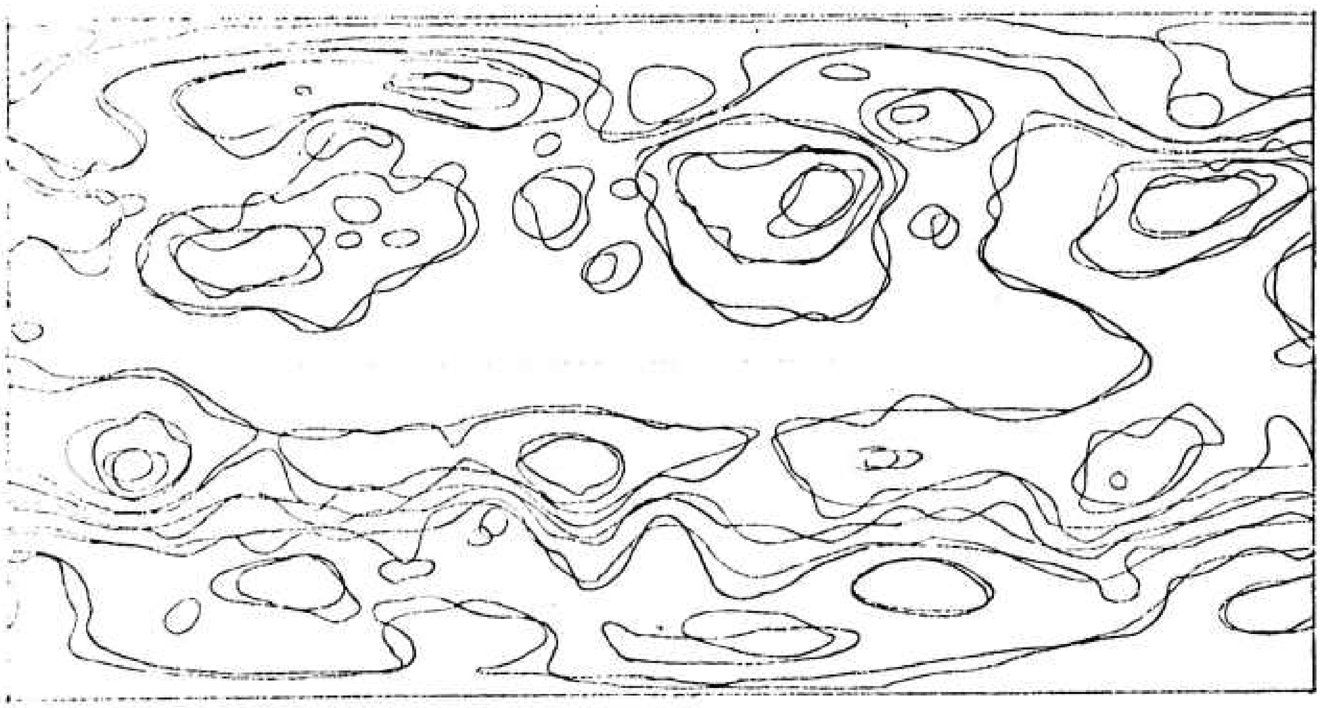

(b)

Figure 9-5

(a) Test Field, Trapezoidal Truncation (M= 9, L=15)
(b) With Untruncated Map Overlay

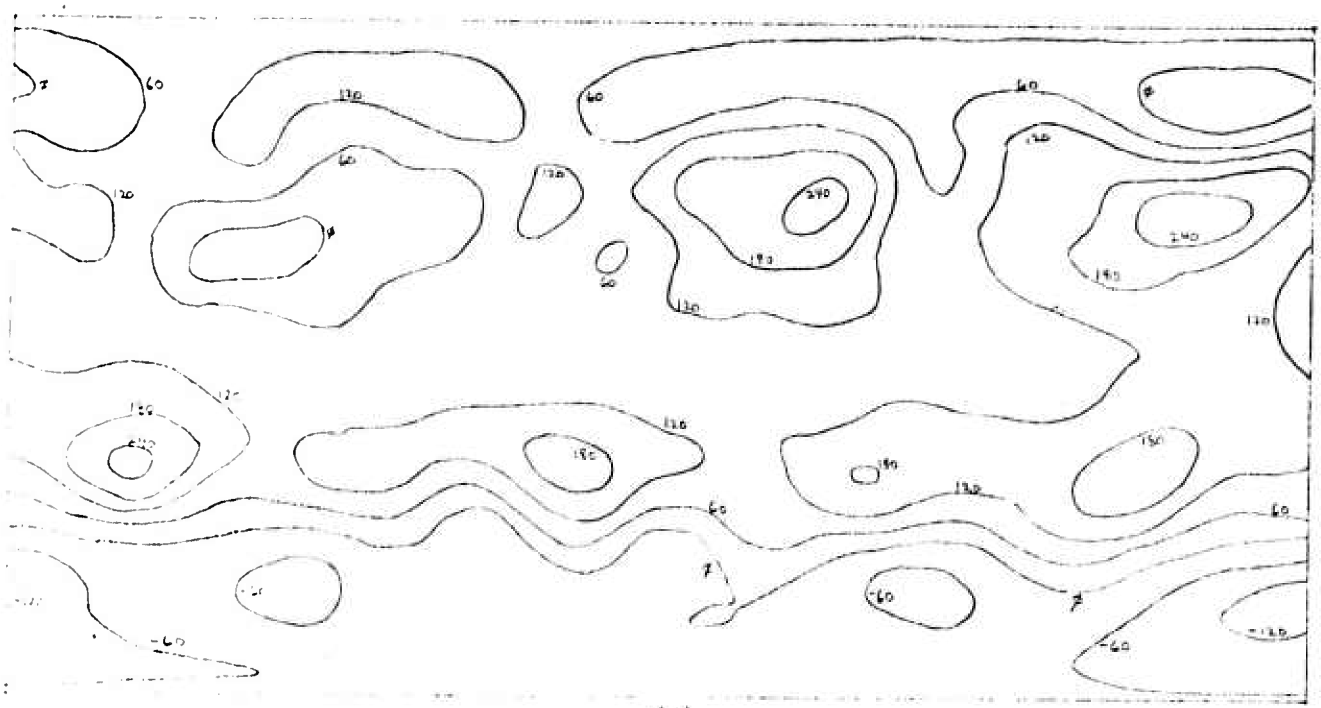

(a)

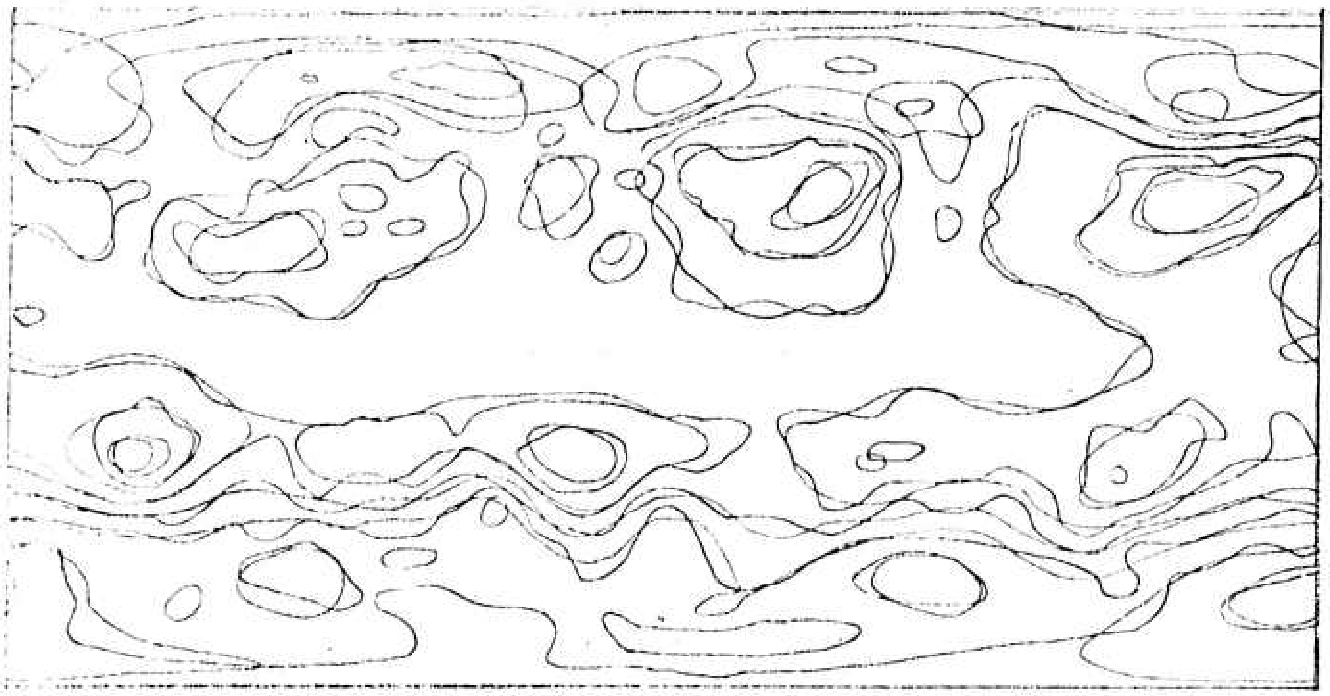

(b)

Figure 9-6

(a) Test Field, Rhomboidal Truncation (M=9, J=9)
(b) With Untruncated Map Overlay

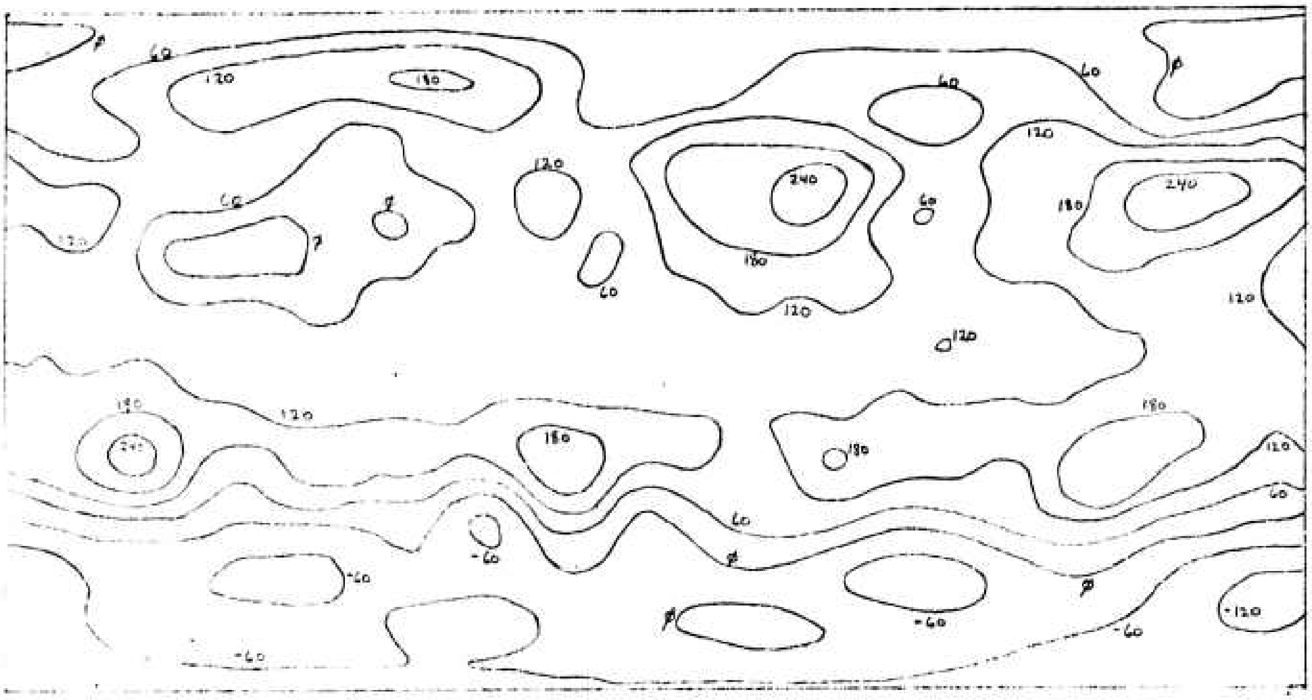

(a)

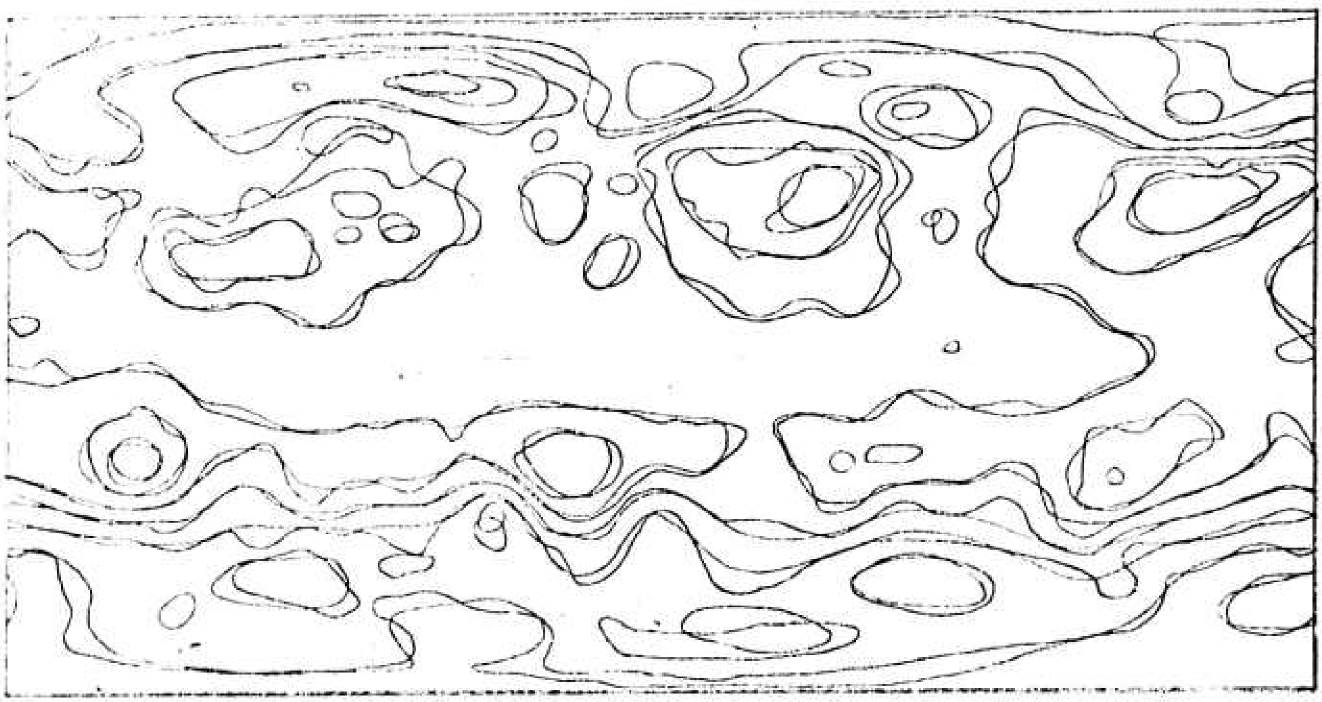

(b)

Figure 9-7

(a) Test Field, Trapezoidal Truncation (M=15, L=15)
(b) With Untruncated Map Overlay

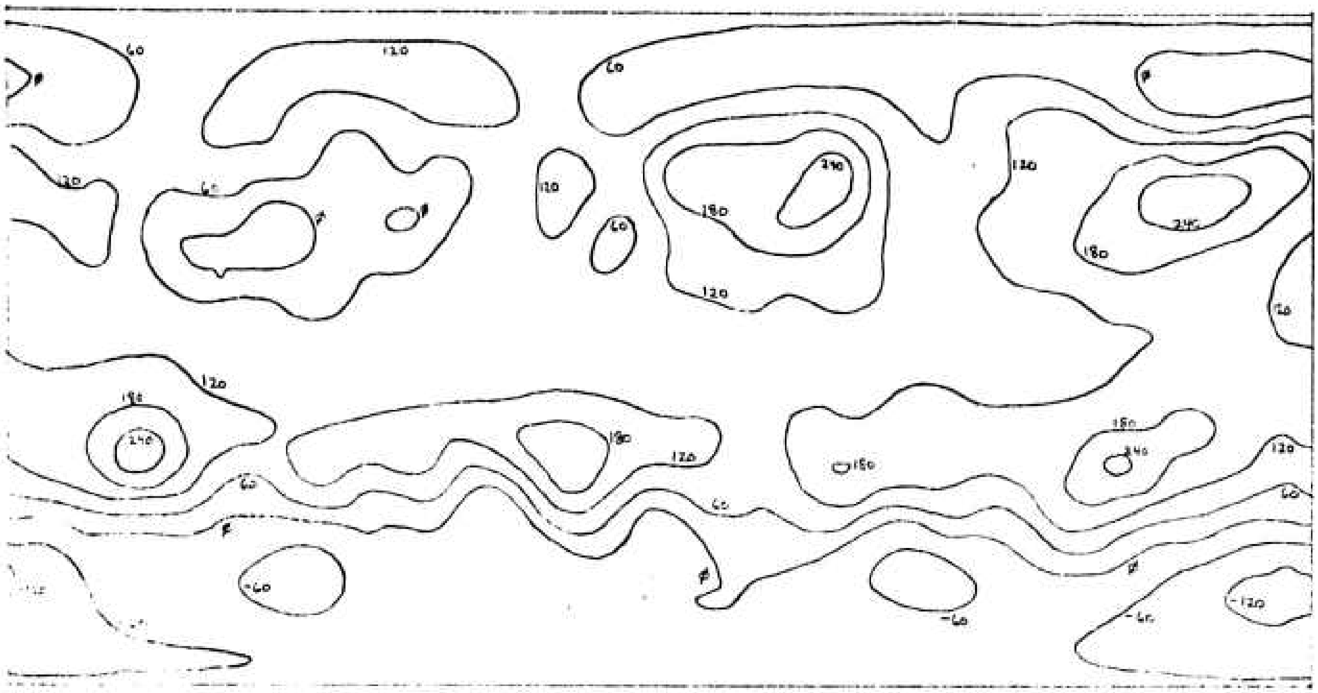

(a)

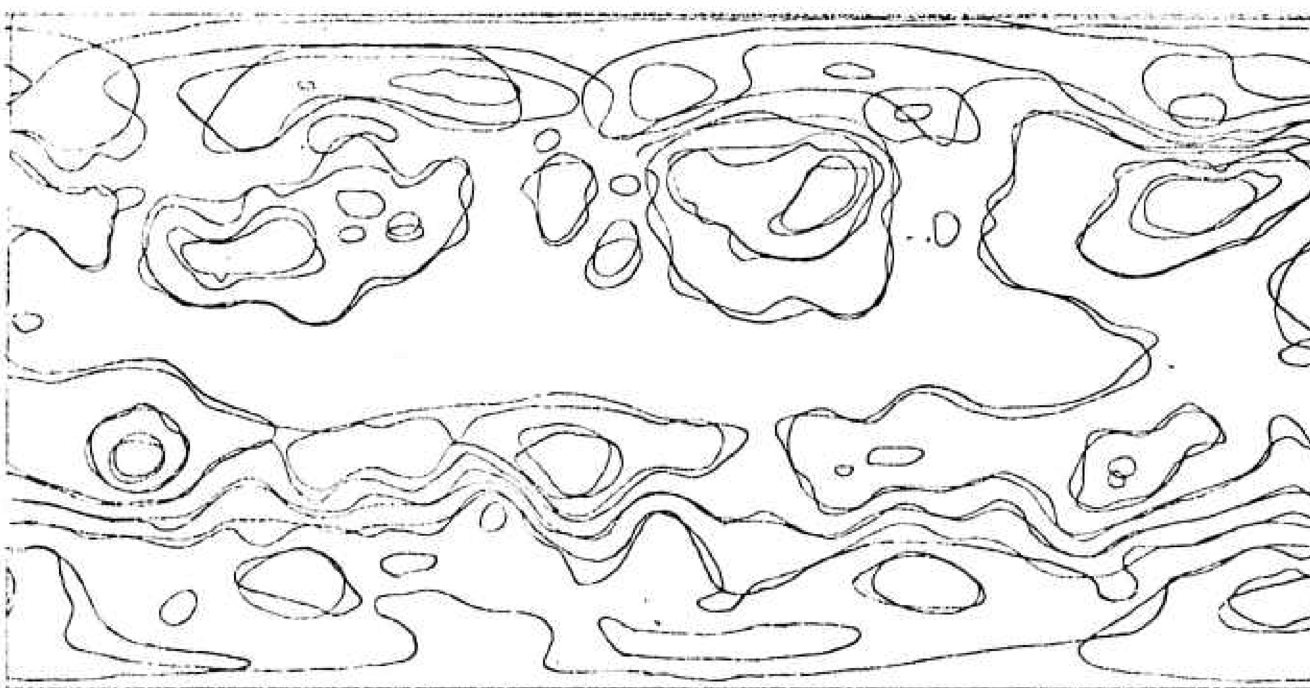

(b)

Figure 9-8

(a) Test Field, Rhomboidal Truncation (M=15, J=9)
(b) With Untruncated Map Overlay

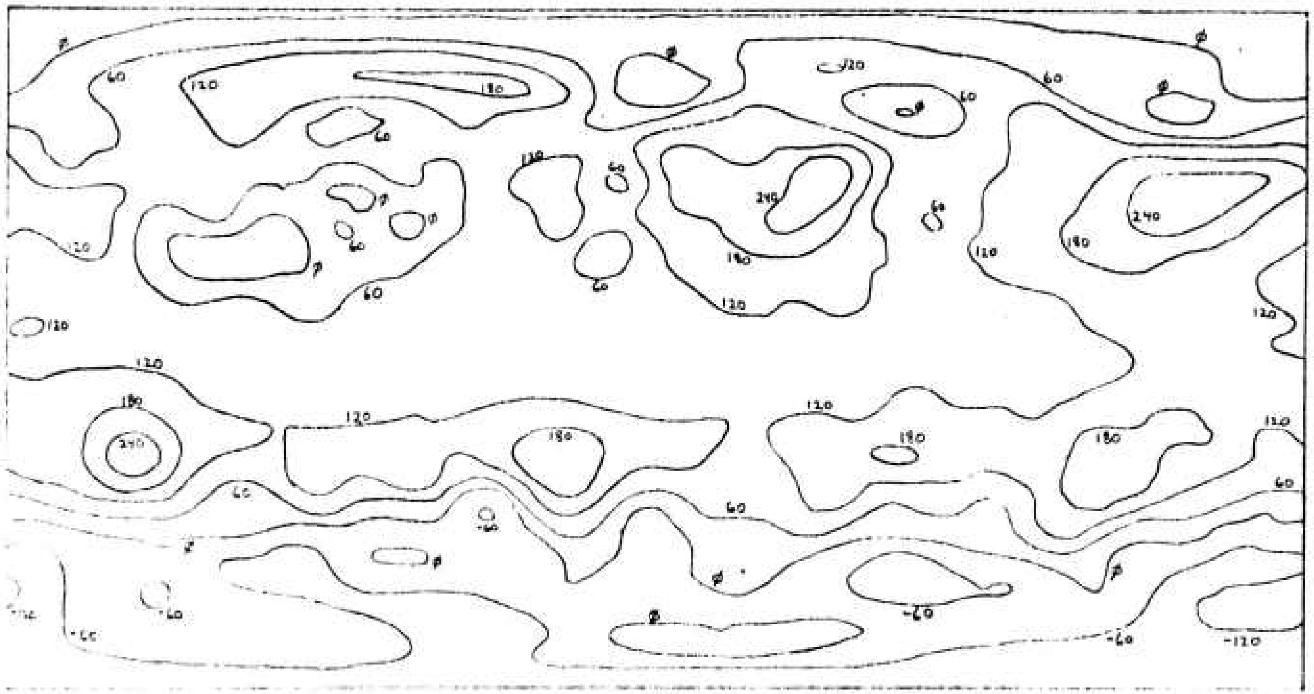

(a)

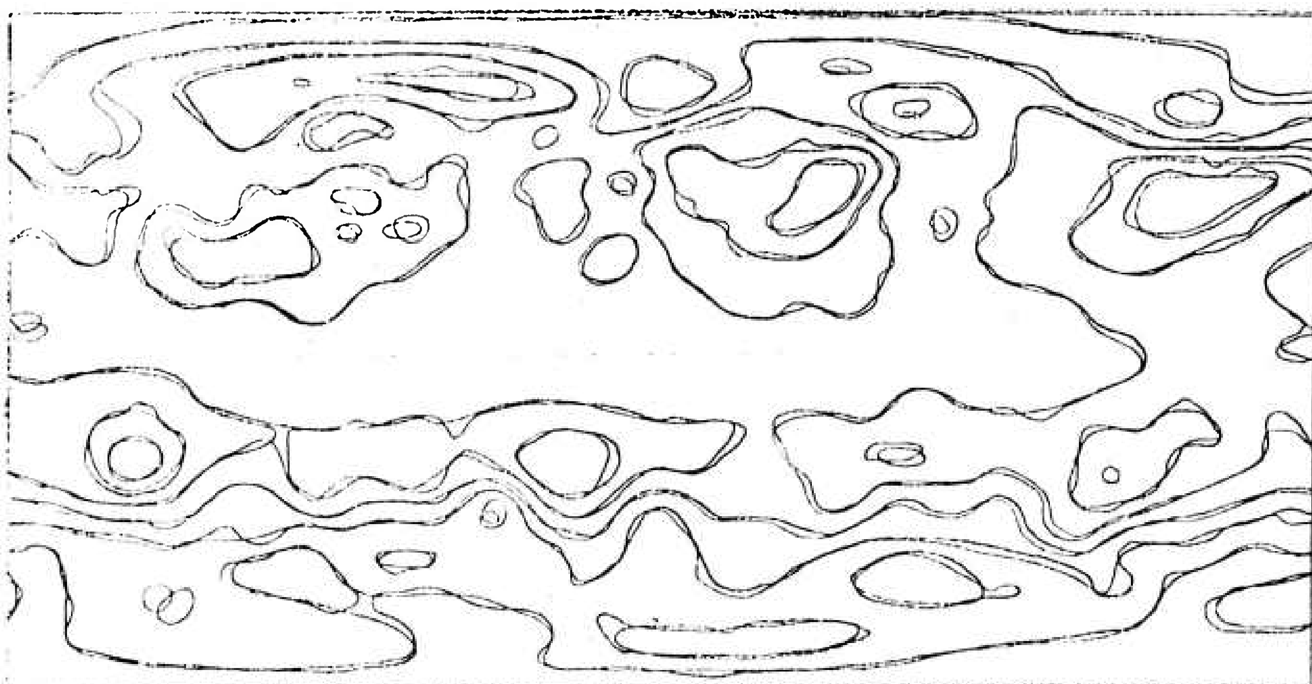

(b)

Figure 9-9

(a) Test Field, Trapezoidal Truncation (M=15, L=25)
(b) With Untruncated Map Overlay

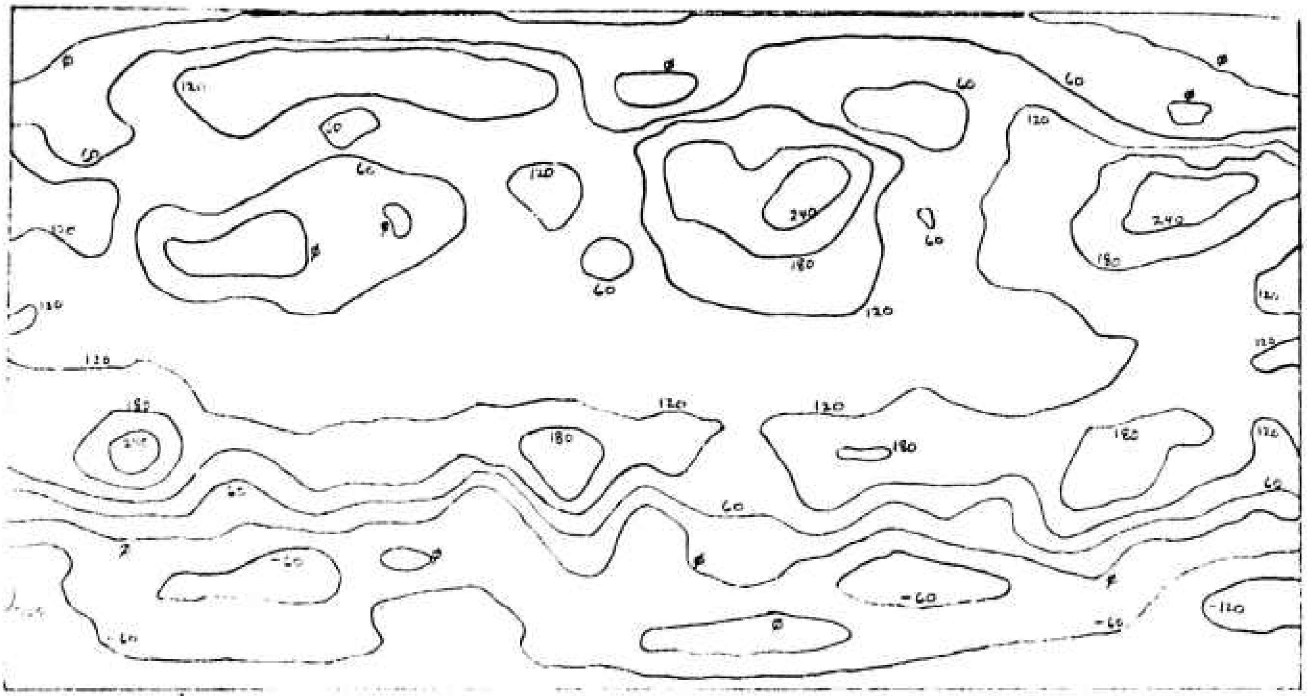

(a)

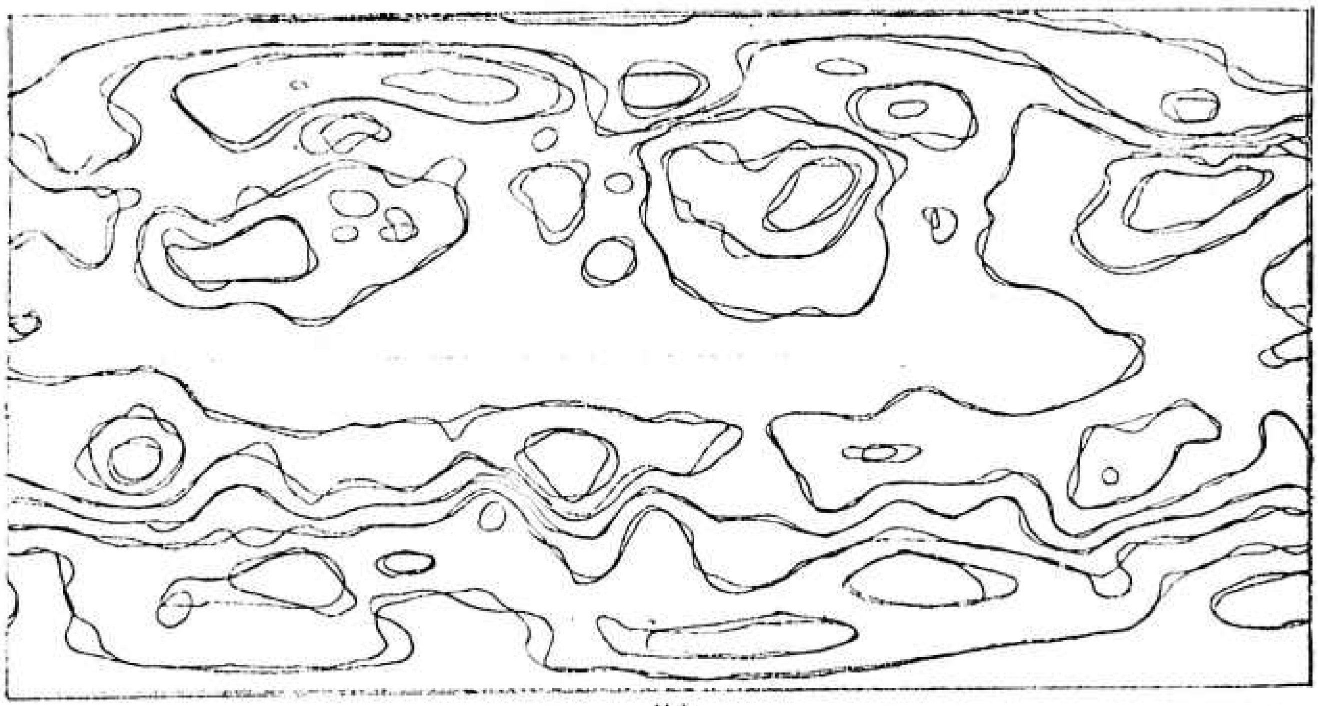

(b)

Figure 9-10

(a) Test Field, Trapezoidal Truncation (M=12, L=20)
(b) With Untruncated Map Overlay

Section 10. TIME STEP EXPERIMENT

The following four maps represent the results of an experiment to determine whether an increase in the time step will make the computation blow up. Four twelve hour predictions were made. The time step used were 10 minutes, 20 minutes, 30 minutes and 40 minutes. We display the results for the 500 mb. pressure height. As one can see the first three maps are almost identical. The 40 minutes time step differs considerable from the other three. As far as the expansion coefficients are concerned, the coefficients for the first three runs differ very little from each other. For the 40 minute runs, the low M and L coefficients are very similar to those of the first three predictions, those with higher M and L values, above 5 say, are considerably different. Values of all coefficients and their time-derivatives have been checked at all layers as has the value of the divergence of the velocity on gridpoints in all layers. There is no indications of any instability setting in. We thus think that the difference as far as the 40 minute time step is concerned is simply a matter of an inaccuracy in integration produced by the time step being too long.

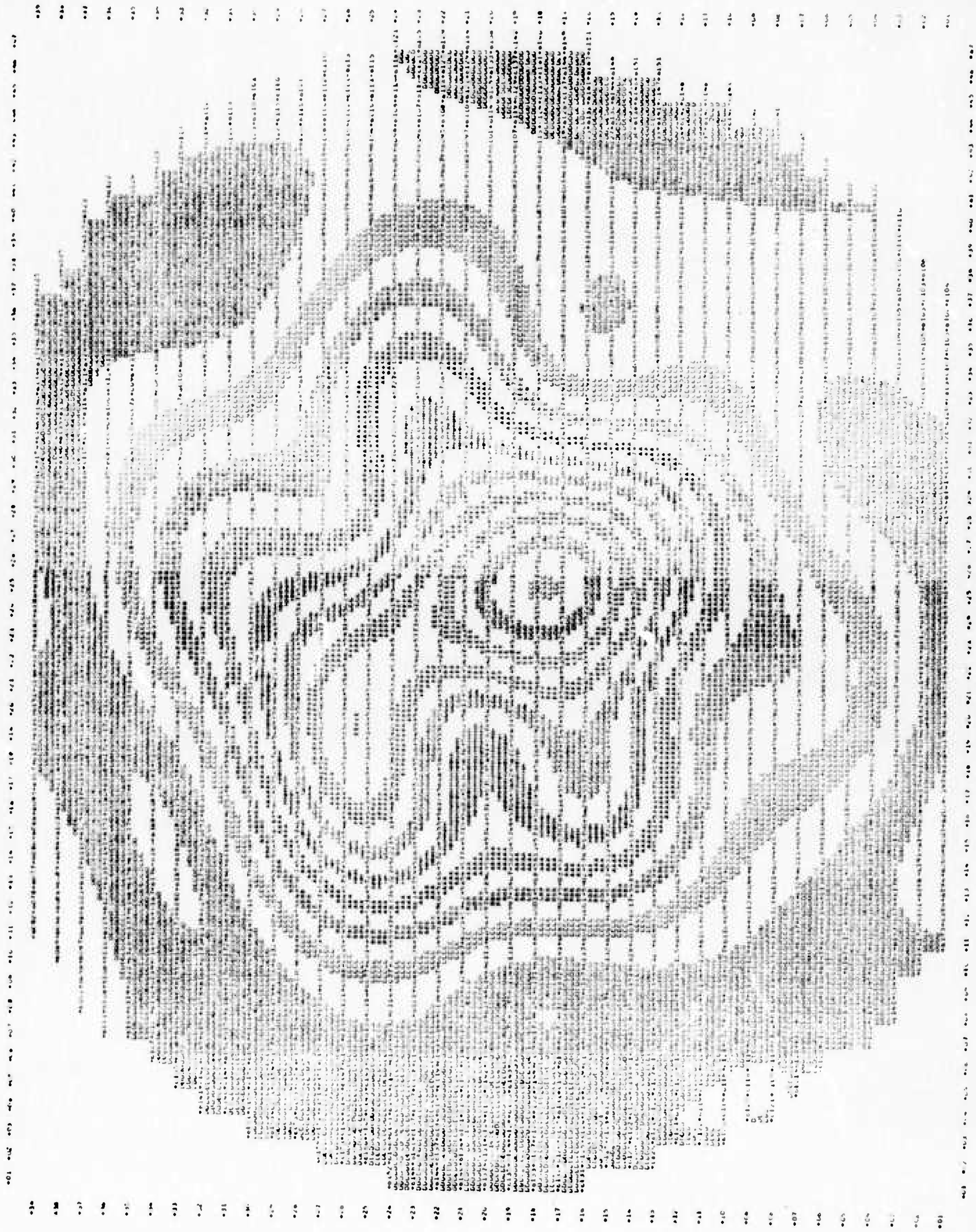

Z, 500 mb, 00Z 2 Dec. 1974, 12 Hour Prediction (10 min. time step)

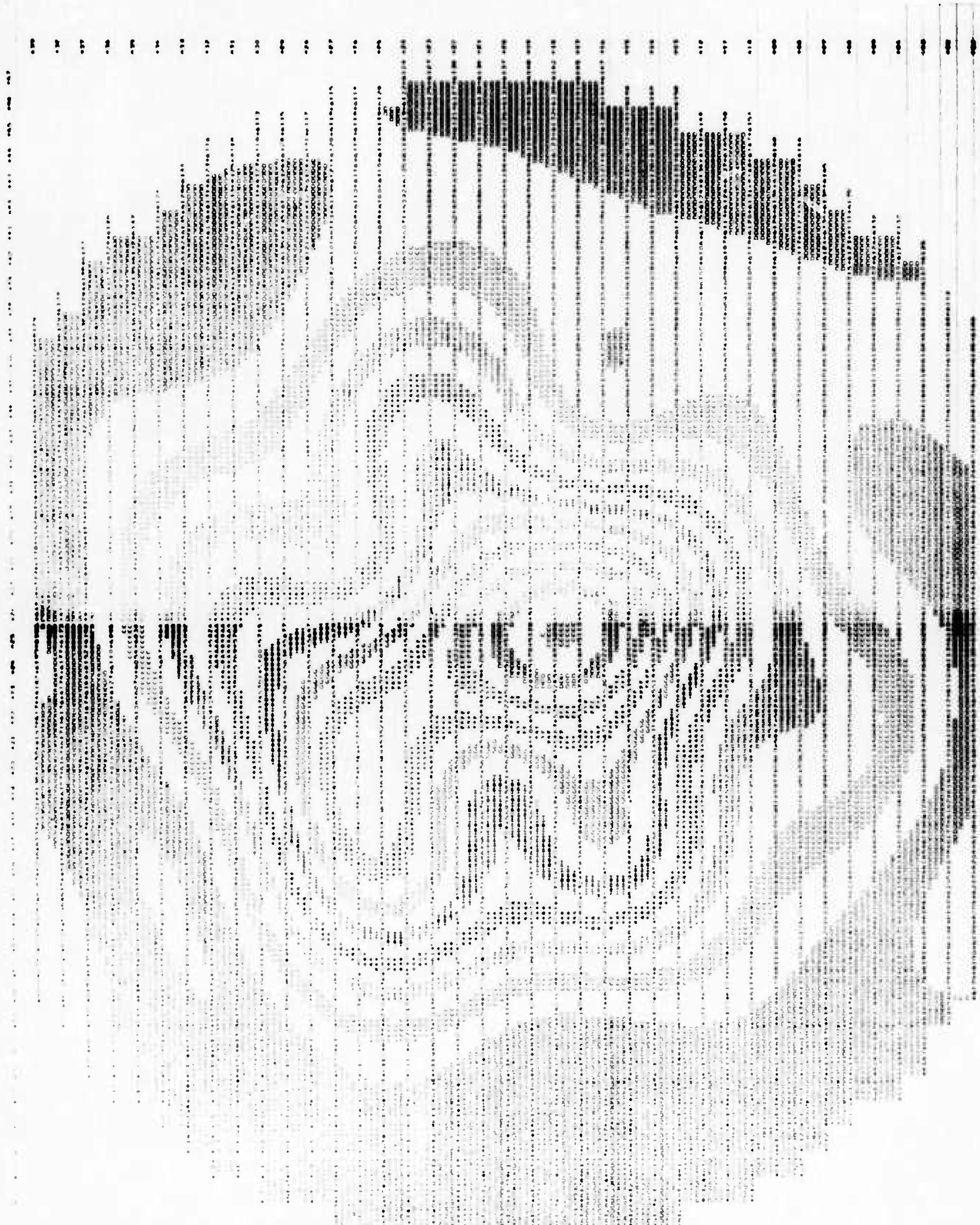

Z, 500 mb, 00Z 2 Dec. 1974, 12 Hour Prediction (20 min. time step)

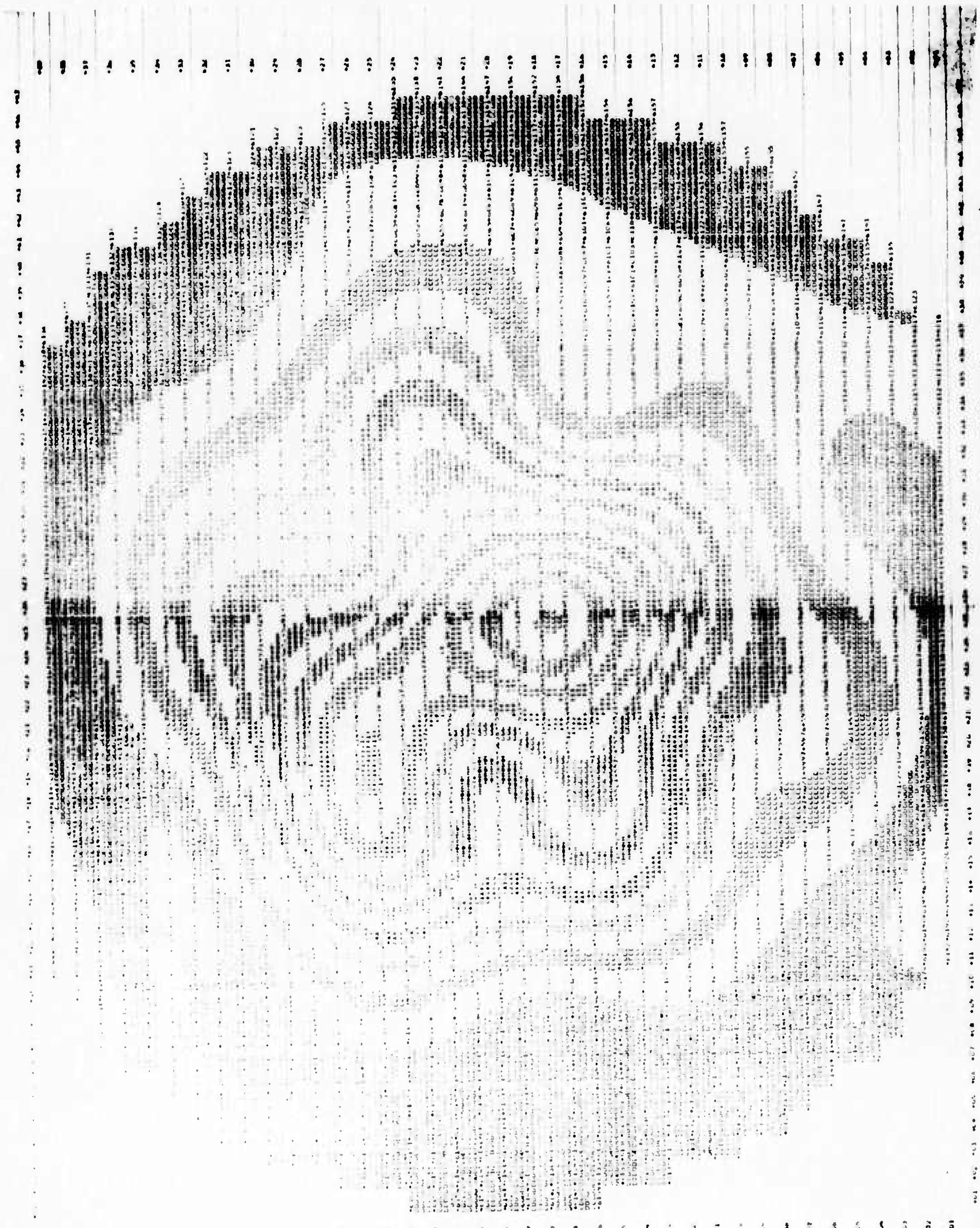

Z, 500 mb, 00Z 2 Dec. 1974, 12 Hour Prediction (30 min. time step)

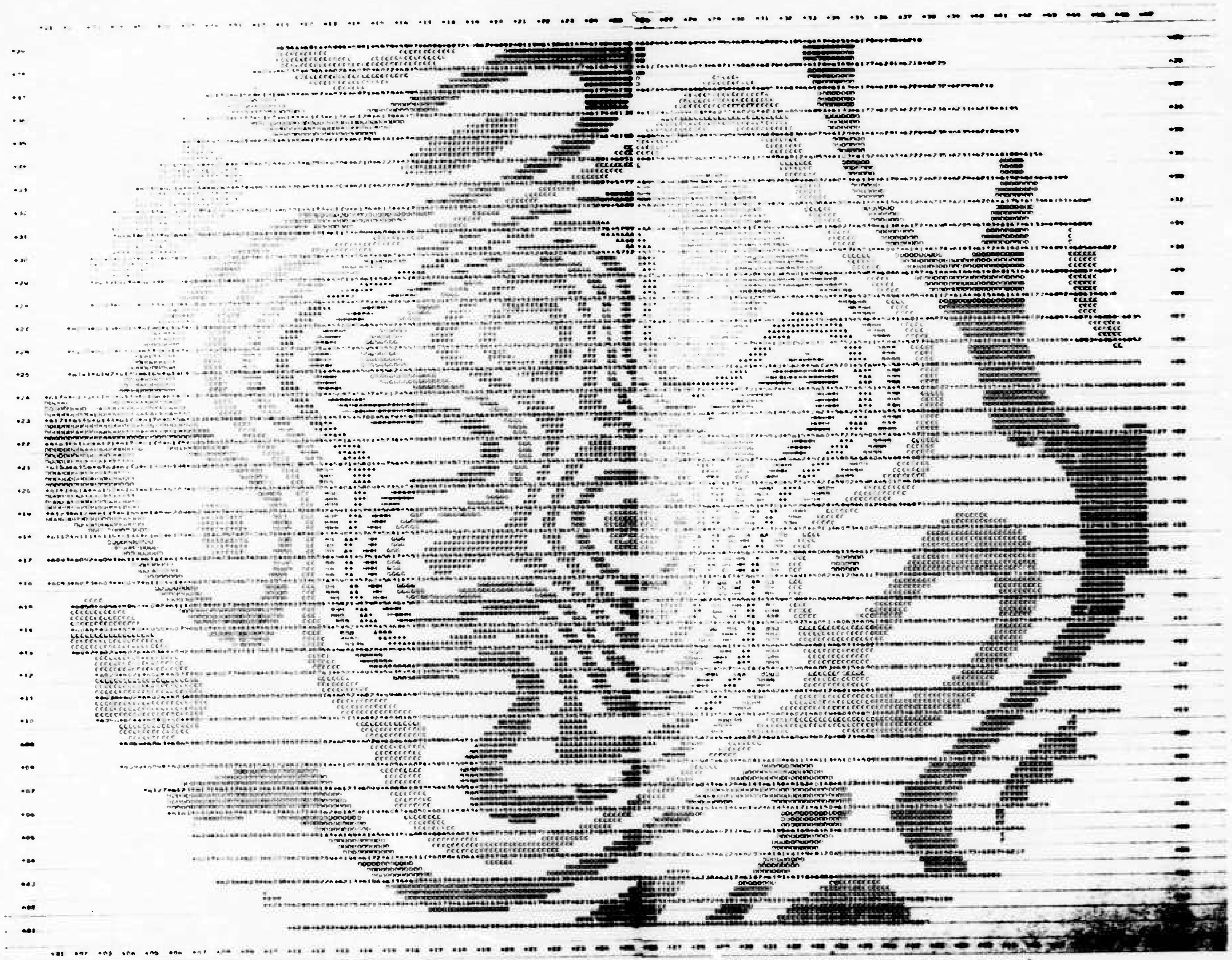

Z, 500 mb, 00Z 2 Dec. 1974, 12 Hour Prediction (40 min. time step)

Section 11. ANGULAR MOMENTUM

The angular momentum vector of a moving fluid of density ρ and velocity $\vec{V}$ is given by

$$\vec{L} = \int \vec{r} \times \rho \vec{v} \, d\tau \tag{1}$$

where $d\tau$ is the volume element and $\vec{r}$ is the radius vector. To begin with consider the case of a sphere surrounded by a atmosphere of spherically symmetric density. $\vec{v}$ can be expanded in the form

$$\vec{V}(\vec{r},t) = \sum_{M,L} \left[a_L^M(r,t) A_L^M(\theta,\varphi) + b_L^M(r,t) B_L^M(\theta,\varphi) + c_L^M(r,t) C_L^M(\theta,\varphi) \right] \tag{2}$$

Remembering that

$$A_L^M(\theta,\varphi) = \hat{e}_r \, Y_L^M(\theta,\varphi) \tag{3}$$

$$B_L^M(\theta,\varphi) = \frac{r \nabla Y_L^M(\theta,\varphi)}{\sqrt{L(L+1)}} \tag{4}$$

$$C_L^M(\theta,\varphi) = -\frac{i \vec{r} \times \nabla Y_L^M(\theta,\varphi)}{\sqrt{L(L+1)}} \tag{5}$$

The contributions for these three kind of terms are then

$$\vec{L}_A = \sum_{ML} \int \rho\, a^M_L(r,t)\, \vec{r} \times \hat{e}_r\, A^M_L(\theta,\varphi)\, d\tau = 0 \tag{6}$$

$$\vec{L}_B = \sum \frac{1}{\sqrt{L(L+1)}} \int \rho\, b^M_L(r,t)\, \vec{r} \times \nabla Y^M_L(\theta,\varphi)\, d\tau$$

$$= \int_0^\infty i\,\rho\, b^M_L(r,t)\, r^2 dr \int_0^{2\pi}\int_0^{\pi} C^M_L(\theta,\varphi) \sin\theta\, d\theta\, d\varphi \tag{7}$$

where

$$C^M_L = T^M_{LL} = \left[\frac{(L-M)(L+M+1)}{2L(L+1)}\right]^{\frac{1}{2}} Y^{M+1}_L \hat{e}_- - \frac{M}{[L(L+1)]^{\frac{1}{2}}} Y^M_L \hat{e}_0$$

$$- \left[\frac{(L+M)(L-M+1)}{2L(L+1)}\right]^{\frac{1}{2}} Y^{M-1}_L \hat{e}_+ \tag{8}$$

Consider the integral

$$\int_0^{2\pi}\int_0^{\pi} C^M_L(\theta,\varphi) \sin\theta\, d\theta\, d\varphi = \sqrt{4\pi} \int_0^{2\pi}\int_0^{\pi} Y^0_0(\theta,\varphi)\, C^M_L(\theta,\varphi) \sin\theta\, d\theta\, d\varphi$$

Using the orthonormality of the Y^M_L's the only non-zero terms for this integral must be those originating in C^M_L's which contain Y^0_0 terms. A look at equation (8) shows that there are no such terms.

Consequently $\vec{L}_B = 0$.

$$\vec{L}_c = \int \vec{r} \times \rho(r) \sum_{M,L} C_L^M(r,t)\, C_L^M(\theta,\varphi)\, d\tau \tag{9}$$

$$= -\sum_{M,L} \int \rho(r)\, C_L^M(r,t)\, \vec{r} \times \frac{i}{\sqrt{L(L+1)}} \left(\vec{r} \times \nabla Y_L^M(\theta,\varphi)\right) d\tau$$

where

$$\vec{r} \times \left(\vec{r} \times \nabla Y_L^M(\theta,\varphi)\right) = \vec{r}\left(\vec{r} \cdot \nabla Y_L^M\right) - \nabla Y_L^M\, r^2$$

$$= -r^2\, \nabla Y_L^M(\theta,\varphi)$$

$$= -r\sqrt{L(L+1)}\; B_L^M(\theta,\varphi) \tag{10}$$

Thus

$$\vec{L}_c = i \sum_{M,L} \int_0^\infty \rho(r)\, C_L^M(r,t)\, r^3\, dr \int_0^{2\pi}\!\!\int_0^{\pi} B_L^M(\theta,\varphi) \sin\theta\, d\theta\, d\varphi \tag{11}$$

$$B_L^M(\theta,\varphi) = \left(\frac{L+1}{2L+1}\right)^{\frac{1}{2}} Y_{L\,L-1}^M(\theta,\varphi) + \left(\frac{L}{2L+1}\right)^{\frac{1}{2}} Y_{L\,L+1}^M \tag{12}$$

Again only terms in B_L^M containing Y_0^0 will contribute. These terms are

$$T^{-1}_{10} = Y^0_0 \hat{e}_- \quad , \quad T^0_{10} = Y^0_0 \hat{e}_0 \quad , \quad T^1_{10} = Y^0_0 \hat{e}_+ \qquad (13)$$

or

$$B^{-1}_1 = \sqrt{\frac{2}{3}}\, T^{-1}_{10} \quad , \quad B^0_1 = \sqrt{\frac{2}{3}}\, T^0_{10} \quad , \quad B^1_1 = \sqrt{\frac{2}{3}}\, T^1_{10} \quad . \qquad (14)$$

Thus we have reached the result that to the approximation that $\rho = \rho(r)$ the only terms capable of having a total angular momentum different from zero are:

$$c^{-1}_1(r,t)\, C^{-1}_1(\theta,\varphi) \;,\; c^0_1(r,t)\, C^0_1(\theta,\varphi) \quad \text{and} \quad c^1_1(r,t)\, C^1_1(\theta,\varphi)$$

Now, of course, two important approximations have been made: the earth was assumed spherical and the density was assumed to depend only on the distance from the center of the earth but not on the angles and . These are, however, pretty good approximations and to a considerable degree, then, the angular momentum of the atmosphere resides in the three terms found above. In particular the term $c^0_1(r,t)$ $C^0_1(\theta,\varphi)$ is the main component of the zonal circulation.

$$C^0_1 = -\frac{i L_\varphi}{\sqrt{2}} \frac{\partial Y^0_1}{\partial \theta} = -i\sqrt{\frac{3}{8\pi}}\, \hat{e}_\varphi \frac{\partial \cos\theta}{\partial \theta} = i\sqrt{\frac{3}{8\pi}}\, \hat{e}_\varphi \sin\theta$$

The imaginary value does not matter, it simply means that $c_1^0(r,t)$ also has to be imaginary to make the velocity and the angular momentum real. The result implies that C_1^0 must be very stable since if we assume that at one instant of time the angular momentum only has a z-component, i.e. $c_1^1 (r,t) = c_1^{-1} (r,t) = 0$, and since the other velocity terms cannot absorb any total angular momentum, the law of conservation angular momentum will keep C_1^0 going. We show below some results from real data and predictions

Section 12. SELECTED EXPANSION COEFFICIENTS

Out of the very large number of expansion coefficients that are contained in the computer printouts we have chosed to display graphically a few generated from 25 July, 1974 NMC data. This is so that the reader can get a feel for how they depend on M and L. For the graphs only M is displayed, the value of L in each group with a given M value goes from M to 9. Of the wind components only the C_1^m coefficients (graph C_1^m expansion coefficient magnitudes) are displayed. C_1^o represent the zonal components and C_1^m, $(M \neq 0)$ represent Rossby, Haurwitz, or Neamtam waves, whatever you choose to be the proper nomenclature.

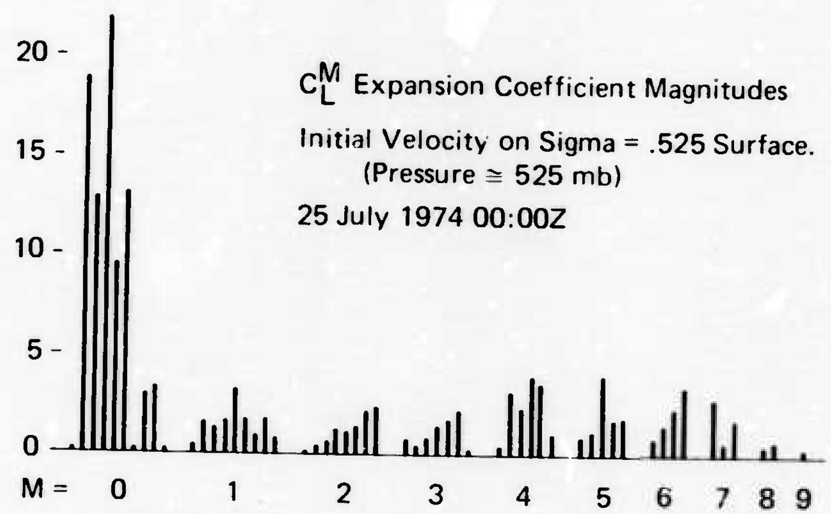
C_L^M Expansion Coefficient Magnitudes
Initial Velocity on Sigma = .525 Surface.
(Pressure ≅ 525 mb)
25 July 1974 00:00Z
20
15
10
5
0
M = 0 1 2 3 4 5 6 7 8 9

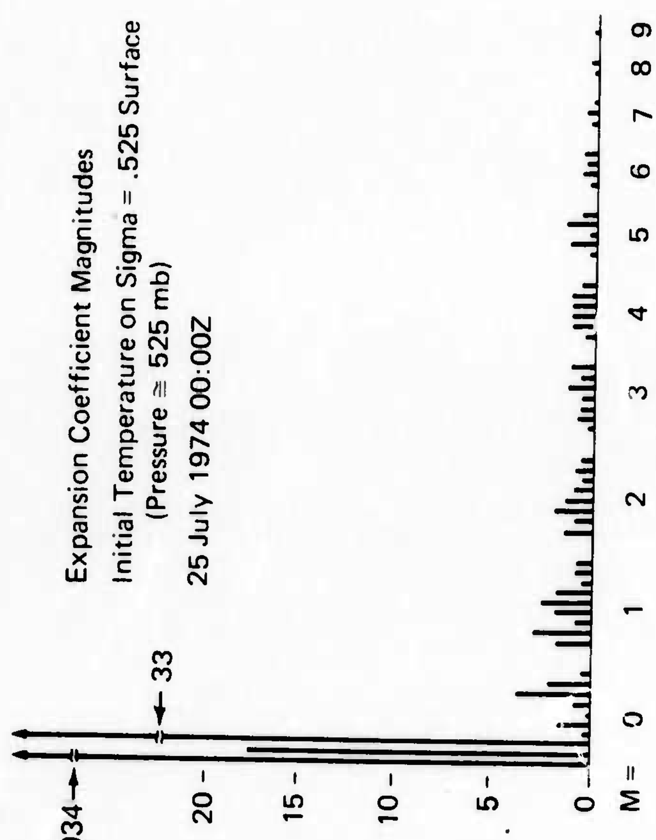
Expansion Coefficient Magnitudes
Initial Temperature on Sigma = .525 Surface
(Pressure ≅ 525 mb)
25 July 1974 00:00Z
934
33
20
15
10
5
0
M = 0 1 2 3 4 5 6 7 8 9

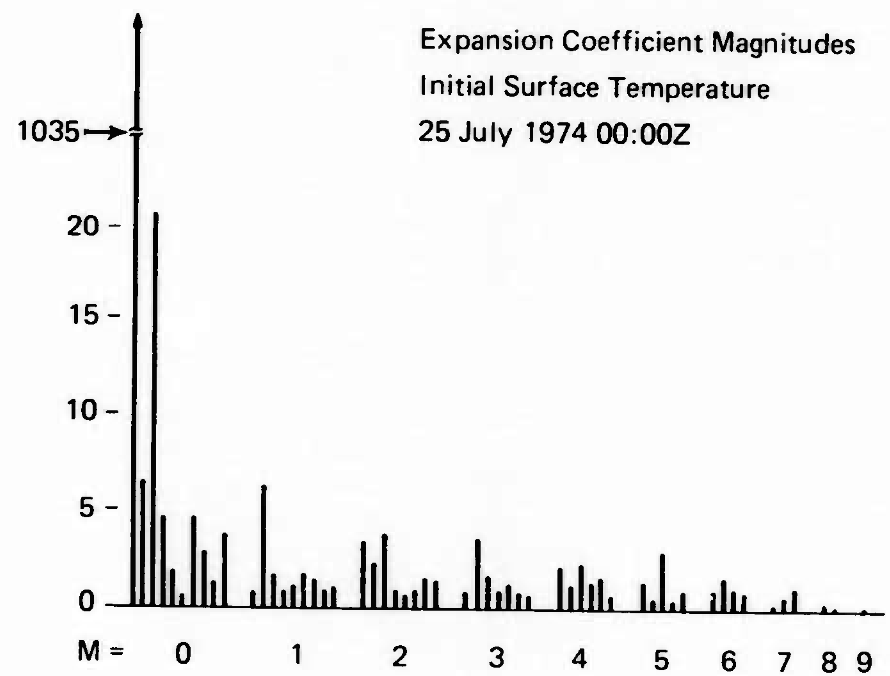
Expansion Coefficient Magnitudes
Initial Surface Temperature
25 July 1974 00:00Z
1035
20
15
10
5
0
M =
0
1
2
3
4
5
6
7
8
9

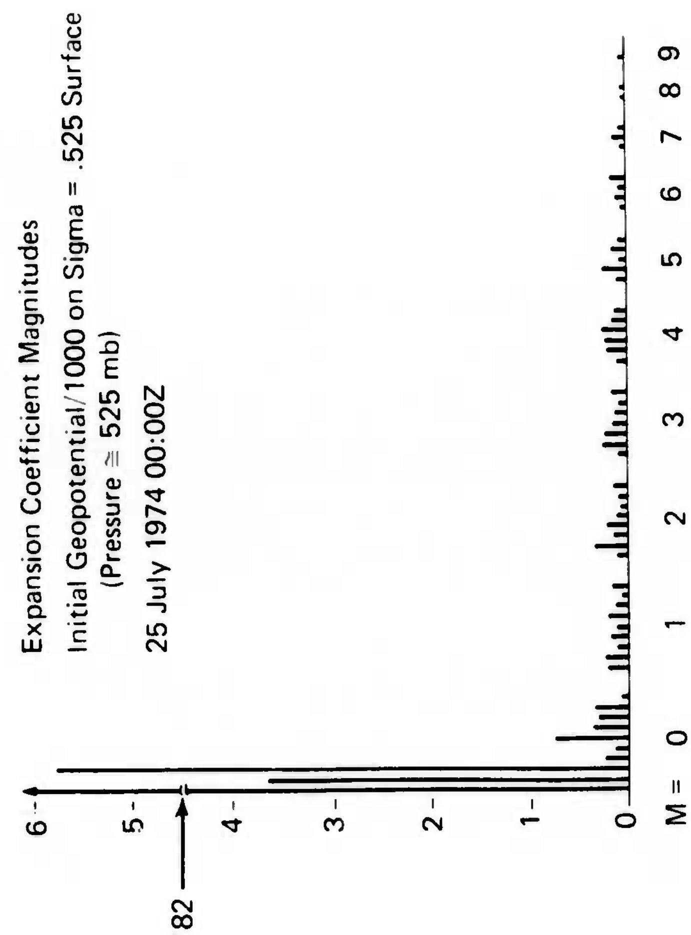

Expansion Coefficient Magnitudes

Initial Geopotential/1000 on Sigma = .525 Surface
(Pressure ≅ 525 mb)

25 July 1974 00:00Z

Section 13. RESULTS FROM = 10 MINUTES PREDICTIONS

We present in the following pages a few selected maps of the 500 mb temperature. As has been discussed before these results are with truncation limits $L_{max.} = M_{max.} = 9$. As the previous discussion on truncation limits shows that these are not reasonable truncation limits. However, in order to save computer time we decided that it was best to first ascertain with these truncation limits that the time step was reasonable, that the model was stable and that the results looked reasonable. The model has been run out to 5 days or 144 hours or 844 time steps. There seems to be quite a good agreement between truncated data and prediction for pressure height to 48 hours and for temperature for a few days more The CPU time on IMB 360/195 is about 18 minutes for a 24 hour prediction with 10 minutes time step with code that has not been optimized for speed but for ease of change and flexibility. We are using the transform method from coefficient to physical space at every time step but not the Fast Fourier Transform since we did not want to be tied down in our experiments to the gridspacing required. Provisions have been made in the program for the inclusion of the F.F.T. No particular initialization has been made for our purposes. We have simply used the N.M.C tapes in the form they have been used by N.M.C. No oscillations to speak of seem to occur in the first 12 hours, which is where we have monitored selected data for every time step. We have computed the kinetic energy of the zonal components every six hours and the fluctuation is of the order of 0.5%. We have monitored the spherically symmetric part of the logarithm of the surface pressure which of course is a measure of the total weight of the atmosphere and found the r.m.s. deviation from the mean to be less than one part in a million for 5 days. We have at every six hours printed 1 out the value of the fivergence of the velocity at every gridpoint in every layer and found no significant oscillations except that the predicted values differ from the data about one order of magnitude. The values in

the data always being smaller. Apparently the divergence is being suppressed in the data. We just after these few comments and maps at this time in order to keep this report to reasonable lengths. We intend to publish a more detailed report after we have had more time to analyze both the data and the prediction and after we have extended the truncation limits.

The maps represent the 500 mb pressure height. NMCIC represents a map printed out from N.M.C is data tape. Prediction is the same pressure height with $L_{max.} = M_{max.} = 9$ and NMC I.C. truncated means that the data has been converted to expansion coefficients for the spherical harmonics with the same truncated limits and then converted to numerical values from the functions on the grid.

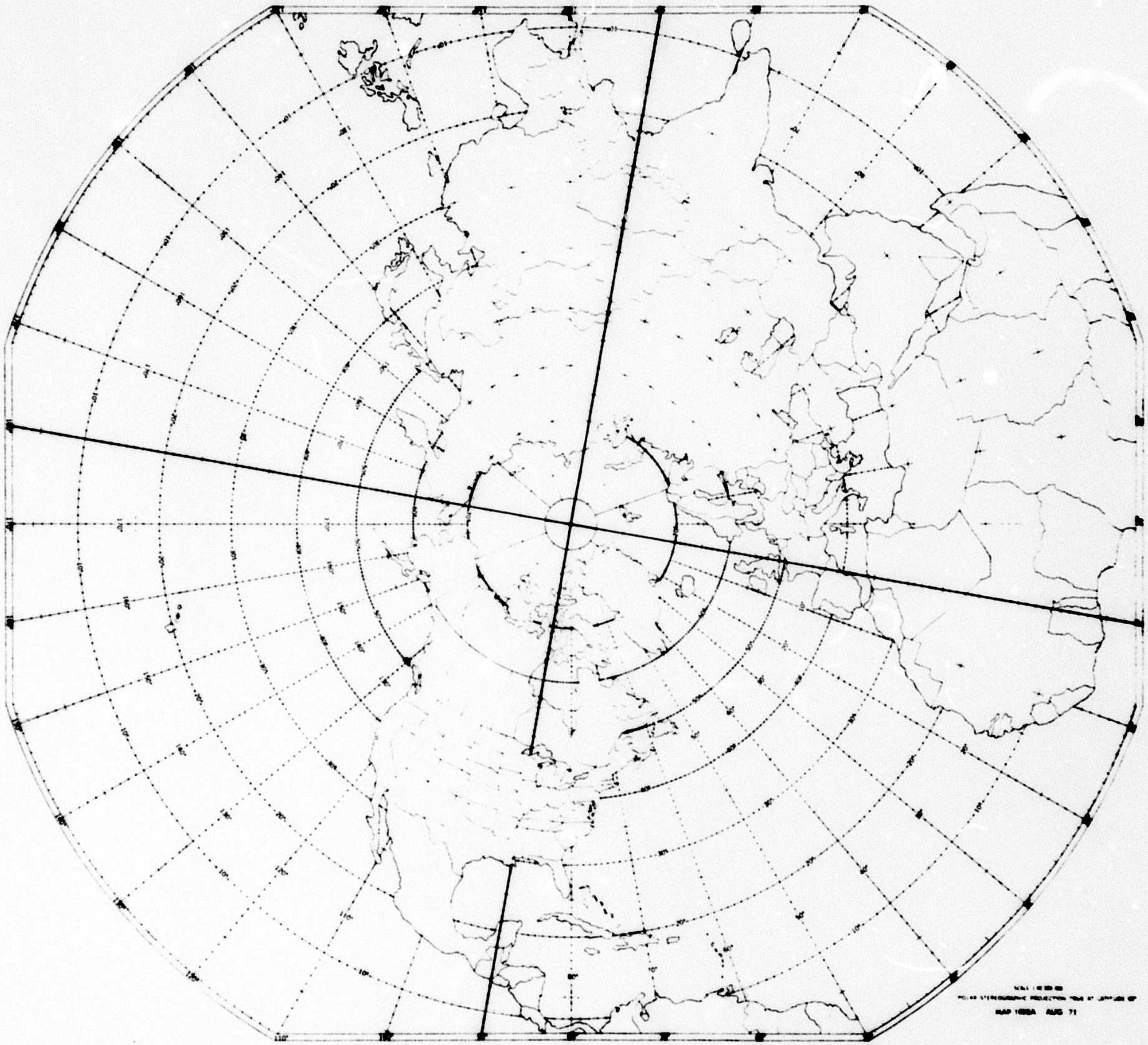

Geographical Orientation of Data Maps

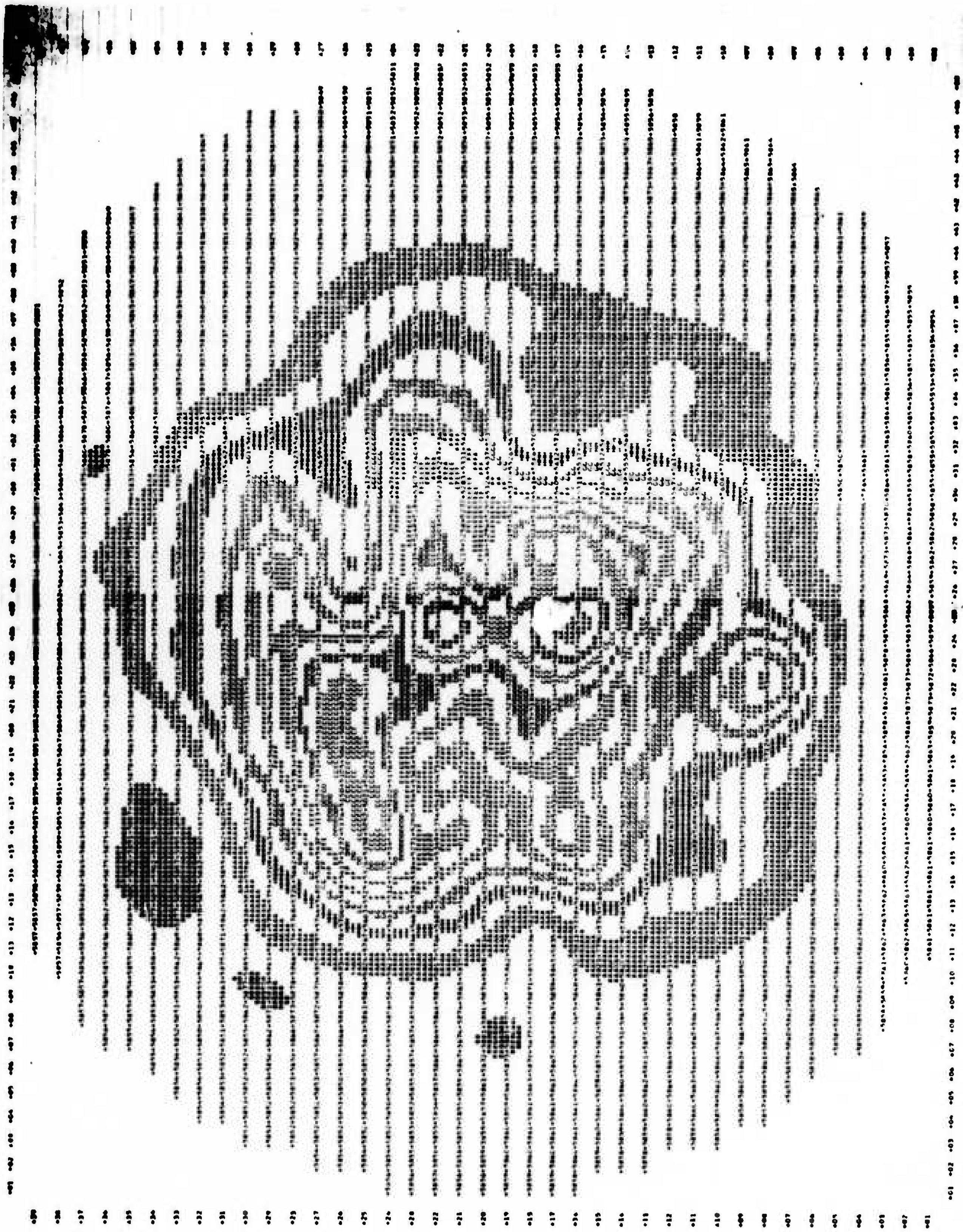

Z, 500 mb, 12Z 1 Dec. 1974, NMC I.C.

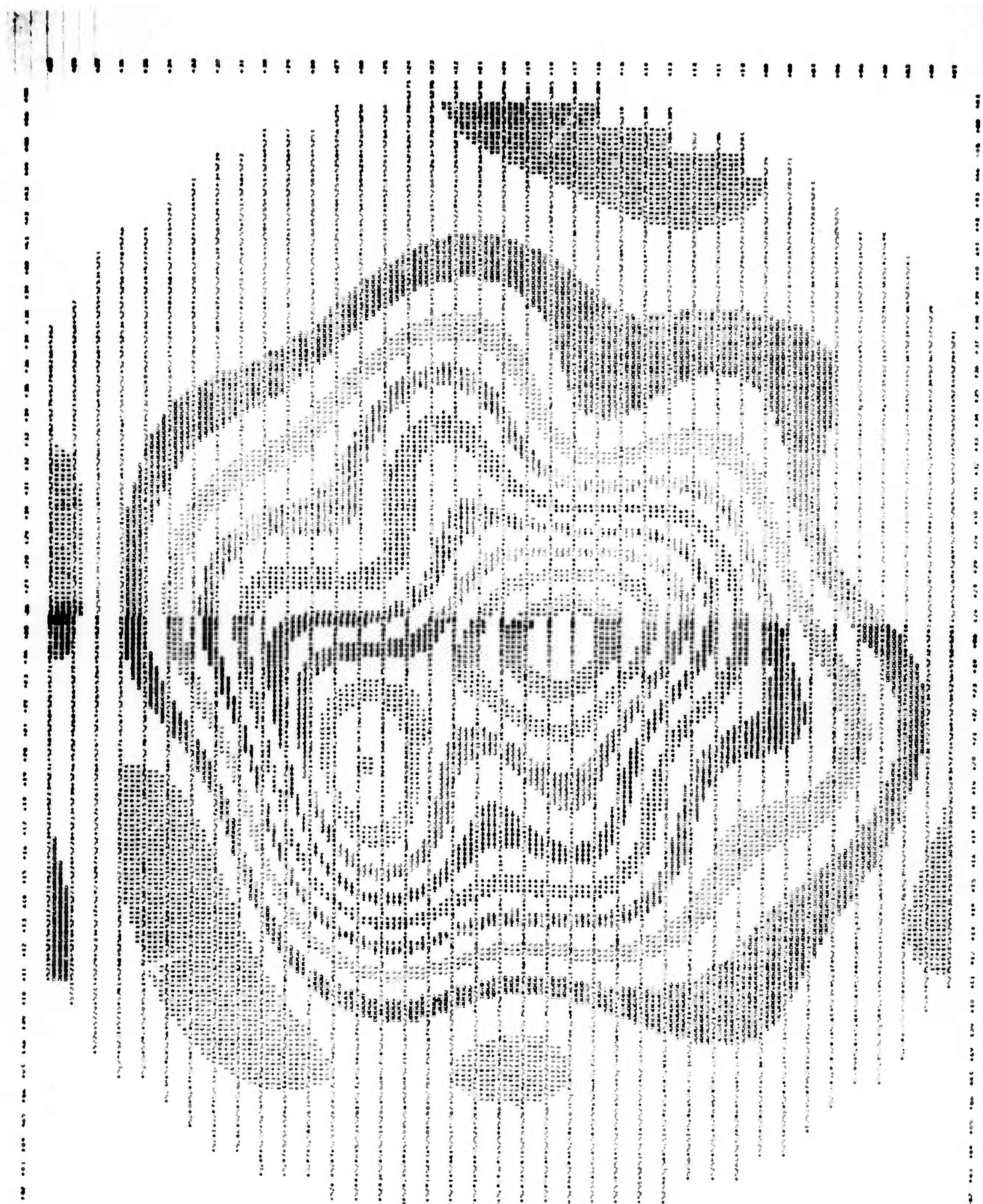

Z, 500 mb, 12Z 1 Dec. 1974, NMC I.C. Truncated

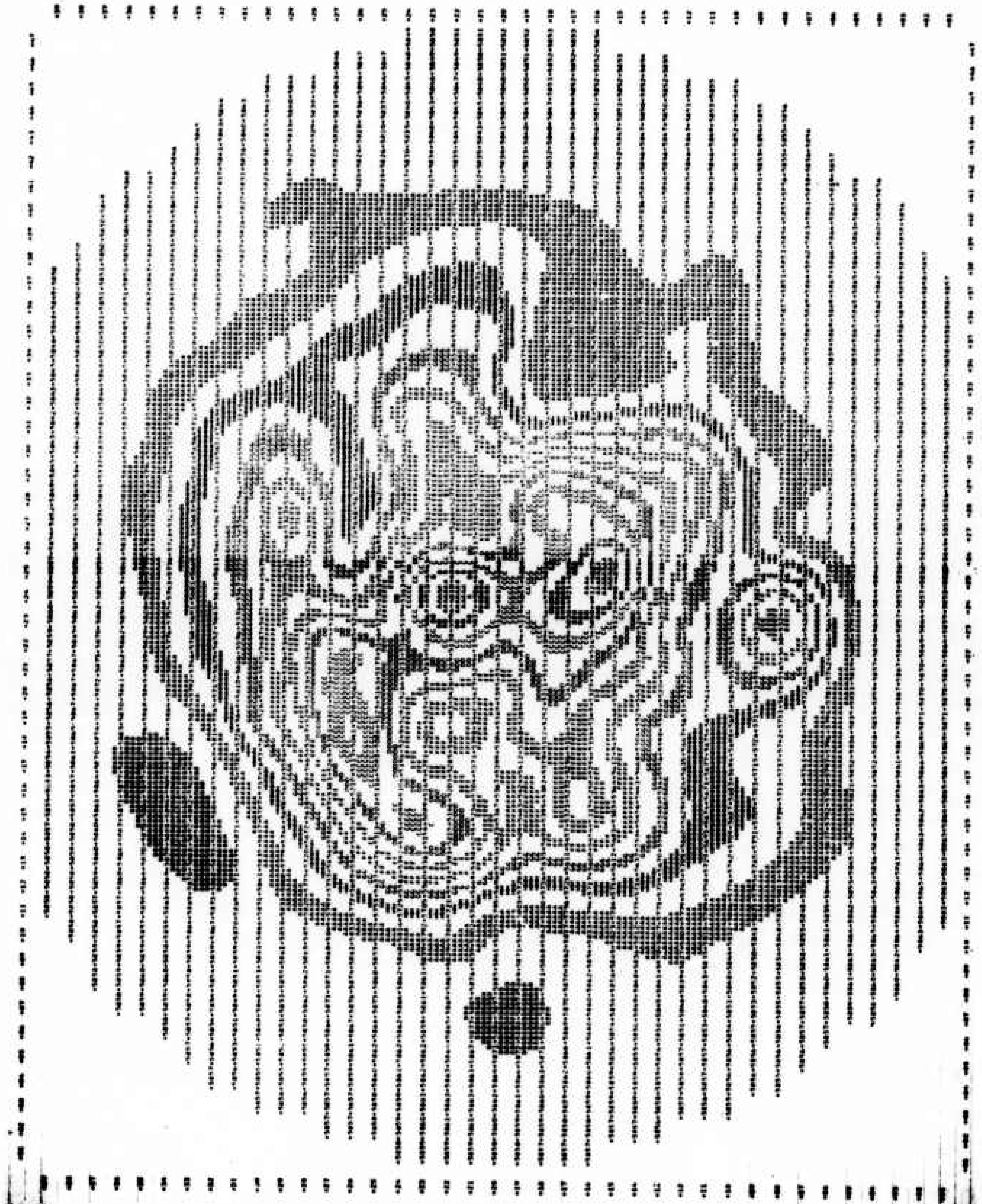

Z, 500 mb, 00Z 2 Dec. 1974, NMC I.C.

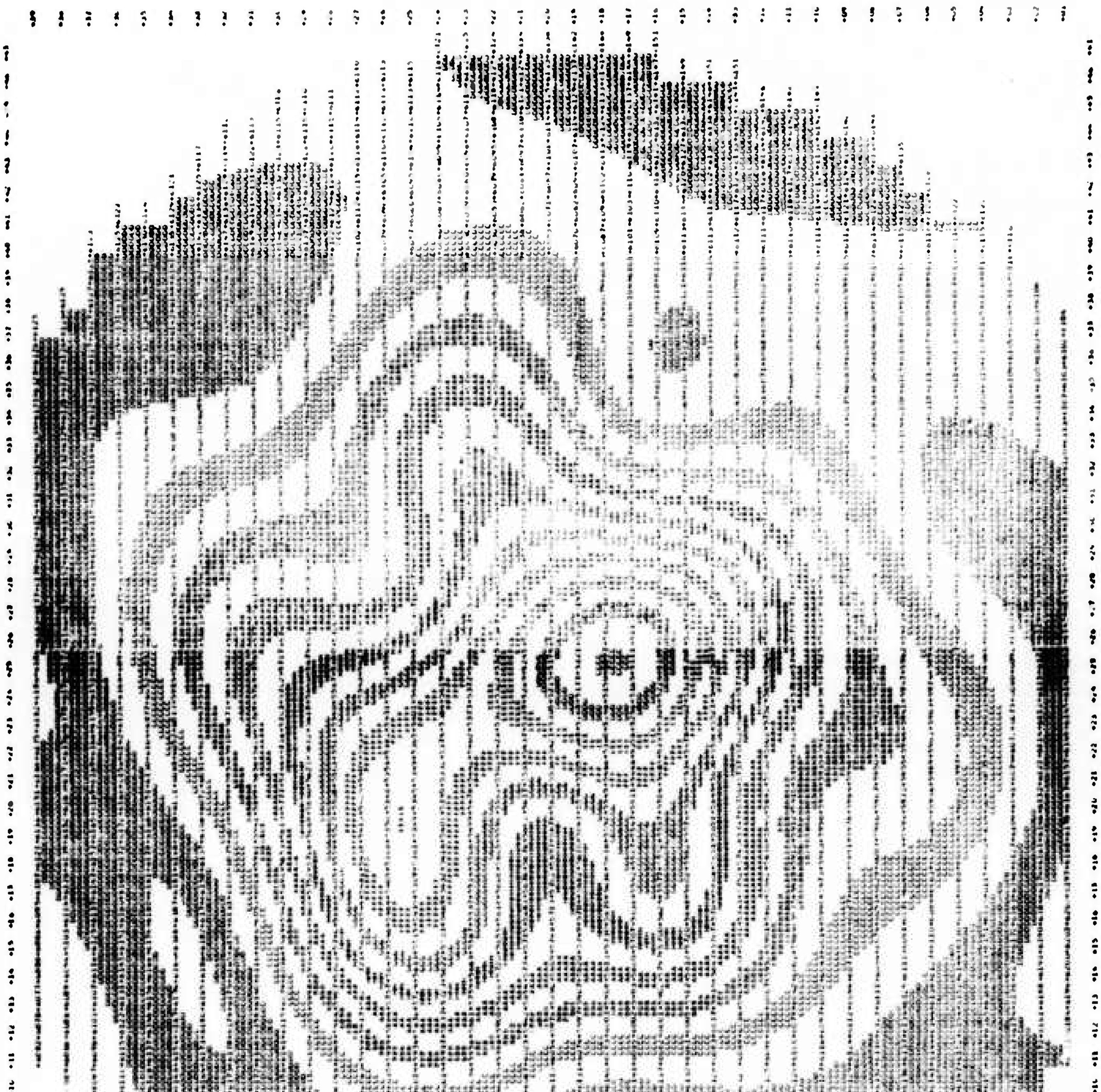

Z, 500 mb, 00Z 2 Dec. 1974, 12 Hour Prediction (10 min. time step)

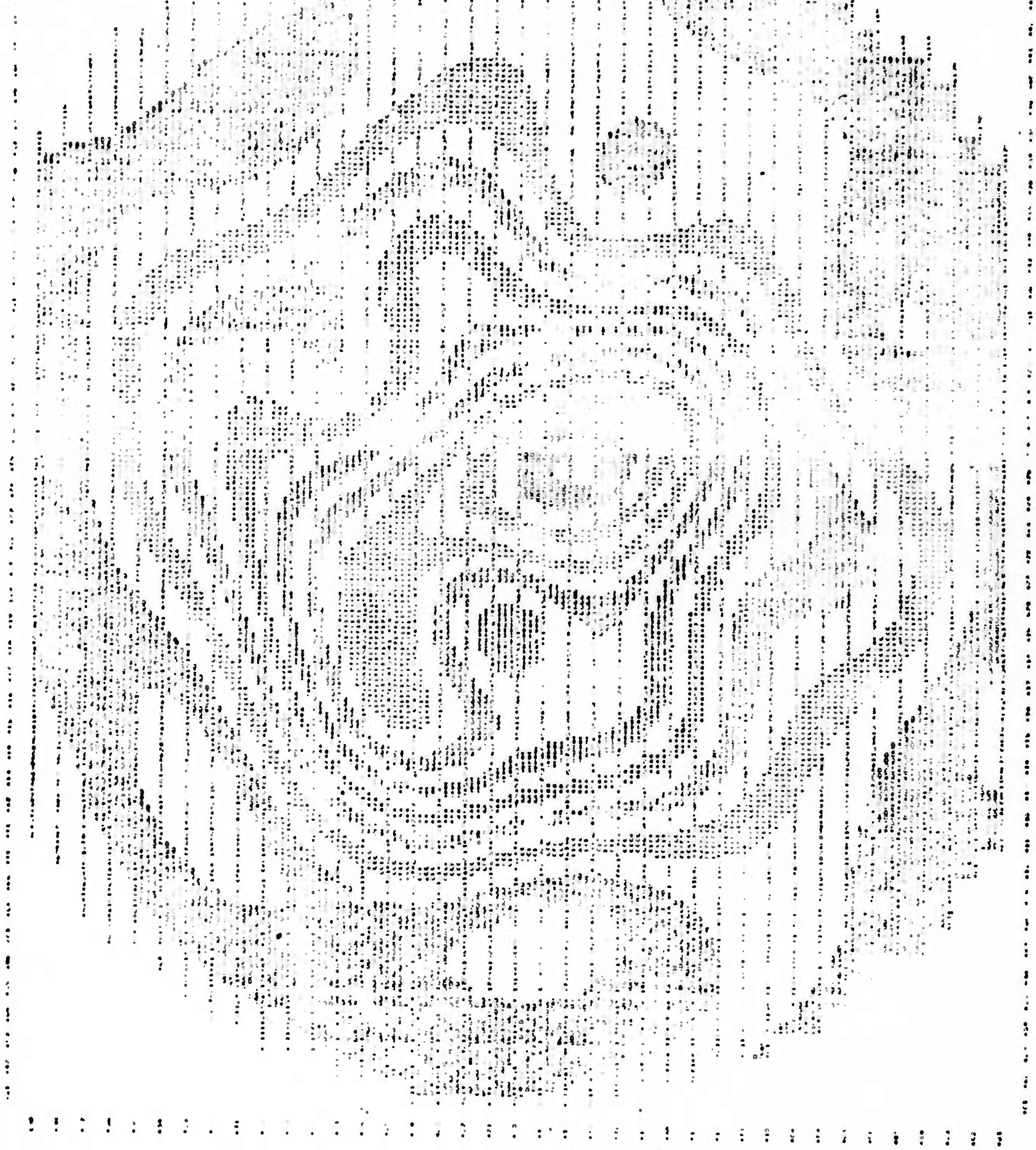

Z, 500 mb, 00Z 2 Dec. 1974, NMC I.C. Truncated

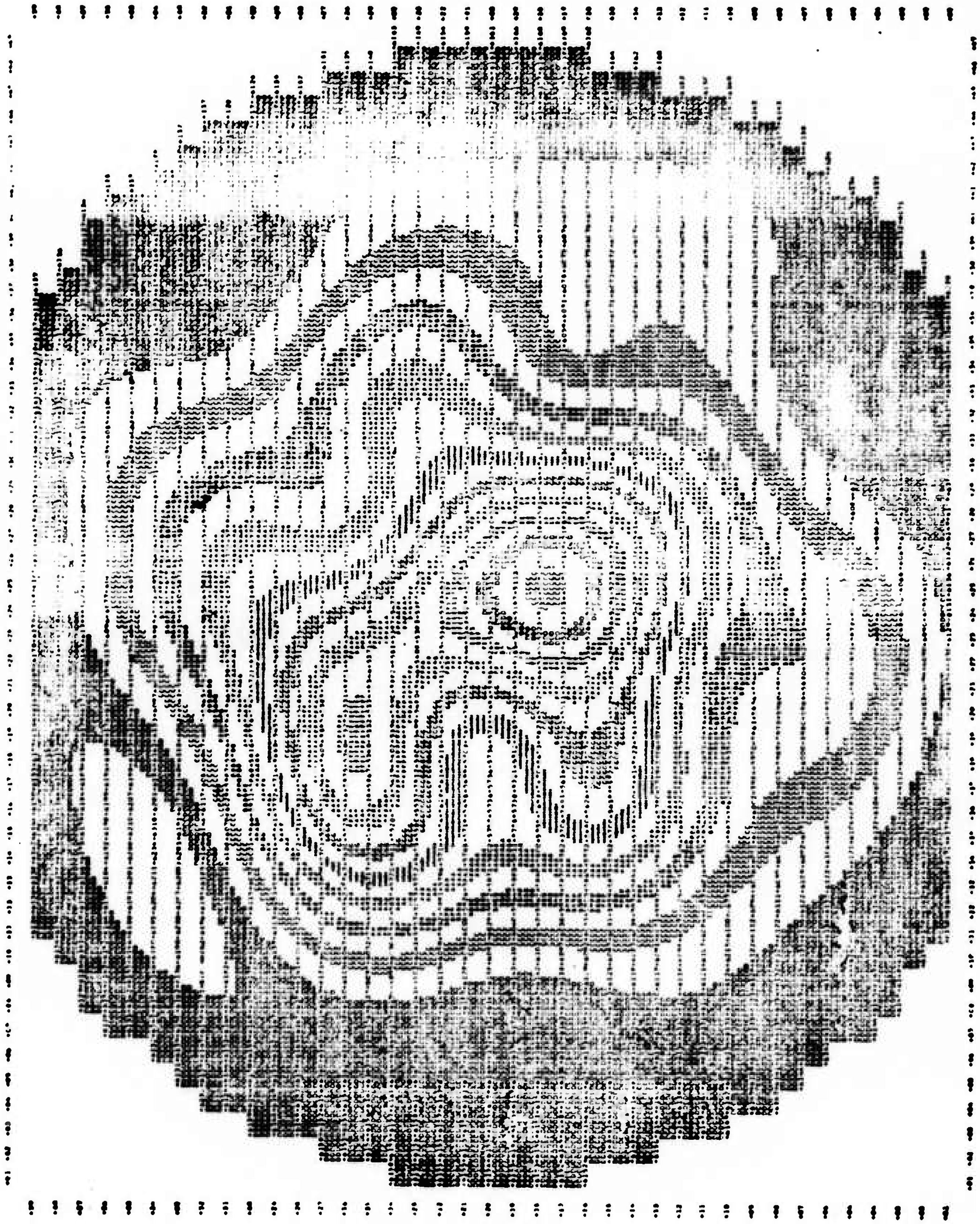

Z, 500 mb, 12Z 2 Dec. 1974, 24 Hour Prediction (10 min. time step)

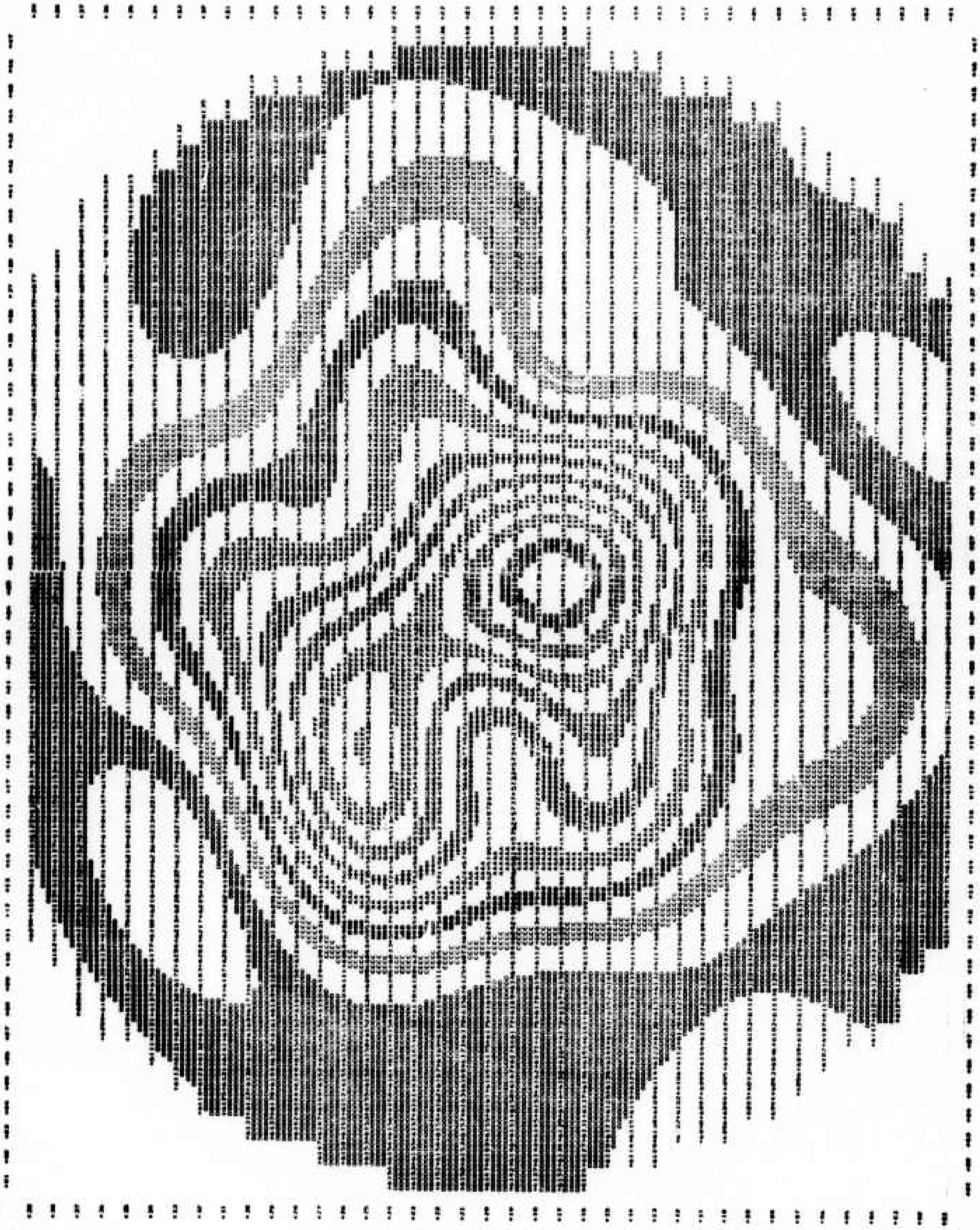

Z, 500 mb, 00Z 3 Dec. 1974, 36 Hour Prediction (10 min. time step)

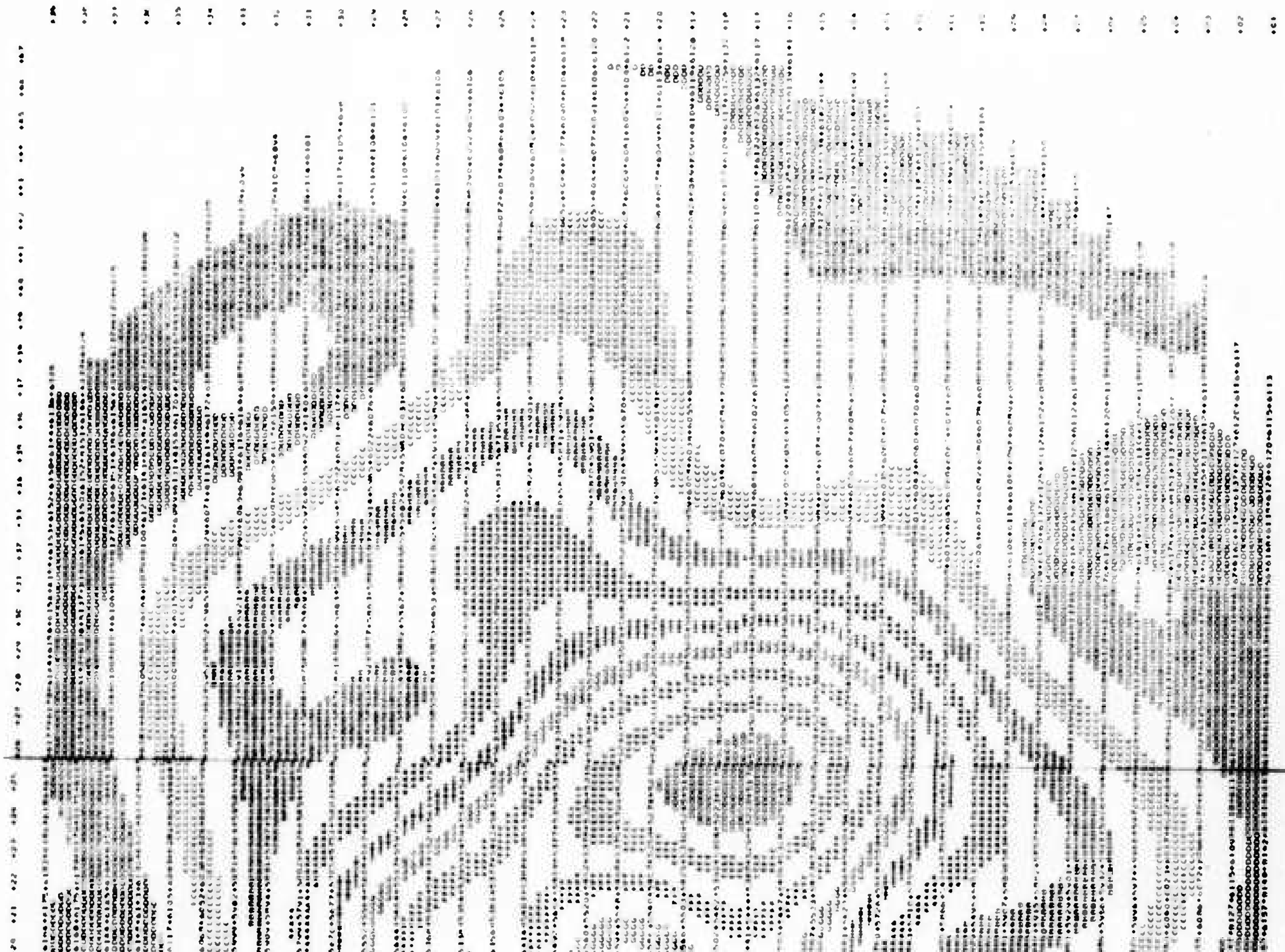

Z, 500 mb, 00Z 3 Dec. 1974, NMC I.C. Truncated

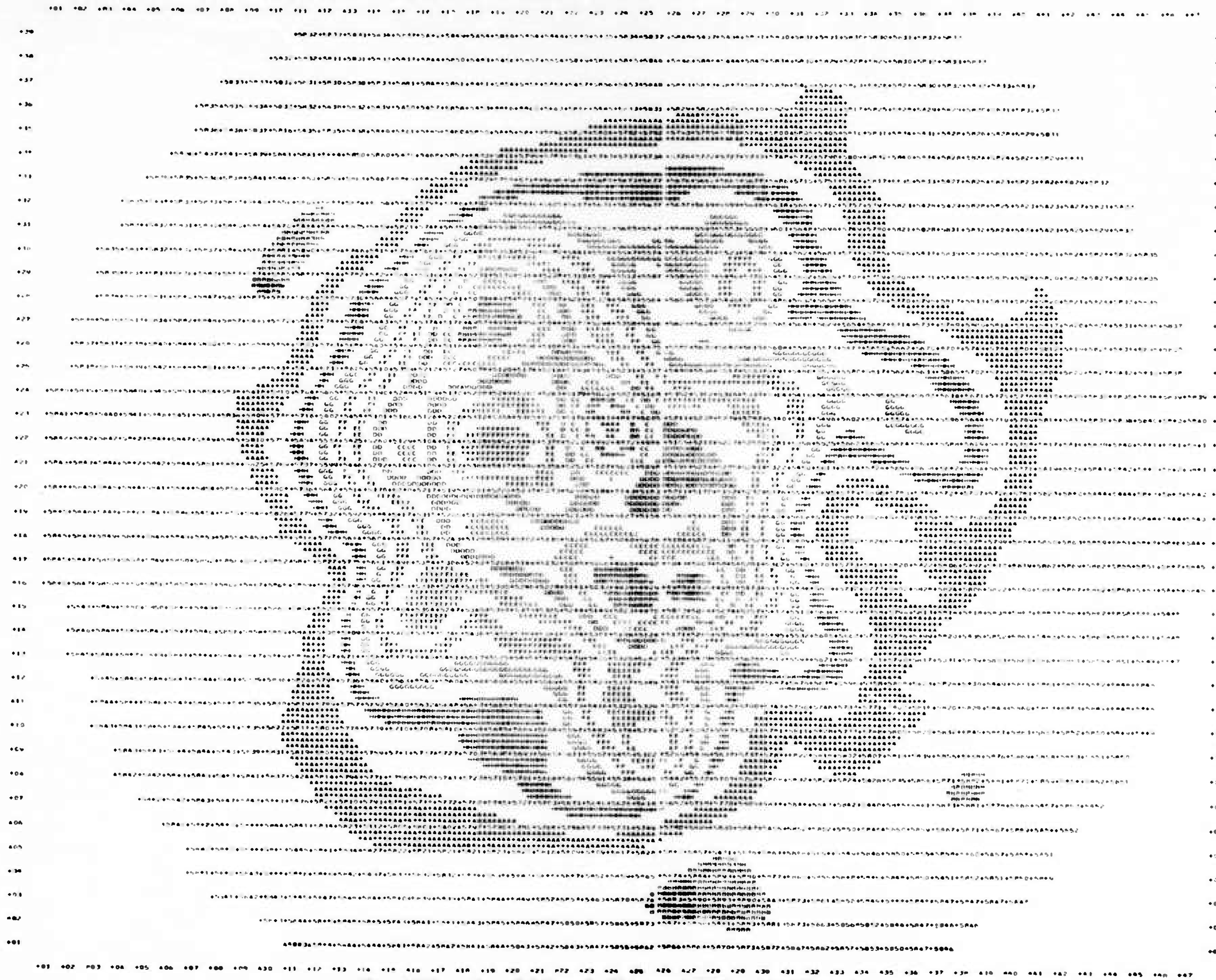

Z, 500 mb, 12Z 3 Dec. 1974, NMC I.C.

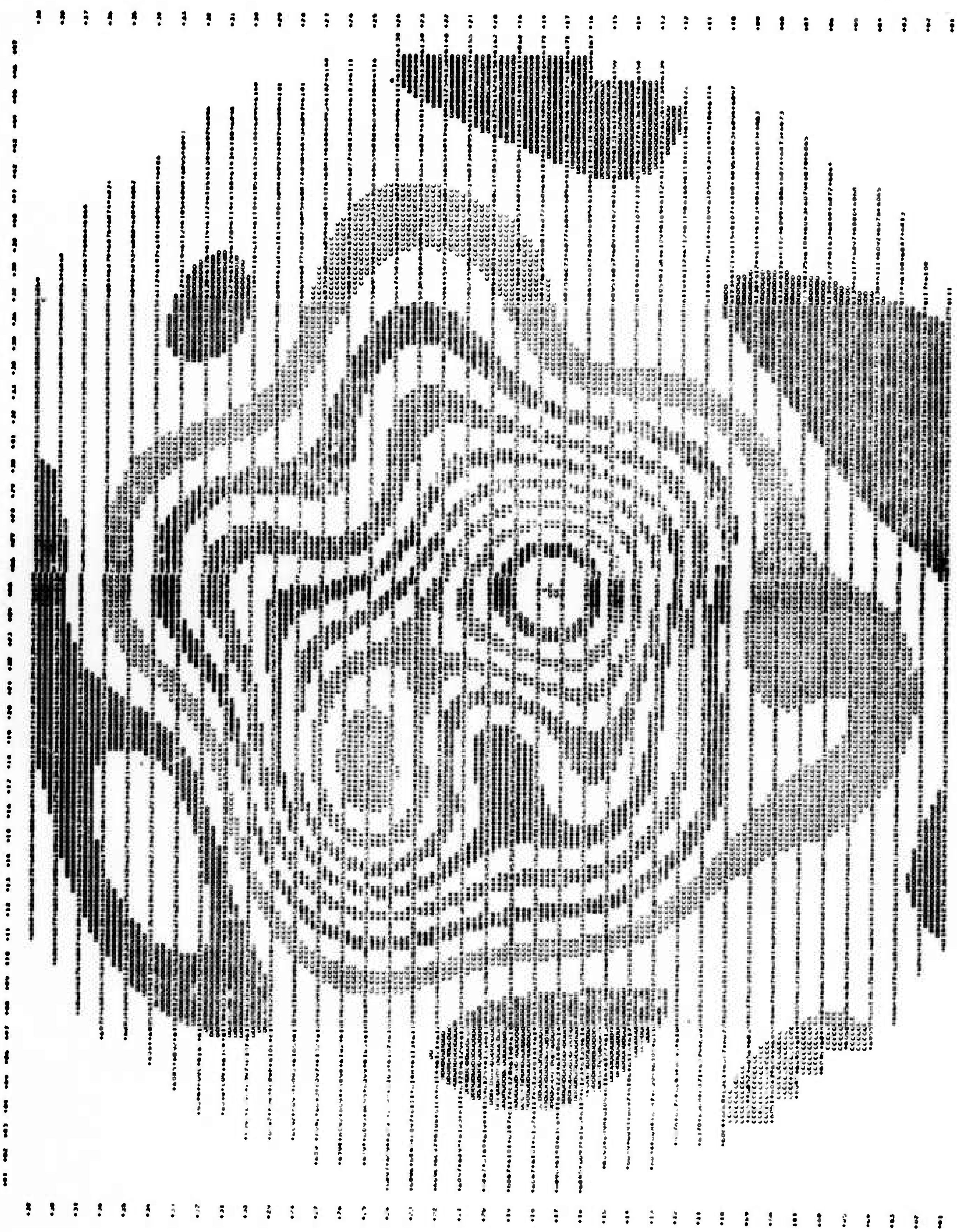

Z, 500 mb, 12Z 3 Dec. 1974, 48 Hour Prediction (10 min. time step)

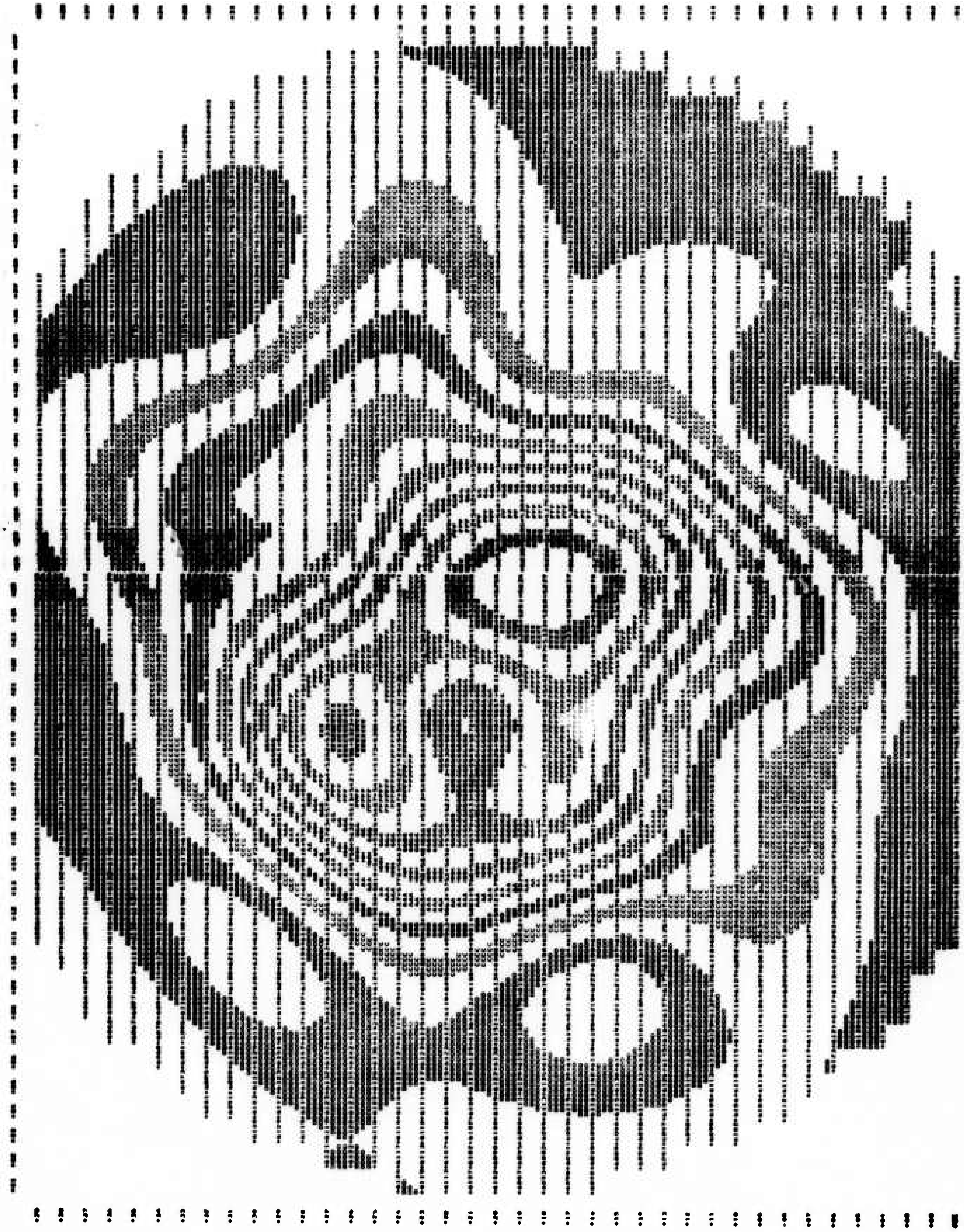

Z, 500 mb, 12Z 3 Dec. 1974, NMC I.C. Truncated

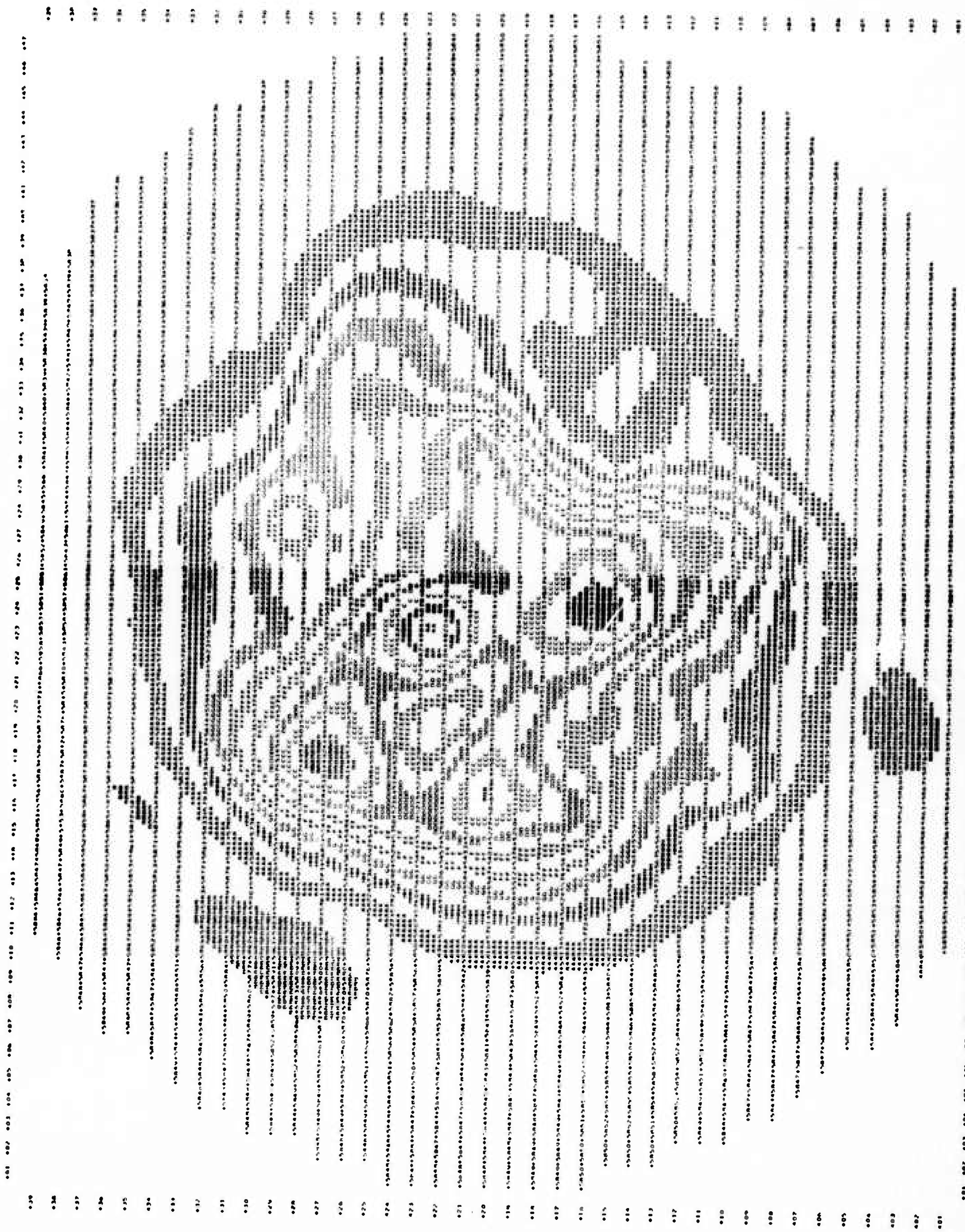

Z, 500 mb, 12Z 5 Dec. 1974, NMC I.C.

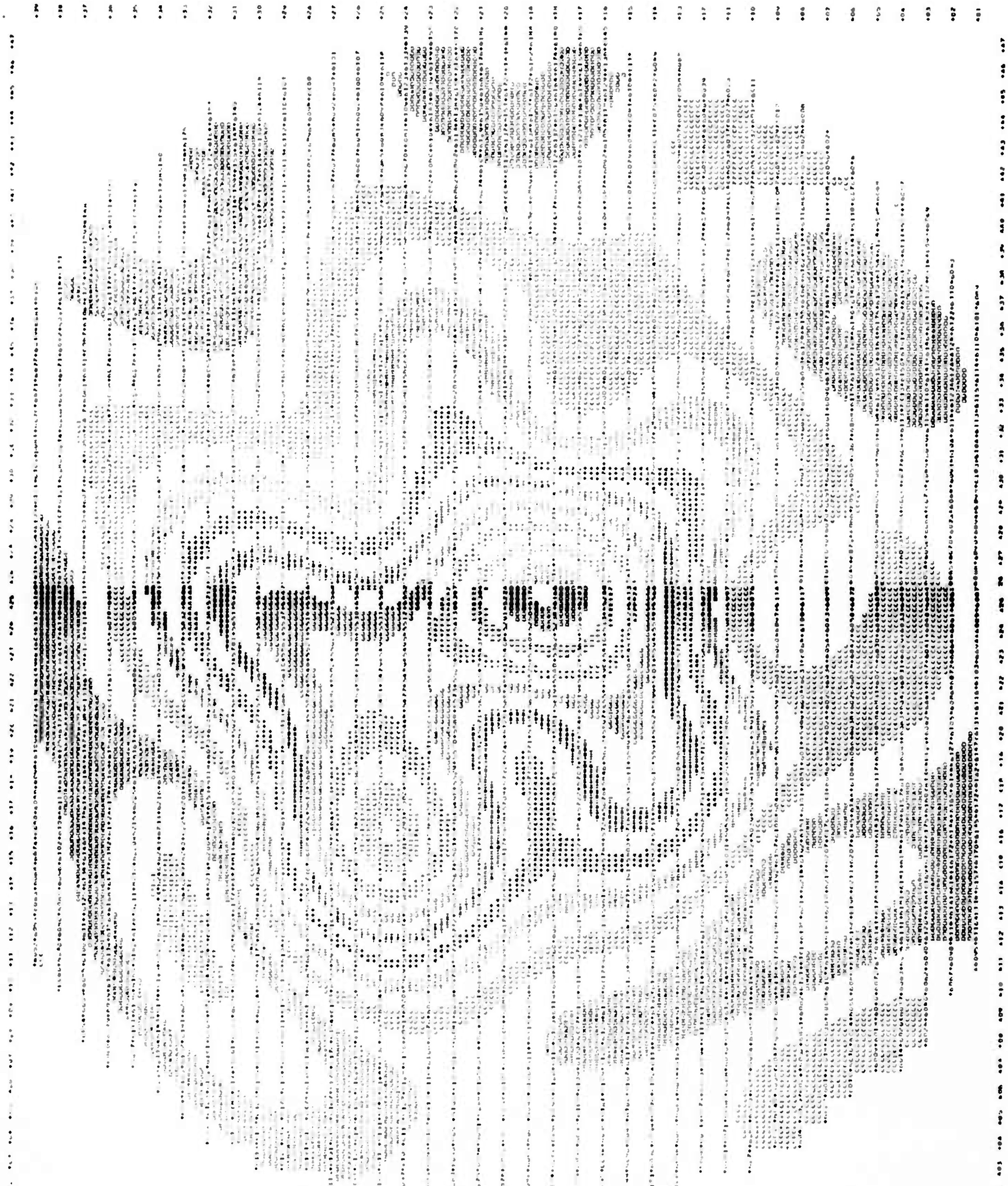

Z, 500 mb, 12Z 5 Dec. 1974, 96 Hour Prediction (10 min. time step)

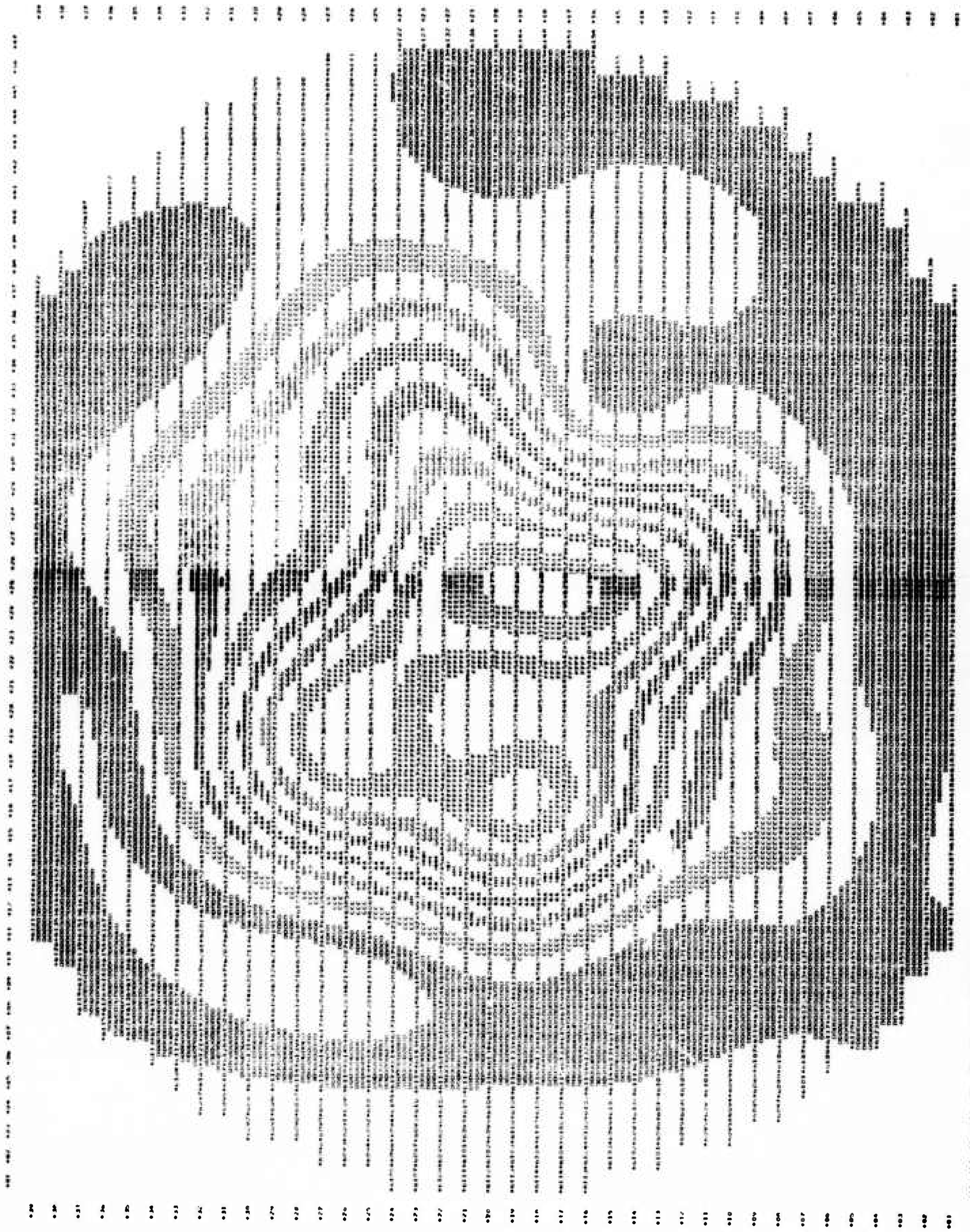

Z, 500 mb, 12Z 5 Dec. 1974, NMC I.C. Truncated

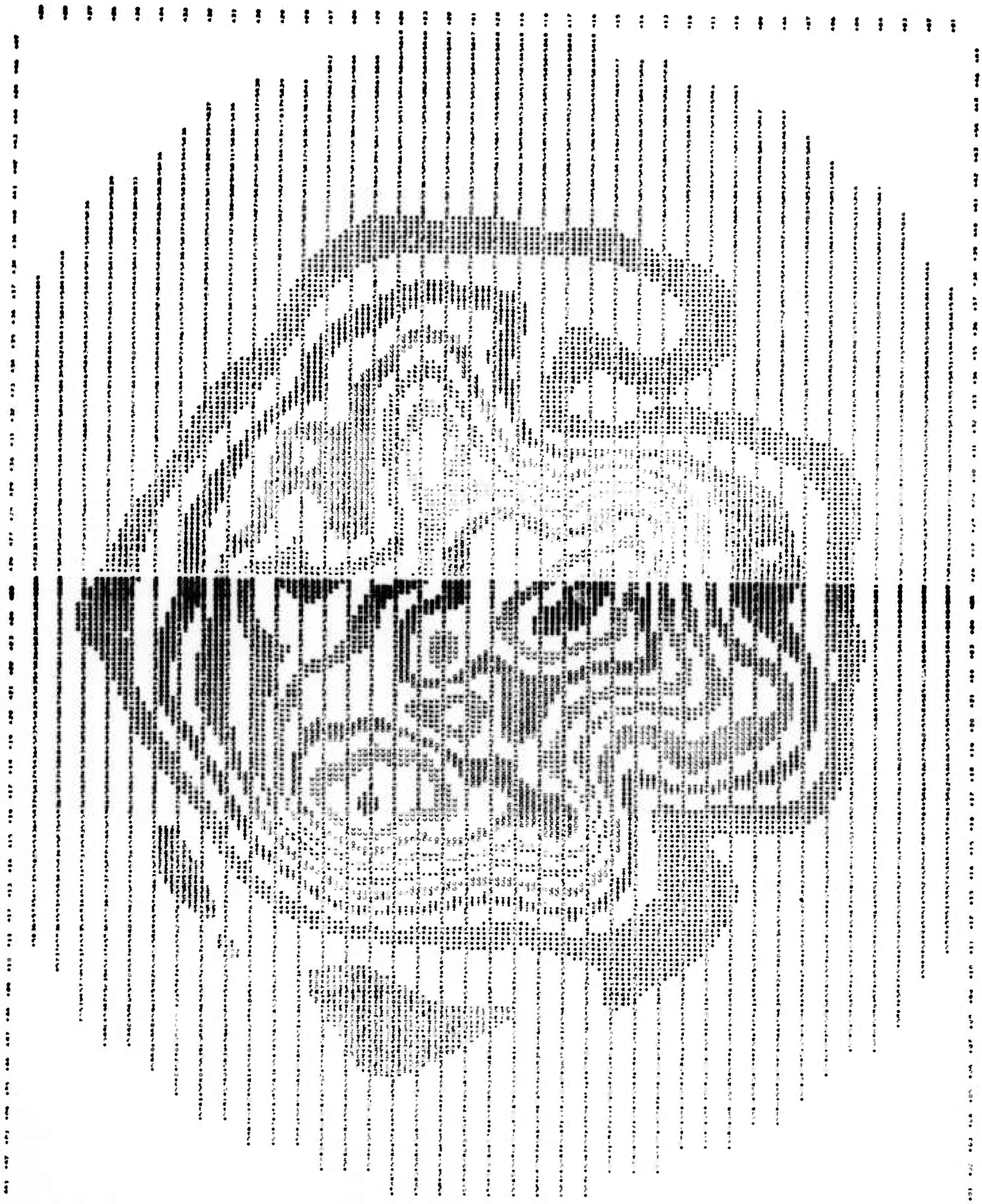

Z, 500 mb, 12Z 7 Dec. 1974, NMC I.C.

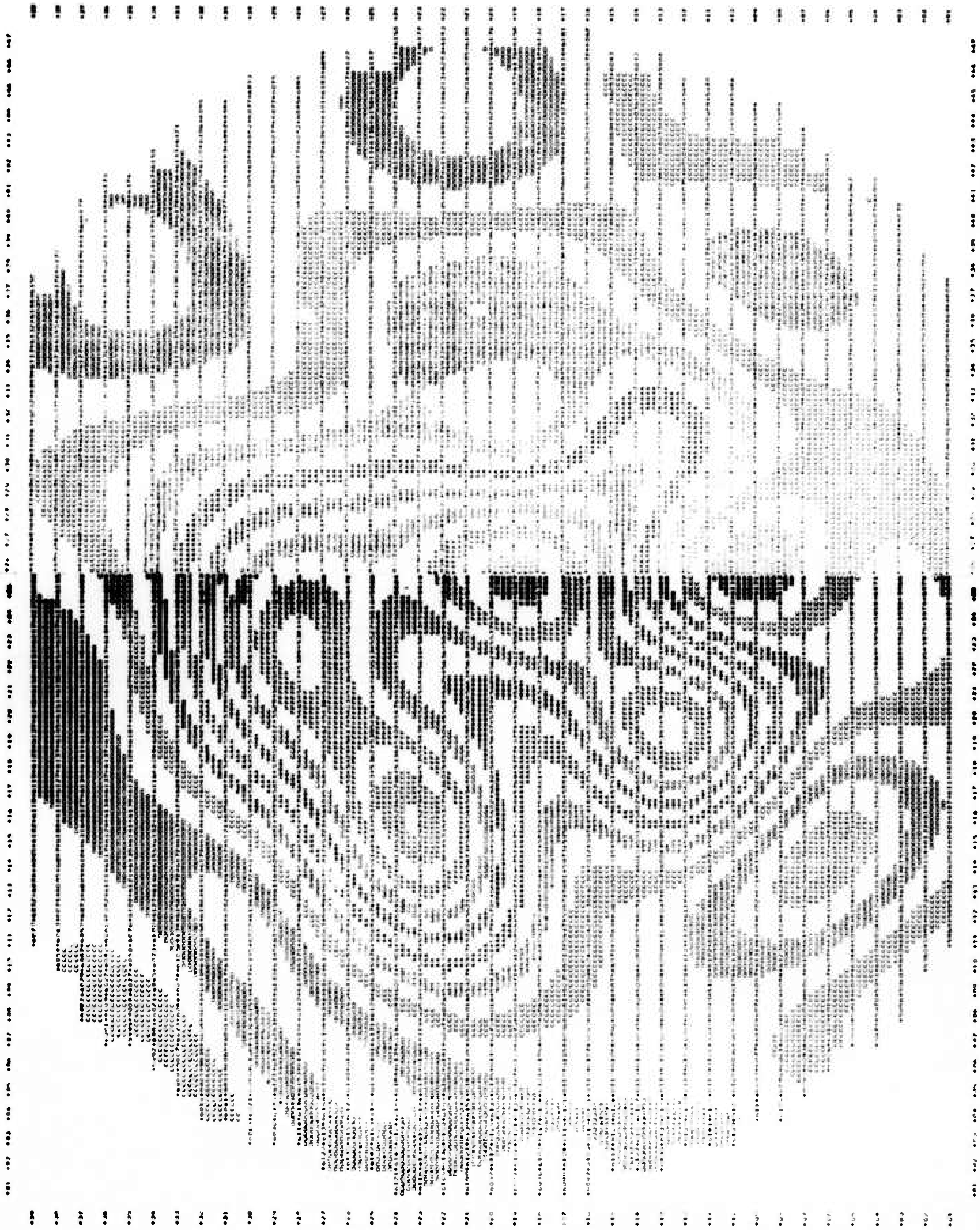

Z, 500 mb, 12Z 7 Dec. 1974, 144 Hour Prediction (10 min. time step)

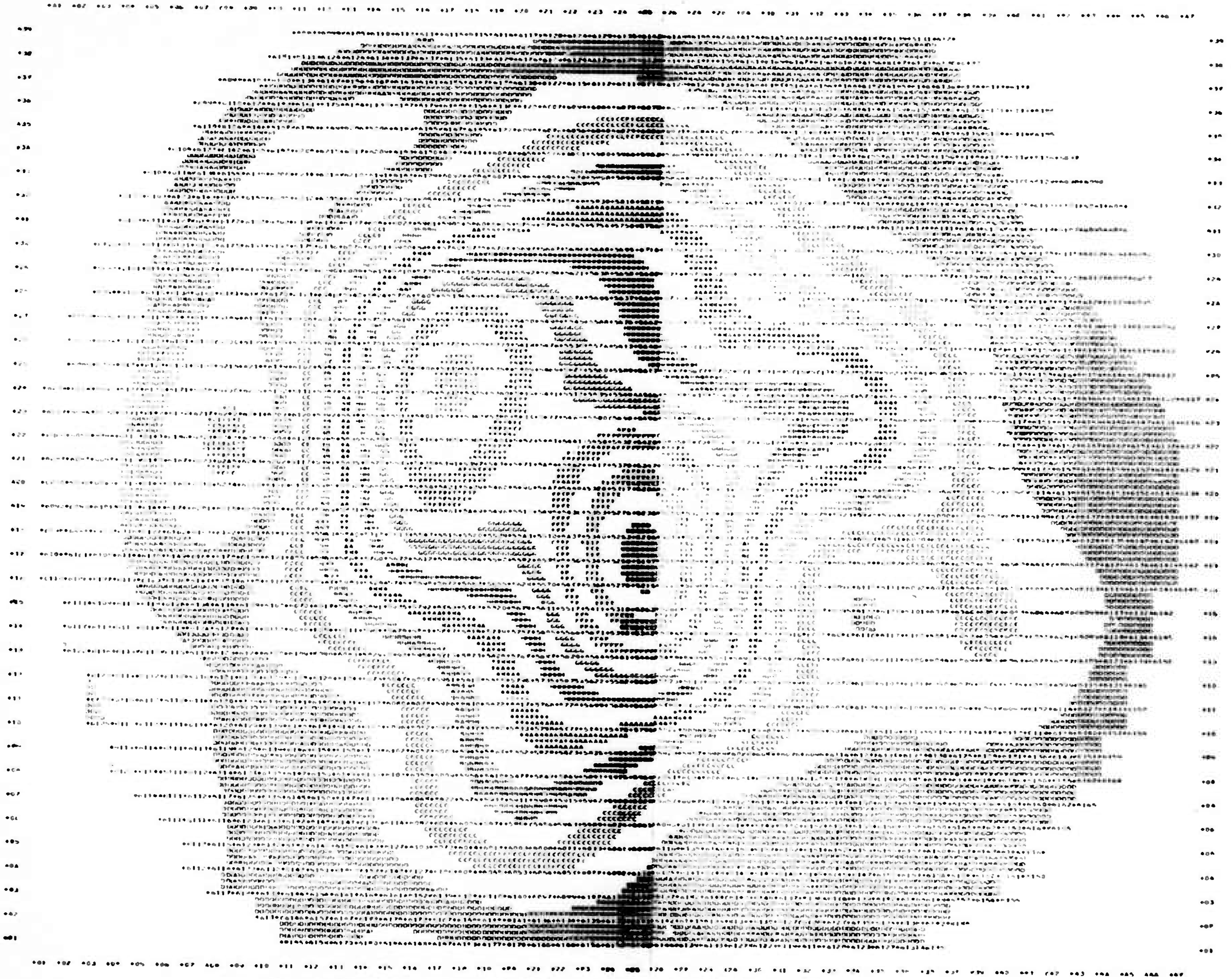

Z, 500 mb, 12Z 7 Dec. 1974, NMC I.C. Truncated

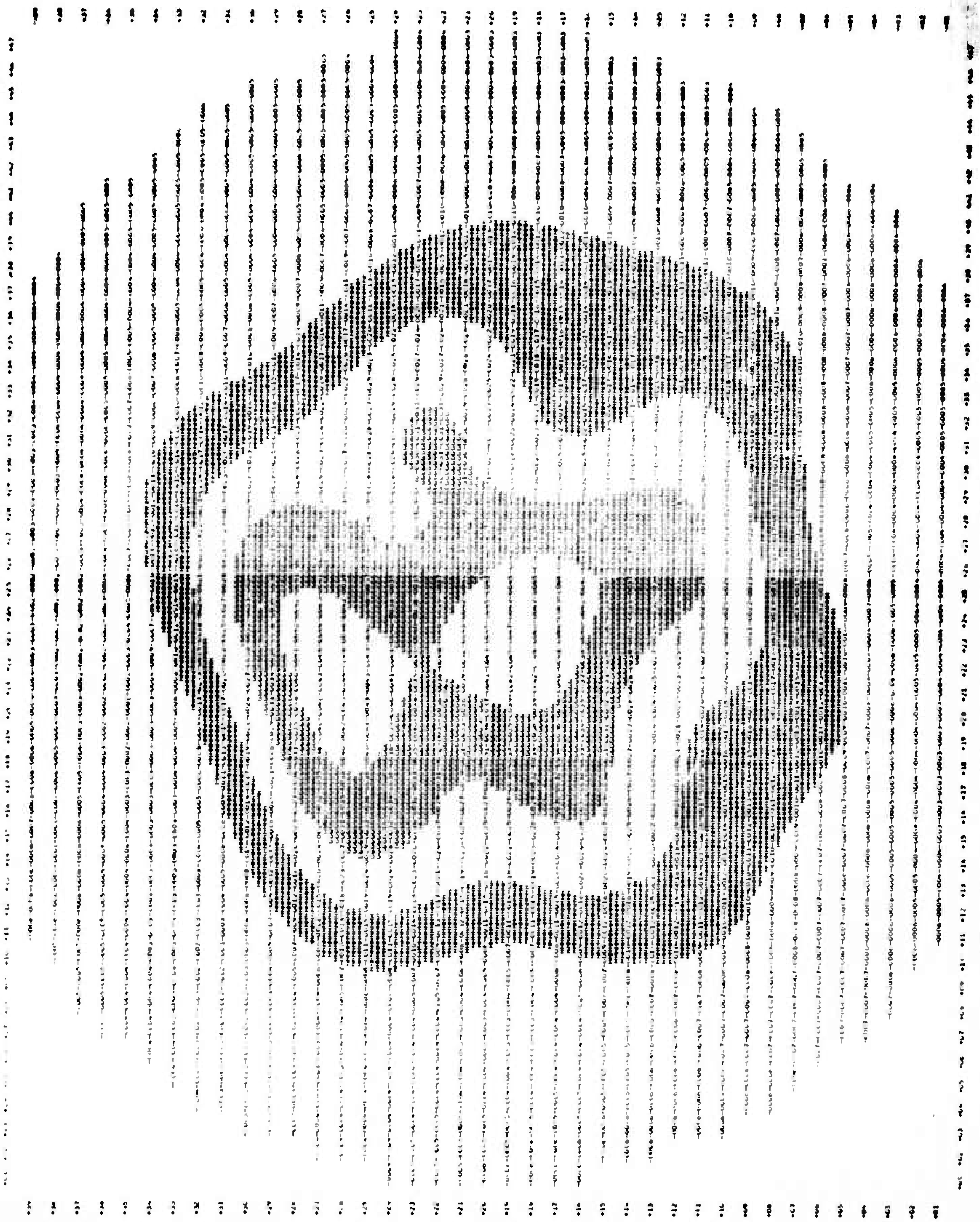

T, 500 mb, 12Z 1 Dec. 1974, NMC I.C. Truncated

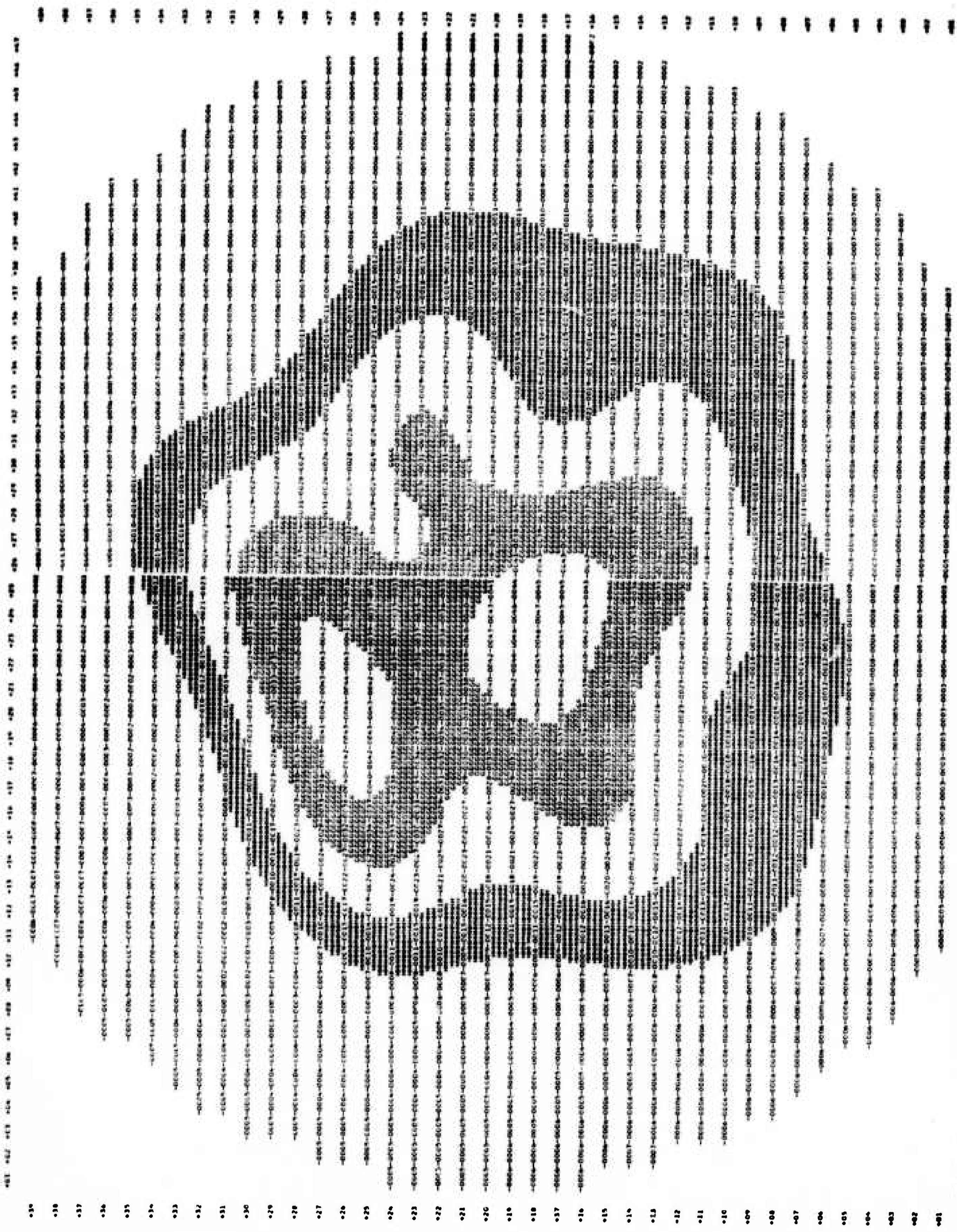

T, 500 mb, 12Z 2 Dec. 1974, 24 Hour Prediction (10 min. time step)

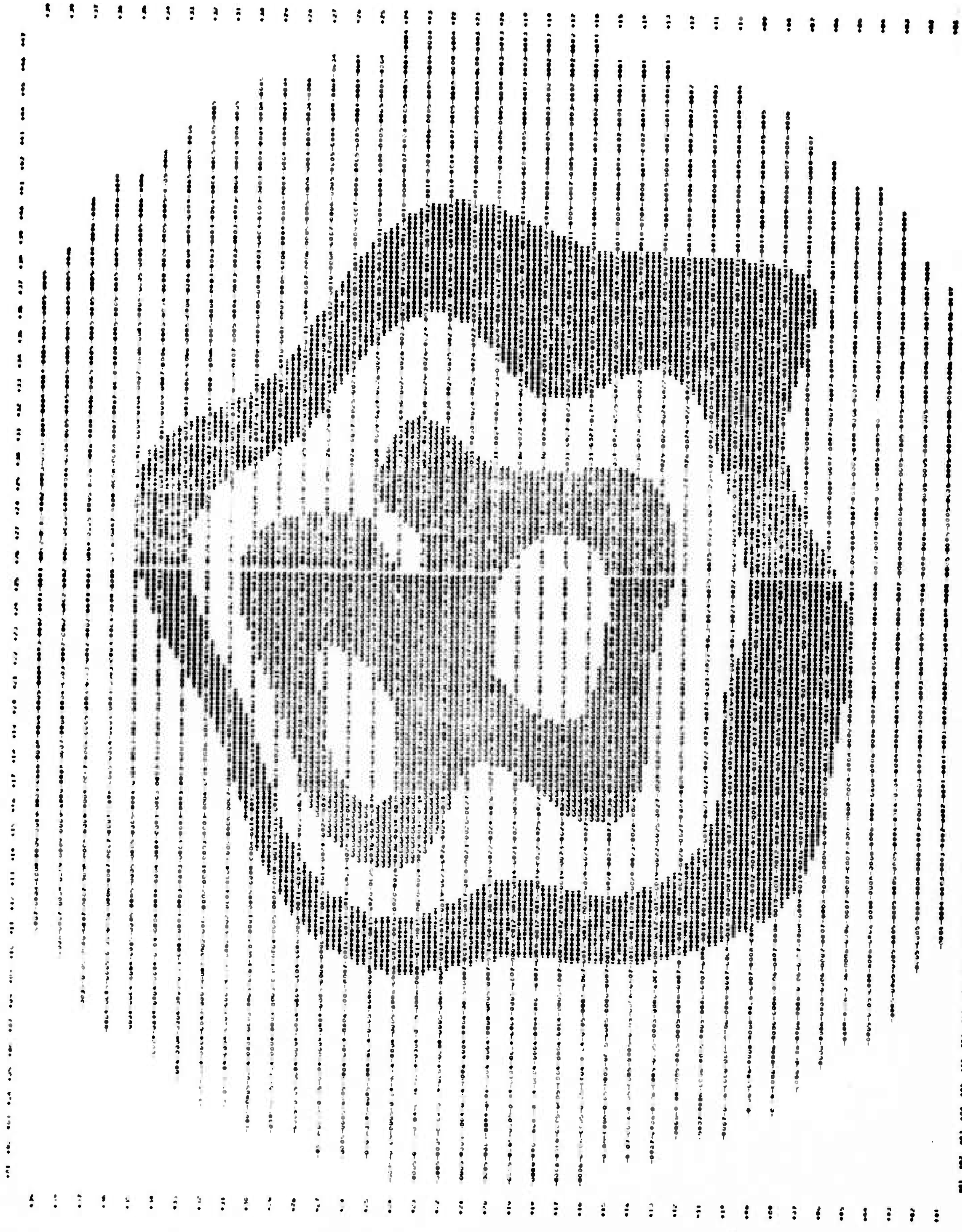

T, 500 mb, 12Z 3 Dec. 1974, 48 Hour Prediction (10 min. time step)

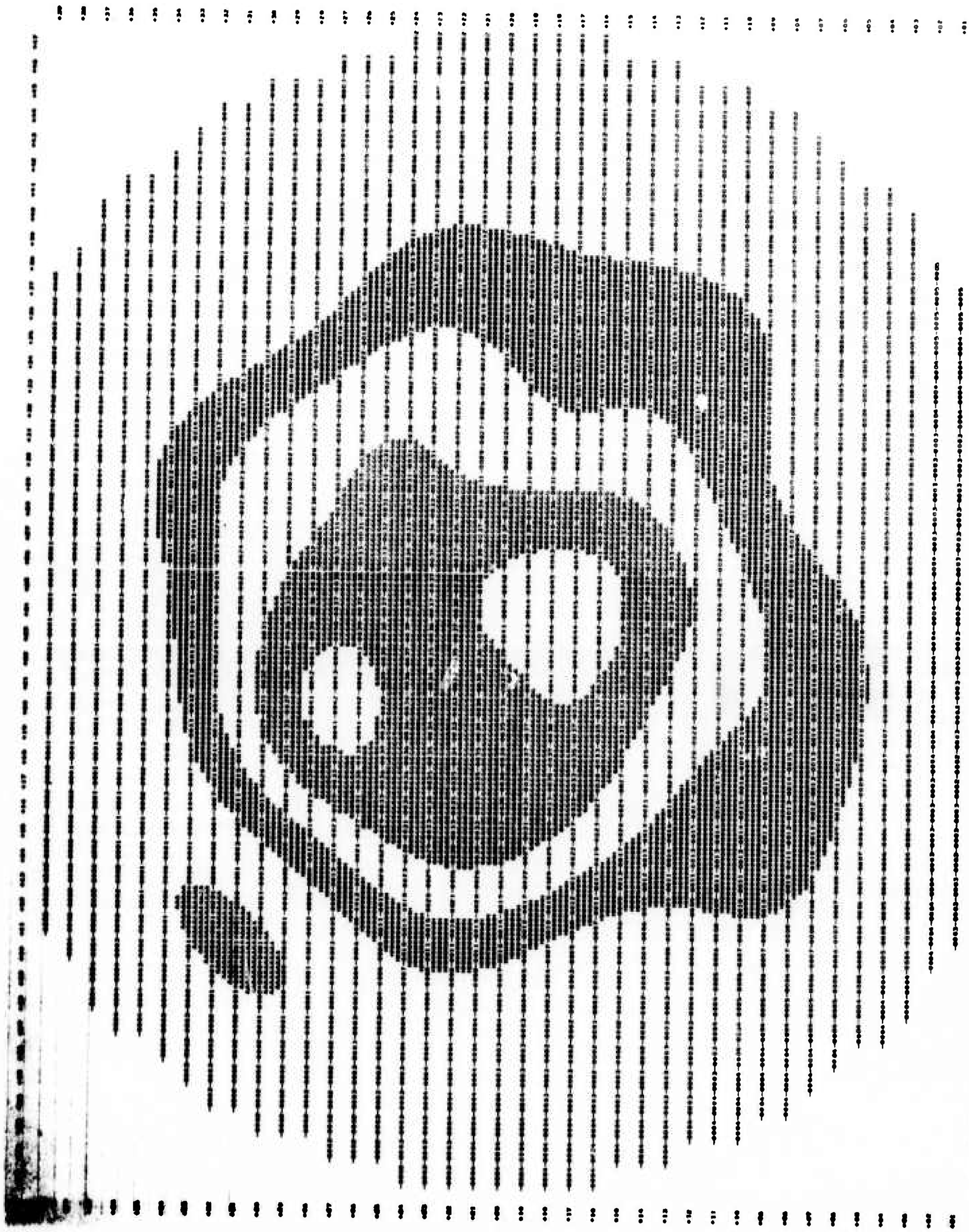

T, 500 mb, 12Z 3 Dec. 1974, NMC I.C. Truncated

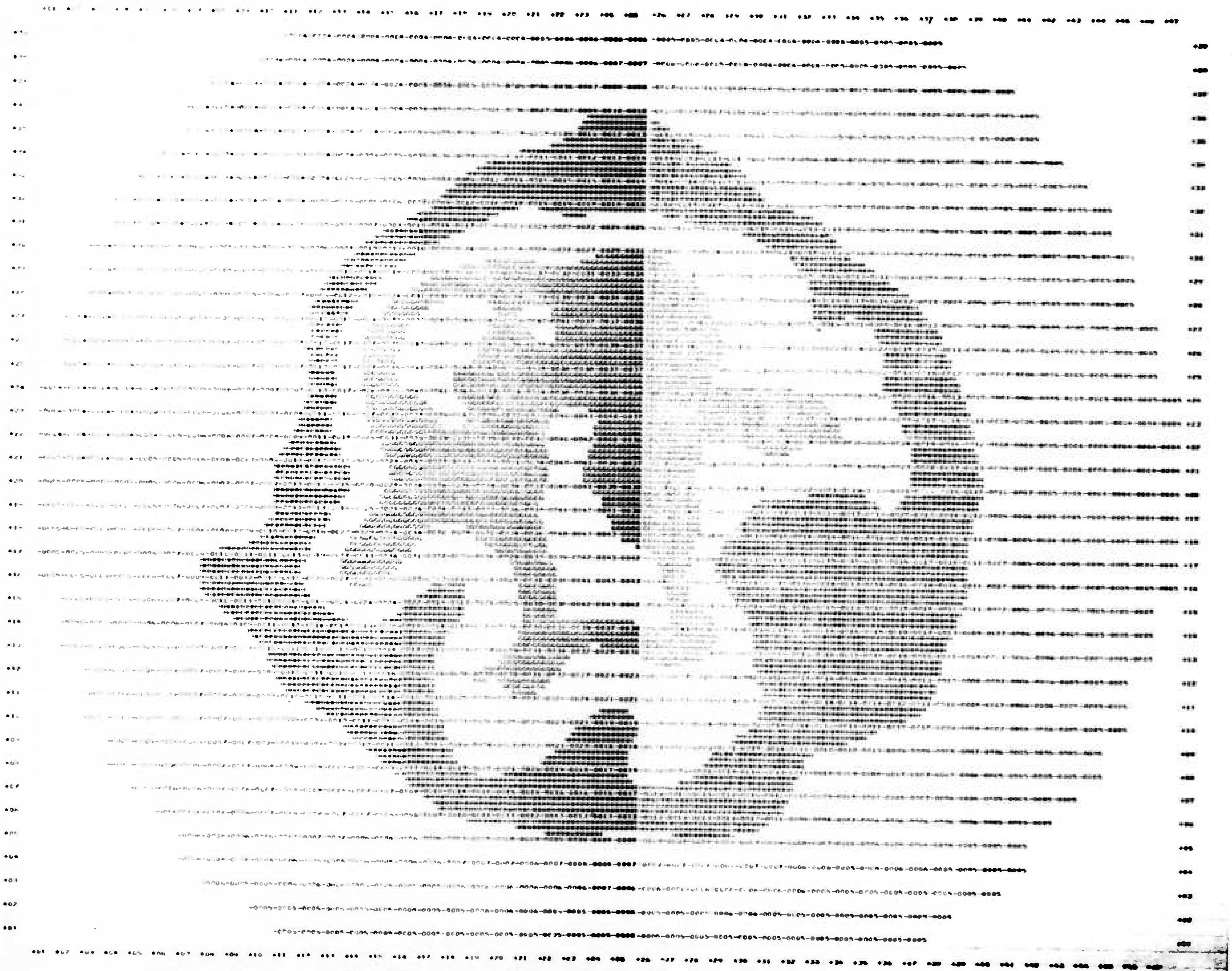

T, 500 mb, 12Z 7 Dec. 1974, NMC I.C.

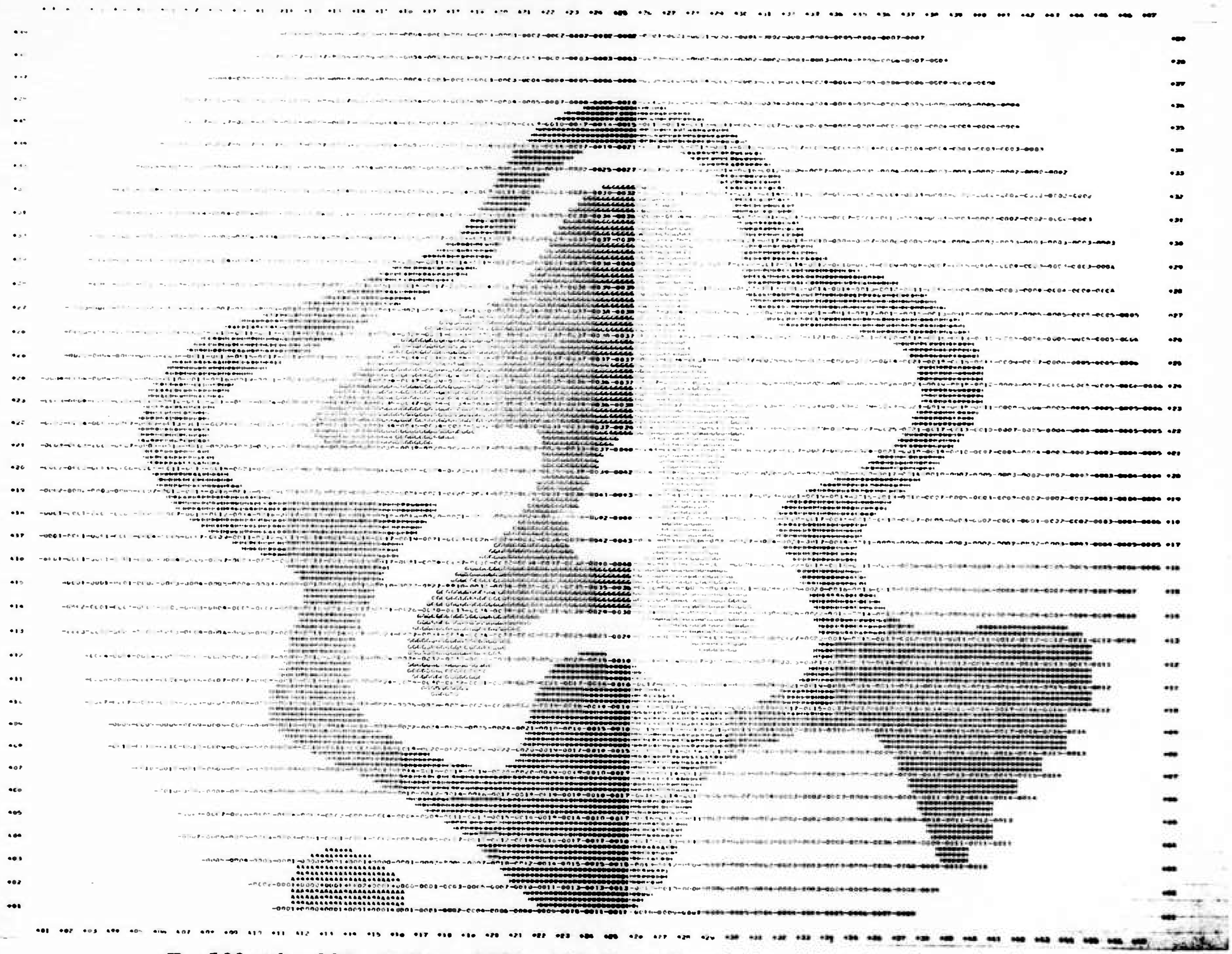

T, 500 mb, 12Z 7 Dec. 1974, 144 Hour Prediction (10 min. time step)

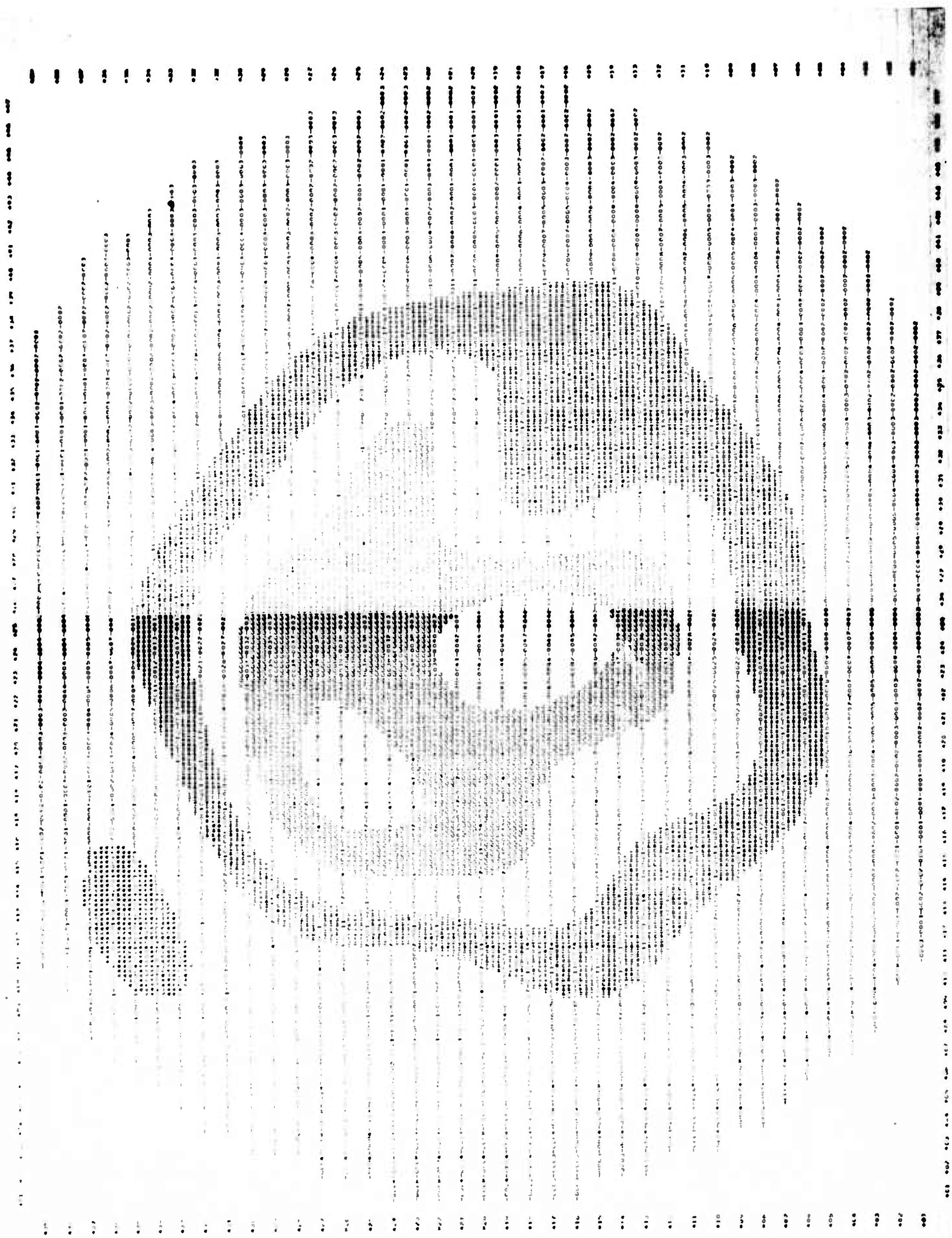

T, 500 mb, 12Z 7 Dec. 1974, NMC I.C. Truncated